Table of Contents

NASA Contractor Report 3381

Roller Skewing Measurements in Cylindrical Roller Bearings

Lester J. Nypan

GRANT NSG-3065
JANUARY 1981

NASA

NASA Contractor Report 3381

Roller Skewing Measurements in Cylindrical Roller Bearings

Lester J. Nypan
California State University, Northridge
Northridge, California

Prepared for
Lewis Research Center
under Grant NSG-3065

National Aeronautics
and Space Administration

**Scientific and Technical
Information Branch**

1981

Table of Contents

Summary

Measurements of roller skewing in a 118 mm bore roller bearing operating at shaft speeds to 12000 rpm are reported.

High speed motion pictures of a modified roller were taken through a derotation prism to record skewing as the roller moved through loaded and unloaded regions of the bearing. Subsequent frame by frame measurement of the photographic film provided information on roller skewing. Radial and tangential skew amplitudes of .4 to .5 degrees were observed with .5 degree misalignment.

Introduction

Rollers in roller bearings may misalign or skew as they roll between the raceways (1)[1]. This is controlled by small clearances between race shoulders and the roller which provide a restoring moment at the ends of the roller to restrain the roller from further skewing. In high speed turbine bearings the skewing and associated rubbing contact can lead to wear on the roller ends, increased skewing, and eventual failure (2). In some instances skewing and wear can be so severe that the roller turns and lodges within the separator pocket (3). This investigation was undertaken to gather experimental data for comparison with theoretical predictions of skewing magnitudes, and also for comparison of one roller bearing design with future improved designs. The investigation reports skewing behavior of a 1.15 length to diameter ratio roller in 118 mm bore roller bearings of 0.18 and 0.21 mm (0.0073 and 0.0083 in.) clearance operating with a 4450 N (1000 lb) radial load at shaft speeds of 4000, 8000, and 12000 rpm with outer race misalignment of 0, 0.25, 0.5, -0.5 degree.

---

[1]Numbers in brackets designate References at end of paper.

Test Bearings

Two test bearings were used in the investigation. They were representative of aircraft gas turbine engine roller bearings and had PWA 541043D markings. The bearings' original out-of-round outer rings were replaced with cylindrical rings having radial clearances of 0.18 and 0.21 mm (0.0073 and 0.0083 in). These radial clearances were calculated as the difference between the average of the outer race measured maximum and minimum inner diameters and the inner race nominal raceway diameter plus two roller diameters. Table I gives dimensions of the bearings used.

Lubrication

While the inner race had grooves for under race cooling and drilled passages for cage and roller lubrication, these were not used. Oil was sprayed onto the rollers through two jet pipes at a total flow rate of 1.8×10^{-3} m^3/min (0.47 gpm). The oil used was a 5-centistoke neopentylpolyol (tetra) ester. This is a type II oil which conforms to specification MIL-L-23699. Test bearing inlet oil was heated and controlled to 339°K (150°F).

Method of Approach

Roller skewing was measured from photographs of a modified roller in a bearing operating at shaft speeds to 12000 rpm. Figure 1a is a schematic of the test shaft assembly. A 16 mm Fastax WF4 camera was used with synchronized Xenon flash tube illumination to photograph a 32 x 24 mm (1.25 x .94 in) area of the bearing at up to 8000 frames per second. The derotation prism apparatus described in ref. (4-7) was used to maintain this area centered on the modified roller and to follow this roller as it orbited through 360 degrees within the bearing. The

32 x 24 mm (1.25 x .94 in) area photographed in 16 mm format included a segment of a fixed outer race protractor, a segment of an inner race protractor, a segment of the roller bearing separator, the modified roller and portions of adjacent rollers. Figure 1b is an enlargement of a data photograph. At the 12000 rpm shaft speed photographs of the modified roller were obtained at 4 to 5 degree intervals as observed on the outer race protractor. The inner race protractor permitted cage to shaft speed ratio determinations. Two to three hundred photographs could usually be obtained before the energy storage capacitors discharged. This permitted photographs of three to four revolutions of the separator and roller orbit to be obtained:

Camera speeds of 6000 frames per second were often used for the 8000 and 4000 rpm bearing speeds with proportionate adjustments to photographic intervals within the bearing and number of separator revolutions available for analysis.

The roller modification to permit frame by frame roller orientation measurements incorporated a 3.18 mm (0.125 in) diameter x 1.59 mm (0.626 in) deep counterbore recess to help to identify the roller center in the photographs. A pin 1.27 mm (0.050 in) in diameter by 6.35 mm (0.250 in) in length is extended out along the roller axis from the roller end. Figure 2 is a photograph of a modified roller.

In the data photographs, the end of the pin appeared superimposed on the image of the counterbore. By measuring radial and tangential distances from the counterbore image center to the pin image center and dividing by the pin length the tangents of the roller orientation angles are obtained. Measurements were made so that the roller orientation angles are radially outward from the bearing center and tangent to the roller path. As the camera axis was oriented along the bearing center line the pin image center is always offset radially on the counterbore image by the "camera angle". The radial roller skew angle appears superimposed on the constant camera angle. Radial and tangential roller skew

angles are thus obtained as a function of roller location within the bearing.

Film Measurement and Error Estimation

A Vanguard Instrument Corporation Motion Analyzer was used to project the films for frame by frame measurement. A template with concentric circles was used to align a Gerber Scientific Instruments measuring and digitizing instrument first on the image of the pin end, and then on the image of the counterbore. Four digit measurements of the tangential and radial coordinates of the circle centers were automatically punched on computer cards at each alignment. A computer program calculated differences, applied scale factors and prepared output to drive a Calcomp 936 plotter to graph the data.

An estimate of the uncertainty and possible errors inherent in the measurement system was obtained by repeatedly measuring the same film frame. These measurements were then processed in the same manner as regular data measurements made on frames taken at 5 degree increments of roller orbit within the bearing. Figure 3 shows the apparent variation in skew angles due solely to the film measurement system. The test indicates that the maximum deviation from the mean of 72 readings was 0.42 degrees. The standard deviation from the mean was 0.028 degrees in radial skew and 0.037 degrees in tangential skew. When the test measurements were subjected to the Fourier analysis described under Results and Discussion, Figure 3F resulted. It may be observed that amplitudes of up to 0.12 degrees are present. The limitations of the measurement system should be considered in evaluating the roller skew data presented in this report.

Load and Bearing Misalignment

A 4450 N (1000 lb) load was used throughout most of the investigation. This was applied to the test bearing by a cable loop over the test bearing as may be seen in Fig. 1a. The outer race protractor was positioned so that 0 (360) degrees was centered under the cable loop. As the derotation prism and camera viewed the protractors and bearing the protractor degree scale increased in a clockwise direction. Due to bearing clearance rollers entered the loaded zone at about 340° and left it at about 20°.

The misalignment of the outer race relative to the inner race was measured with a dial indicator on a bar bolted to the end of the test shaft. The bar was perpendicular to the shaft center line. Measurements were made by indicating on a machined surface of the test bearing housing. This machined surface of the housing was also perpendicular to the shaft center line when the zero misalignment cases were set up. What is referred to as positive misalignment in this report was produced by forcing the housing at 90° towards the prism and camera while simultaneously forcing the housing at 270° away from the prism and camera by turning nuts on studs extending from the test machine frame. Back-up nuts were kept tight to keep the housing positively positioned. The shaft was turned over by hand and indicator readings written down at 45° intervals over a shaft revolution. Nuts forcing misalignment and back-up nuts were readjusted until the desired misalignment condition was attained. Negative misalignment was produced in a similar fashion by using the nuts and studs at 90° and 270° to force the 90° housing location away from the prism and camera while forcing the 270° housing location towards the prism and camera.

By adjusting the nuts constraining the housing at 90 and 270 degrees the outer race was pivoted about an axis through 0 and 180 degrees on the outer race protractor. Misalignment was maximum at 90 and 270 degrees and minimum at 0 and 180 degrees. Rollers entered the loaded zone at

about 340 degrees with the misalignment decreasing, passed the most heavily loaded point at 0 degrees with the raceway surfaces most nearly parallel, and exited with roller to raceway contact force decreasing as the roller encountered increasingly non-parallel raceway surfaces.

While it had originally been proposed to study misalignment of 0, 0.25 and 0.50 degrees, a reversed misalignment of -0.50 degrees was added to the test program to determine the effect of a reversal of misalignment on roller skewing behavior and the measurement system.

Test Program and Data Organization

The chronological sequence of tests may be followed through the dates and film sequence numbers identifying films and data obtained from the films. Testing began with the 0.21 mm (0.0083 in.) clearance bearing with 0 degree misalignment with films being taken at 4000, 8000, and 12,000 rpm under the 4,450 N (1,000 lb) load. Table 2 lists data presented in the report, and summarizes the organization and figure identification system for the bearing clearance, misalignment, and speed cases studied.

As indicated in Table 2, Figures 4 through 7 are results obtained with the 0.18 mm (0.0073 in.) clearance bearing. Figures 4a, b, c are data at 0 degree misalignment and 4000, 8000, and 12,000 rpm. Figures 5a, b, c; 6a, b, c; and 7a, b, c are results at 0.25, 0.50, and -0.50 misalignment. As more than one roller orbit or revolution of the roller through the bearing could sometimes be read from the film taken for each of these figures a further number is added as 5b-1, 5b-2, to identify the revolution or reading of the film. Figures 8 through 11 show similar information for the 0.21 mm (0.0083 in.) clearance bearing.

Results and Discussion

To plot radial and tangential roller skew angle simultaneously on the same axes without overlap, the camera angle

of about 4.7 degrees was plotted along with the radial skew angle. The camera angle appears in the data photographs because the roller center is radially distant from the bearing-camera center line by the bearing pitch radius. Radial roller skew motions are superimposed on the camera angle.

A fast Fourier transform (FFT) program was used to estimate the frequency components of the data. The FFT program requires N equally spaced data points and N must be a power of 2. These data points were obtained by linearly interpolating 128 points over the 360 degrees of roller orbit measured in each film. Plots of tangential and radial skew angle amplitude absolute value (degrees) as a function of frequency are presented on pages facing the original data figures and are numbered with the original figure number followed by F. Phase (degrees) is also plotted.

Output from the FFT program was manipulated so that the amplitudes are the square root of the sum of the squares of the a_i and b_i coefficients of the Fourier series sine and cosine terms for each frequency. The phase angles are the arc tangent of the a_i/b_i coefficients. Fourier analysis figures are plotted so the first amplitude is the average value of the data in the original figure, the second amplitude is the amplitude of a sine function of 360 degree roller orbit period, the third amplitude is the amplitude of a sinusoid of two cycles in the 360 degrees of roller orbit, etc.

The average value of the radial skew data includes the camera angle. In order to make this point plot together with the other roller skew amplitudes of 0.4 degree or less, this first point was plotted at a tenth of its true value so that the first radial skew amplitude plotted at 0.47 degrees indicates an average radial skew plus camera angle of 4.7 degrees.

Figure 4a shows a result obtained with the 0.18 mm (0.0073 in.) clearance bearing at 0° misalignment and 4000 rpm. It was plotted from 202 frames taken every

1.8 degrees of roller position within its orbit. [illegible] any reading could be in error by as much as 0.4 [illegible] the errors are probably of the order of 0.04 degrees [illegible] indicated in the paragraphs on Film Measurement and Error Estimate. An average skew angle is evidently present along with amplitudes associated with a number of frequencies. Figure 4a and 4aF together indicate a tangential skew averaging -0.33° over the roller orbit, a one-cycle-per-orbit skew amplitude of 0.05°, a 2-cycle-per-orbit skew amplitude of 0.02°, a 3-cycle-per-orbit skew amplitude of 0.05°, a 4-cycle-per-orbit skew amplitude of 0.13°, an 8-cycle-per-orbit skew amplitude of 0 08°, and a 12-cycle-per-orbit skew amplitude of 0.28°. The radial skew plots indicate a camera angle plus average radial skew angle of 10 times 0.47 or 4.7°; 2, 3, 4, and 12-cycle-per-orbit amplitudes of 0.04, 0.03, 0.02, and 0.31°. In view of the 0.12° amplitude noted in repeated measurements on the same film frame described under Film Measurement and Error Estimation amplitudes less than 0.12 may not be significant.

The 12-cycle-per-roller-orbit frequency which appears strongly in all the data corresponds to the roller frequency as the ratio of outer raceway circumference to roller circumference is 12.42. This is the roller to cage speed ratio. This investigator has not been able to make use of information in the phase angle data.

Figures 4b, and 4c show the effect of increasing speed at 0° misalignment. The amplitude at 4 cycles per orbit continues to be evident in the tangential skew, and the sharp peak at 12 cycles that was evident in Figure 4a broadens to include 11 and 14 cycles.

Figures 5a, 5b-1, 5b-2, 5c-1, and 5c-2 are results at 0.25° misalignment. A radial skew amplitude of about 0.18° with a 1-cycle-per-roller-orbit frequency is evident in all of these Figures. Figures 5b-1, 5b-2, 5c-1 and 5c-2 show differences in consecutive revolutions. The amplitude associated with the roller frequency is up to 0.39° in

Figure 5a and extends from 11 to 15 cycles-per-roller-orbit with smaller amplitude in Fig. 5c-2.

Figures 6a, 6b, 6b-2, 6c-1, 6c-2, and 6c-3 show results with the bearing misaligned by 0.5°. The radial skew amplitude is 0.33 to 0.43° at one cycle per orbit. The original data plots resemble a negative sine function. Radial and tangential skew amplitudes associated with the roller frequency again appear to broaden in frequency extent as speed increases. It was not possible to read data beyond 320° in the second roller orbit for Fig. 6b-2, and a Fourier analysis was not obtained for this figure. Some lower frequency components appear consistently in the 3 roller orbits through the bearing that are followed through Figures 6c-1, -2, and -3.

Figures 7a-1, 7a-2, 7b-1, 7b-2, 7c-1, and 7c-2 show the result of a reversed misalignment of 0.5°. Radial skew amplitude are typically 0.47° at one cycle per orbit, and the original data plots resemble a positive sine function of one period per orbit. Comparing this one cycle per orbit information with the one cycle per orbit radial skew information in Figures 5 and 6, it seems that the one cycle per orbit radial skew is the misalignment of the outer race which is being followed by the roller. A noticeable amplitude in both radial and tangential skew at 4 cycles per orbit is present in a number of these figures. It was possible to follow 2 orbits at each of the 8000 and 12,000 rpm speed cases. There appear to be differences in roller behavior from orbit to orbit. Successive revolutions in Figure 7a-1 and 7a-2 differ as the amplitude of one cycle per orbit radial skew is more apparent in Figure 7a-2. As the outer ring circumference is not an integer multiple of the roller circumference, the roller may not enter the loaded zone with the same skew angles on successive revolutions.

Figure 8a, 8b, and 8c show results for the 0.21 mm (0.0083 in.) clearance bearing with 0° misalignment at the 4000, 8000, and 12,000 rpm speeds. There appears to be no significant amplitude at low frequencies, but a skewing amplitude of 0.19 to 0.26° at the 12 cycle per roller orbit frequency.

Figures 9a, 9b, and 9c show results for the larger clearance bearing with 0.25° misalignment. There is radial skew amplitude of 0.1 to 0.23° at one-cycle-per-roller orbit. Both tangential and radial skew amplitudes of 0.18 to 0.26° are present at the 12 cycles-per-roller orbit frequency. Some broadening of the 12 cycle appears as speed increases.

Figures 10a, 10b-1, 10b-2, 10c-1, 10c-2, 10c-3, and 10c-4 show the effect of 0.5° misalignment. A one-cycle-per-orbit amplitude ranging from 0.18 to 0.45° is present in radial skew angle with the original data again resembling minus sine function. A 12-cycle-per-orbit amplitude ranging from 0.12 to 0.36° is present. The 4000 rpm speed case has the highest amplitude and most sharply defined 12 cycle frequency. As speed increases the 12 cycle amplitude seems to decrease, and broadens to extend to lower frequencies. Figures 10b-1 and 10b-2 at 8000 rpm show some variation in consecutive revolutions. Figures 10c-1, 10c-2, 10c-3, 10c-4, 10c-5, and 10c-6 at 12,000 rpm further indicate differences from revolution to revolution.

Figures 11a, 11b-1, 11b-2, 11c-1, 11c-2, and 11c-3 show the result of a reversal of the 0.5° misalignment. Radial skew amplitudes of 0.39 to 0.55° appear at one-cycle-per-roller orbit with the original data again resembling a positive sine function. Tangential and radial skew amplitudes of 0.12 to 0.32° appear to be associated with the roller frequency. Figure 11a appears to indicate there may be a tangential and radial skew amplitude of 0.12° at 20-to 24-cycle-per-roller orbit frequency. This may be a 2 times a roller revolution skewing behavior that could be seen only in 4000 rpm speed studies as the camera frame rate gives data at about 2, 4, and 6 degrees of roller orbit at 4000, 8000, and 12,000 rpm shaft speeds. This limits the frequencies

observable in the data. This frequency does not appear as prominently in other 4000 rpm speed cases. Data from consecutive revolutions again appears to differ slightly. Figures 11c-2, and 11c-3 show the effect of missing frames over 90 to 160° of roller orbit. The film was not measureable over this sector of the bearing, but could provide information over the rest of the roller orbit. The missing frames are interpolated as a straight line in the FFT program which makes the frequency analysis information difficult to evaluate.

Conclusion

Radial skew amplitudes of 0.4 to 0.5° at the roller orbit frequency were observed with 0.5° bearing misalignment. Radial and tangential skew amplitudes of 0.4° associated with the roller frequency were observed. These generally decreased in amplitude and extended in frequency at higher speeds. The 0.21 mm (0.0083 in.) larger clearance bearing generally had slightly smaller roller skew amplitudes than the 0.18 mm (0.0073 in.) clearance bearing. Differences in roller skewing are apparent in successive orbits of the roller.

Further work which should be undertaken is the investigation of roller skewing with misalignment oriented so that the loaded zone of the bearing includes raceway surfaces of maximum misalignment.

References

1. Savage, M. and Loewenthal, S.H., "Kinematic Stability of Roller Pairs in Free-Rolling Contact", NASA Technical Note D-8146, 1976.

2. Savage, M. and Pinkston, B.H., "Roller Bearing Geometry Design", NASA CR-135082, October 1976.

3. Greby, D.F., "What Turbine Technology Is Teaching Us About High-Speed Roller Bearings", Machine Design, April 30, 1970, pp 229-234.

4. Signer, H.R., "Experimental Ball Bearing Dynamics Study", NASA CR-134528, October 1973.

5. Nypan, L.J., "Ball to Separator Contact Forces in Angular Contact Ball Bearings Under Thrust and Radial Loads", NASA CR-2976, April 1978.

6. Nypan, L.J., "Roller to Separator Contact Forces and Cage to Shaft Speed Ratios in Roller Bearings", NASA CR-3048, September 1978.

7. Nypan, L.J., "Measurement of Separator Contact Forces in Ball Bearings Using a Derotation Prism", Journal of Lubrication Technology, Trans. ASME, Series F, Vol. 101, No. 2, April 1979, pp. 180-189.

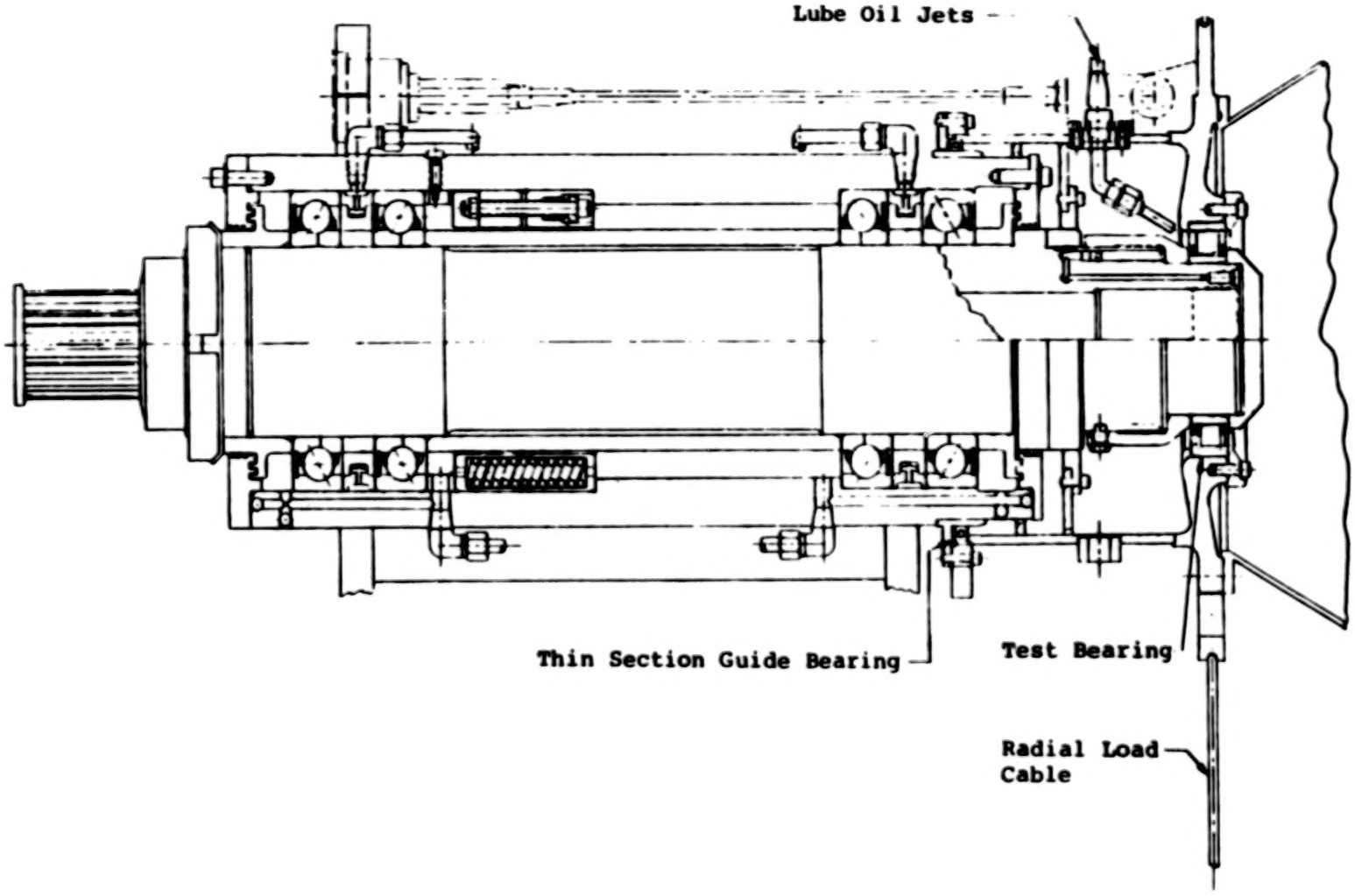

Figure 1a Schematic of Shaft Assembly

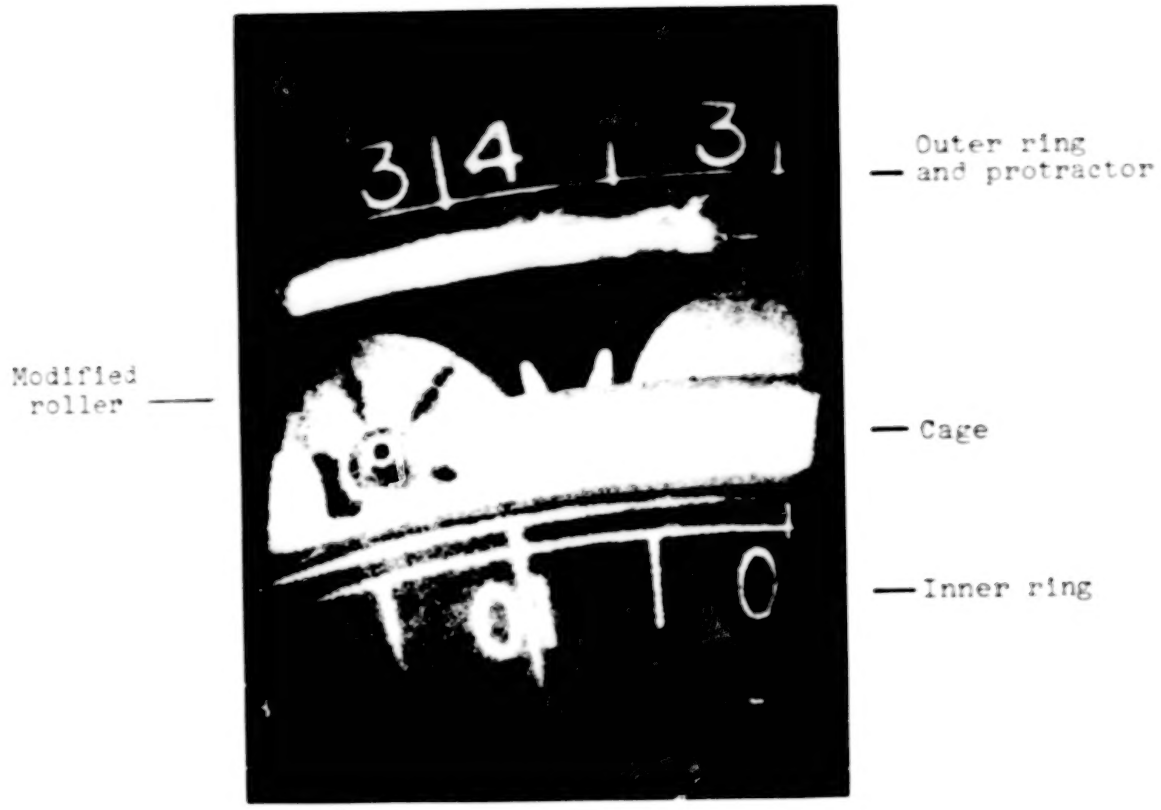

Figure 1b Enlargement of Data Photograph

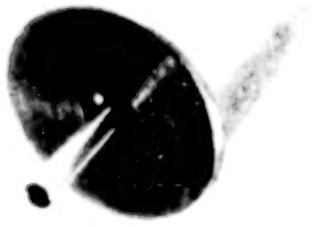

Figure 2 Modified Roller

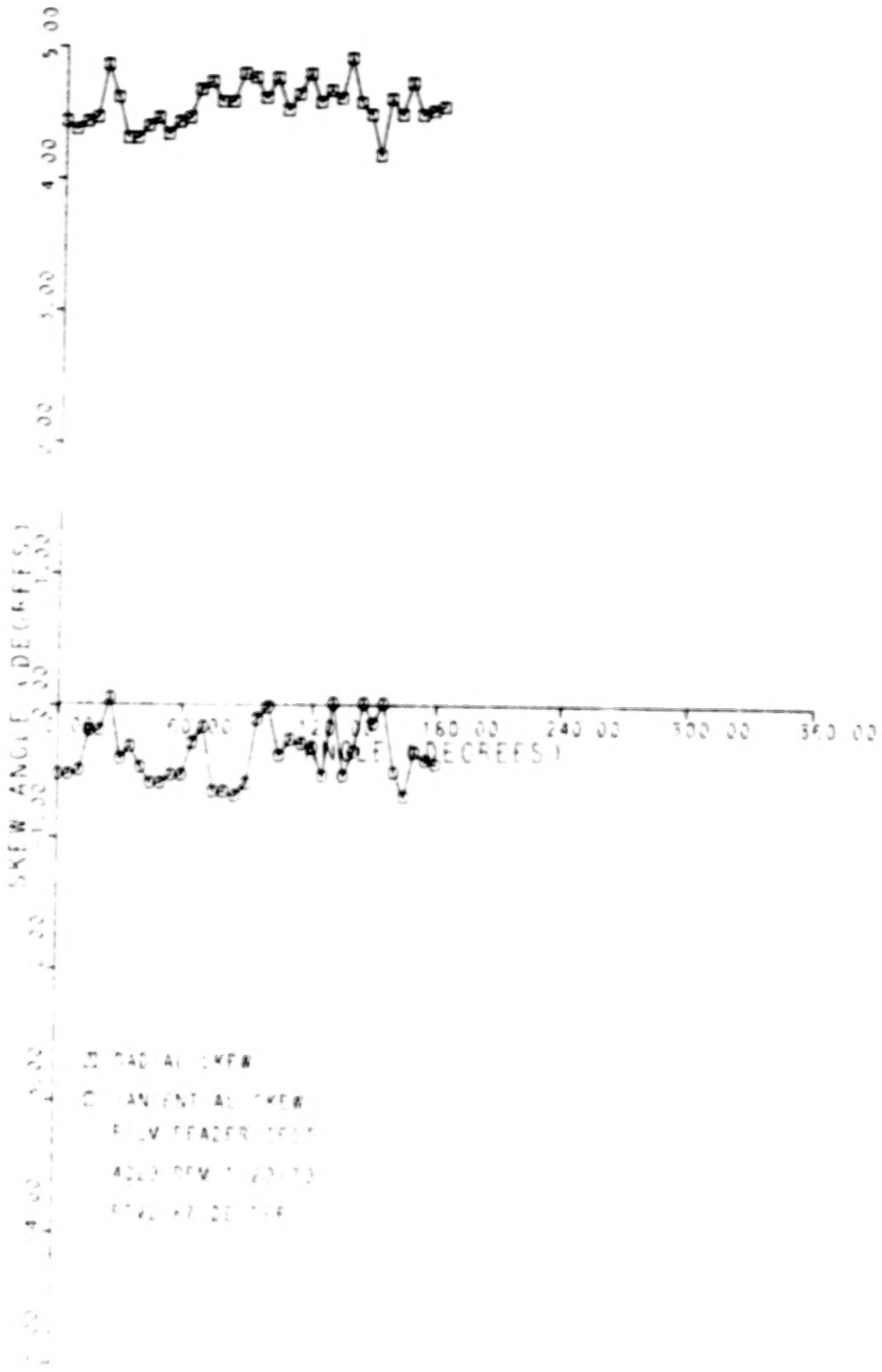

Figure 3 Variability in Skew Angle
Due to Film Measurement

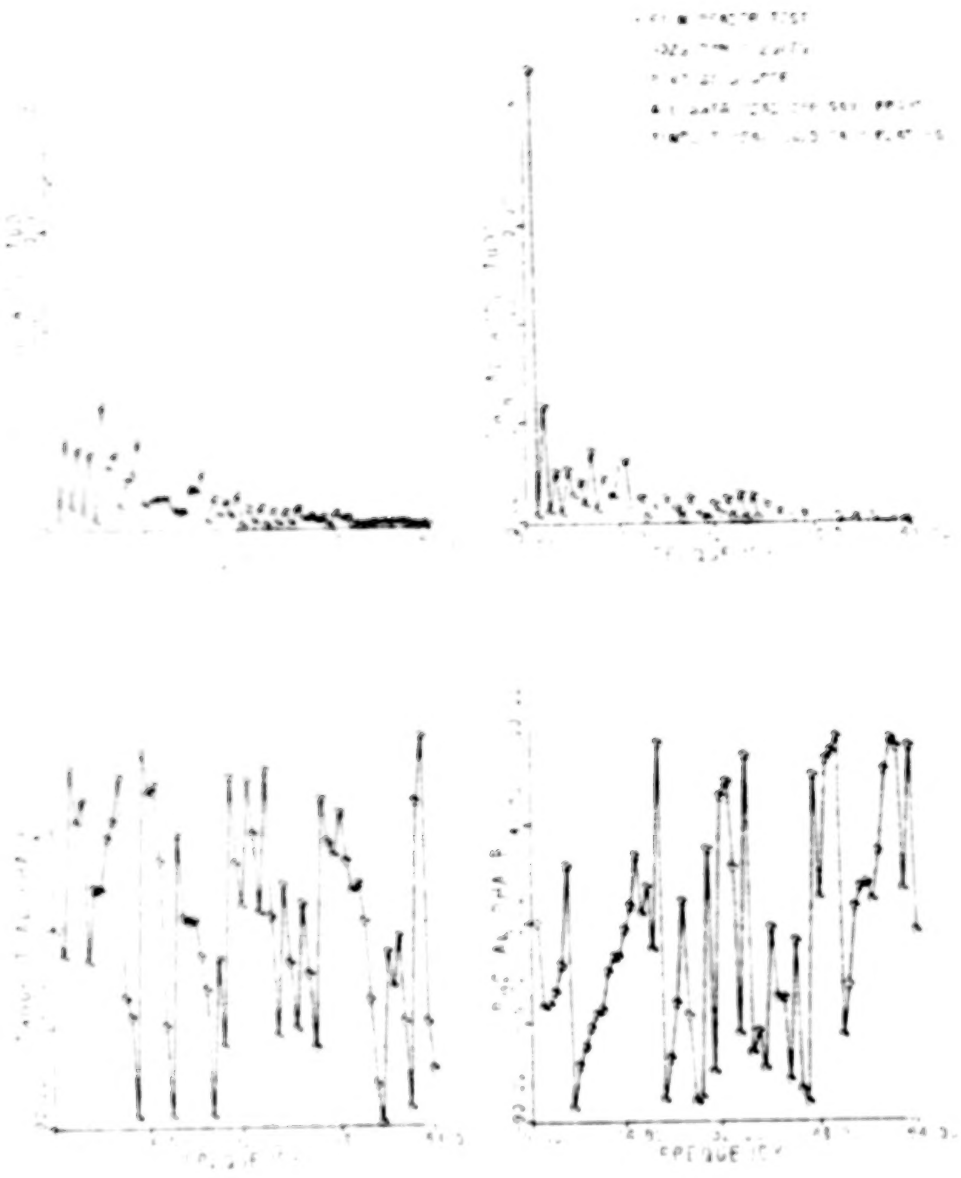

Figure 3F Fast Fourier Transform of Data in Figure 3

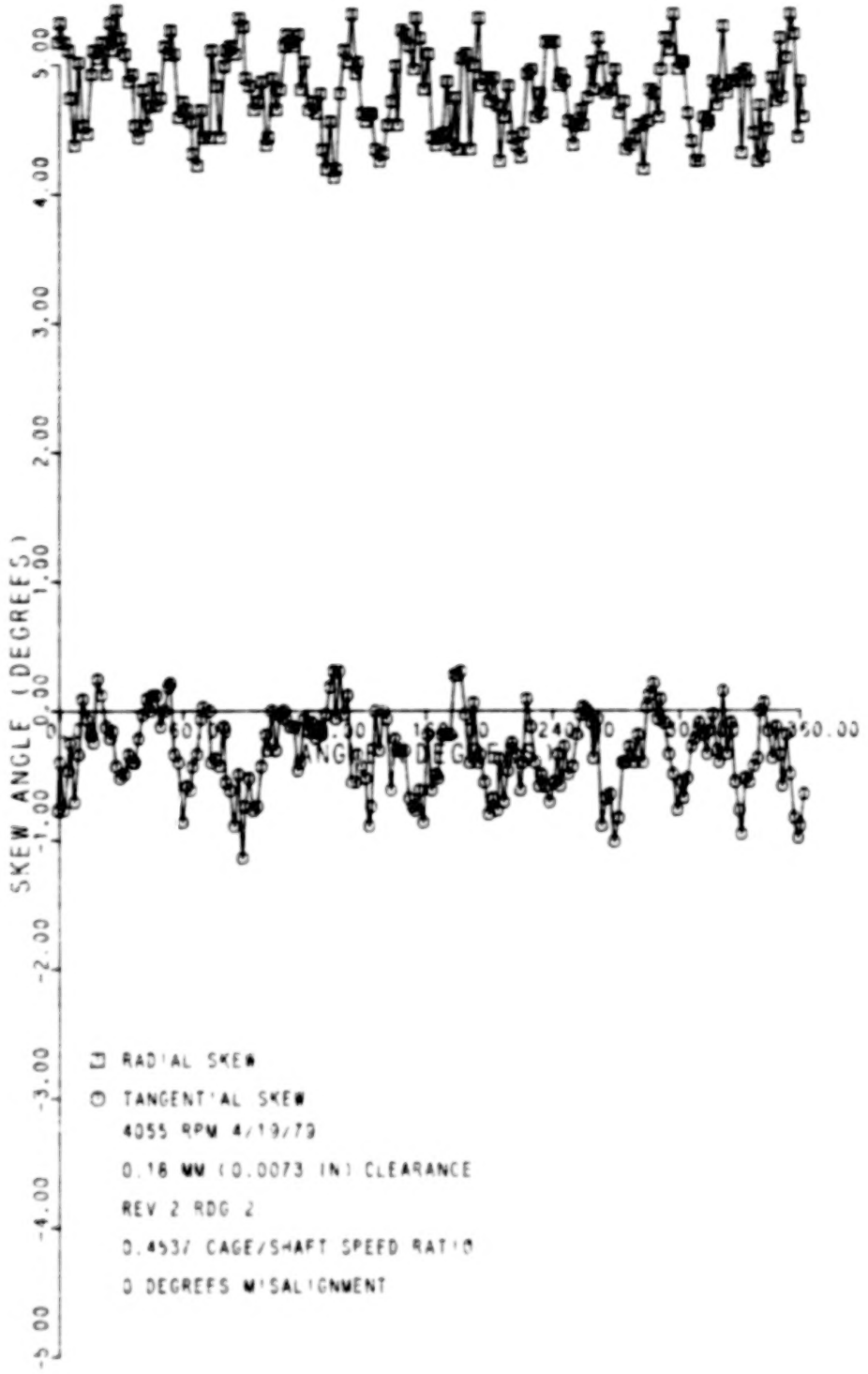

Figure 4a Roller Skew, 0.18 mm Clearance Bearing, 0^{o} Misalignment

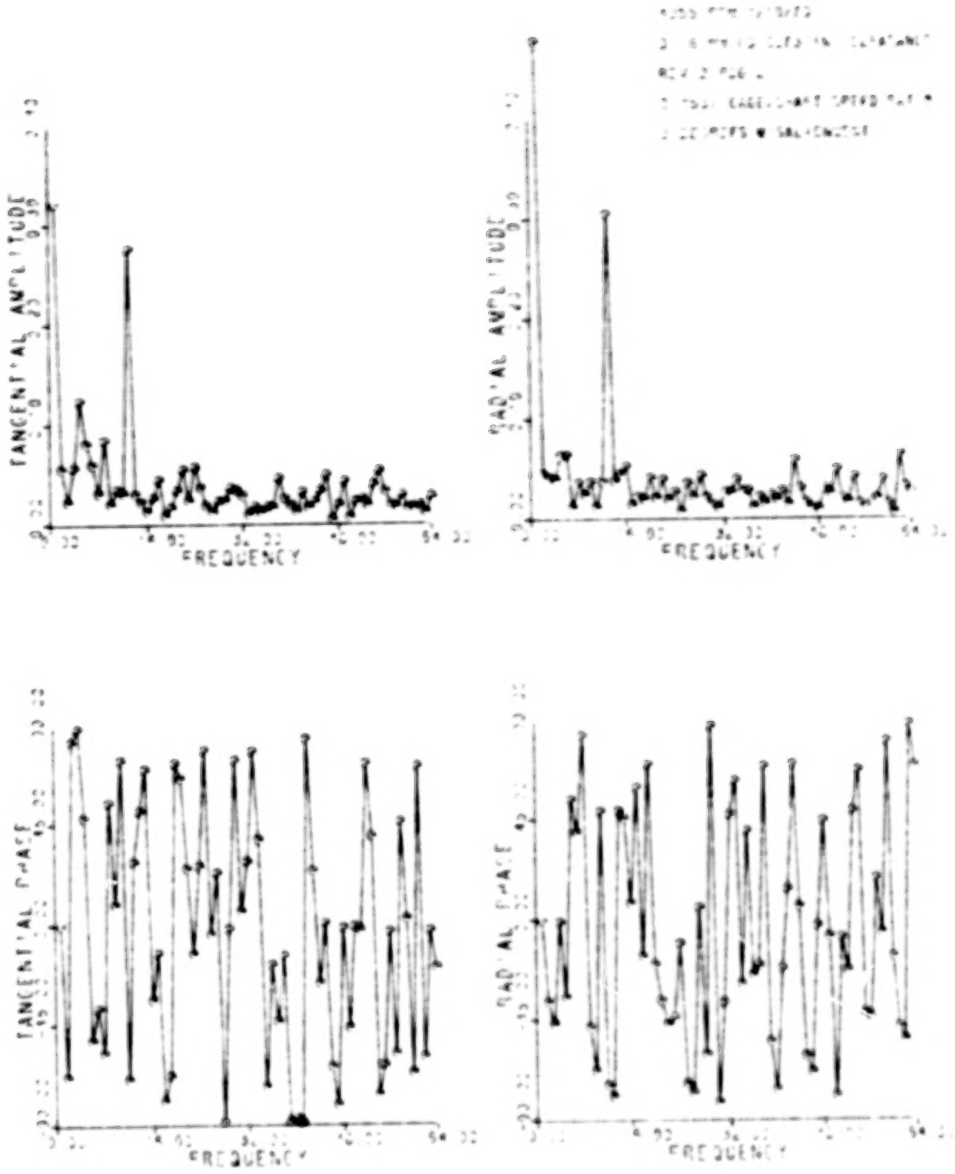

Figure 4aF Fast Fourier Transform of Data in Figure 4a

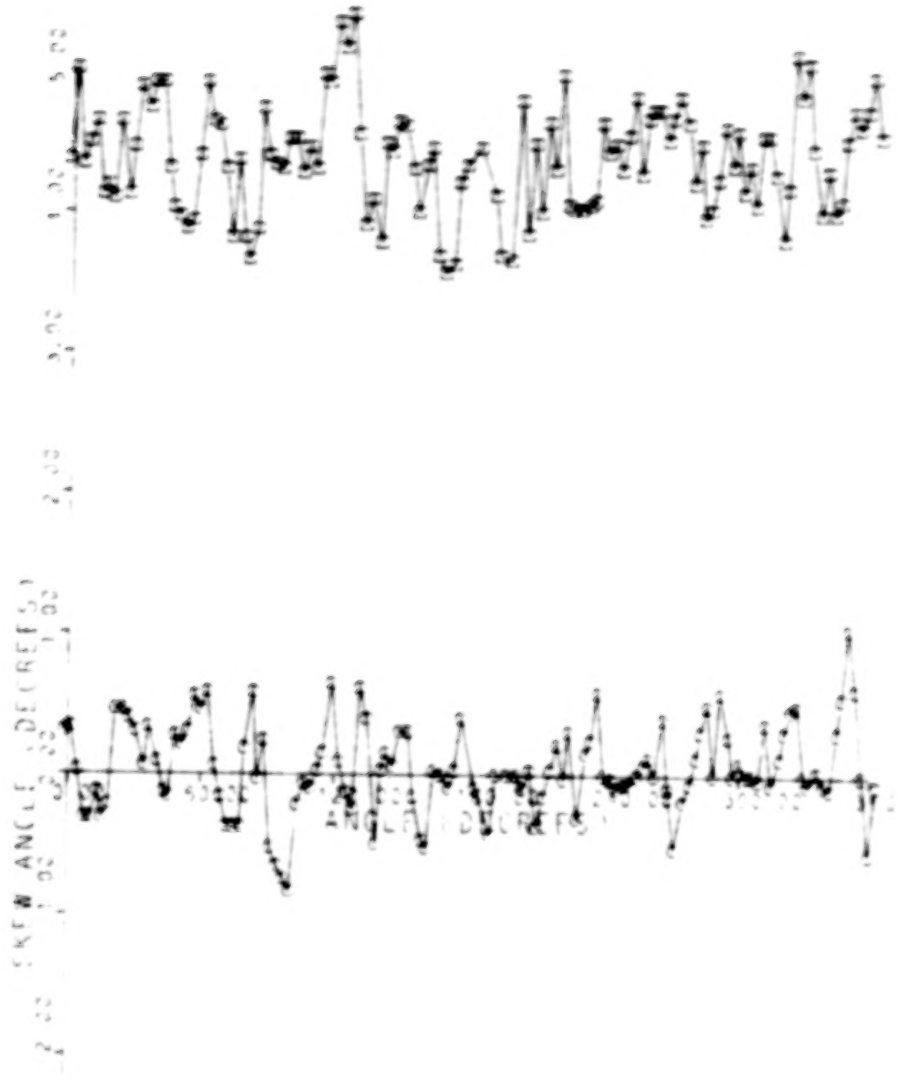

Figure 4b Roller Skew, 0.18 mm Clearance
, Bearing 0° Misalignment

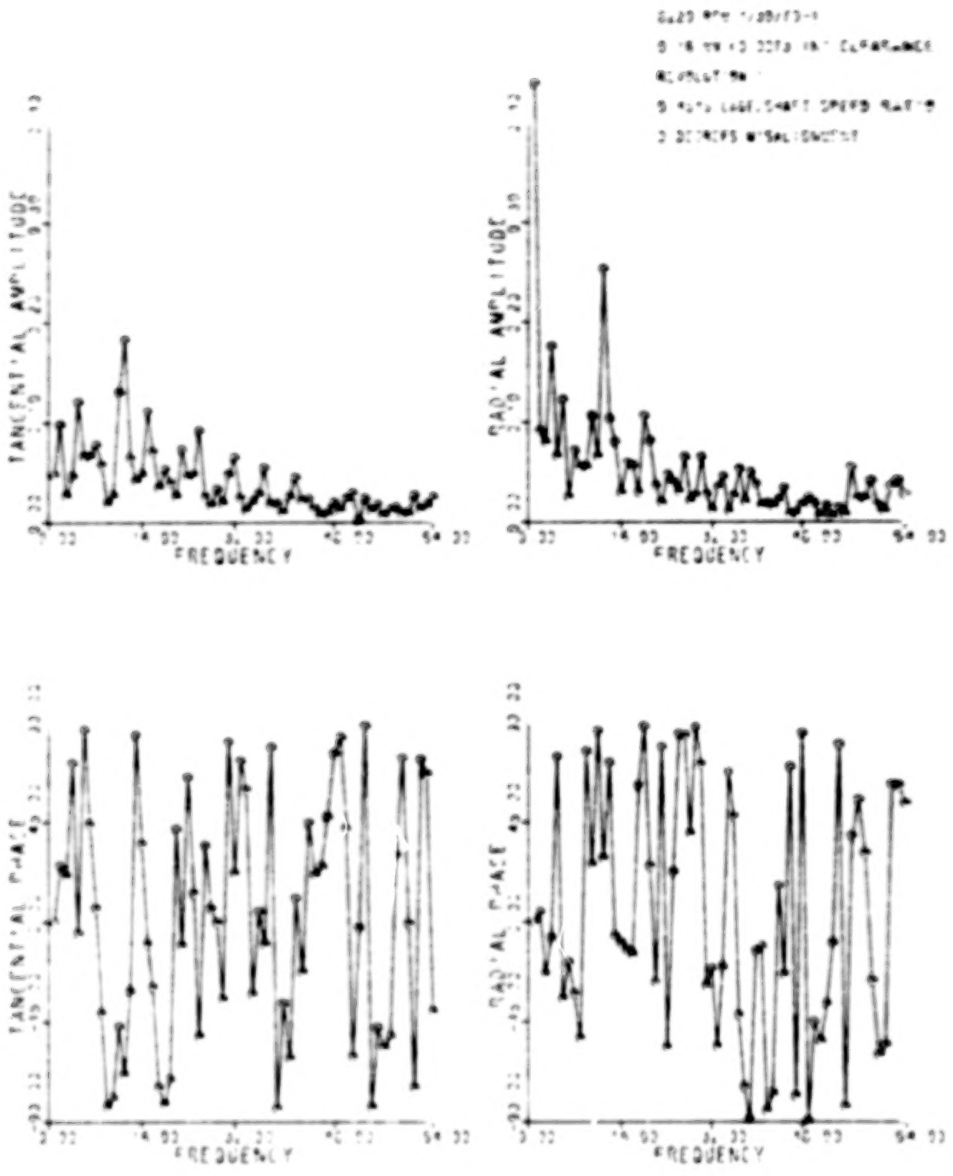

Figure 4bF Fast Fourier Transform of Data in Figure 4b

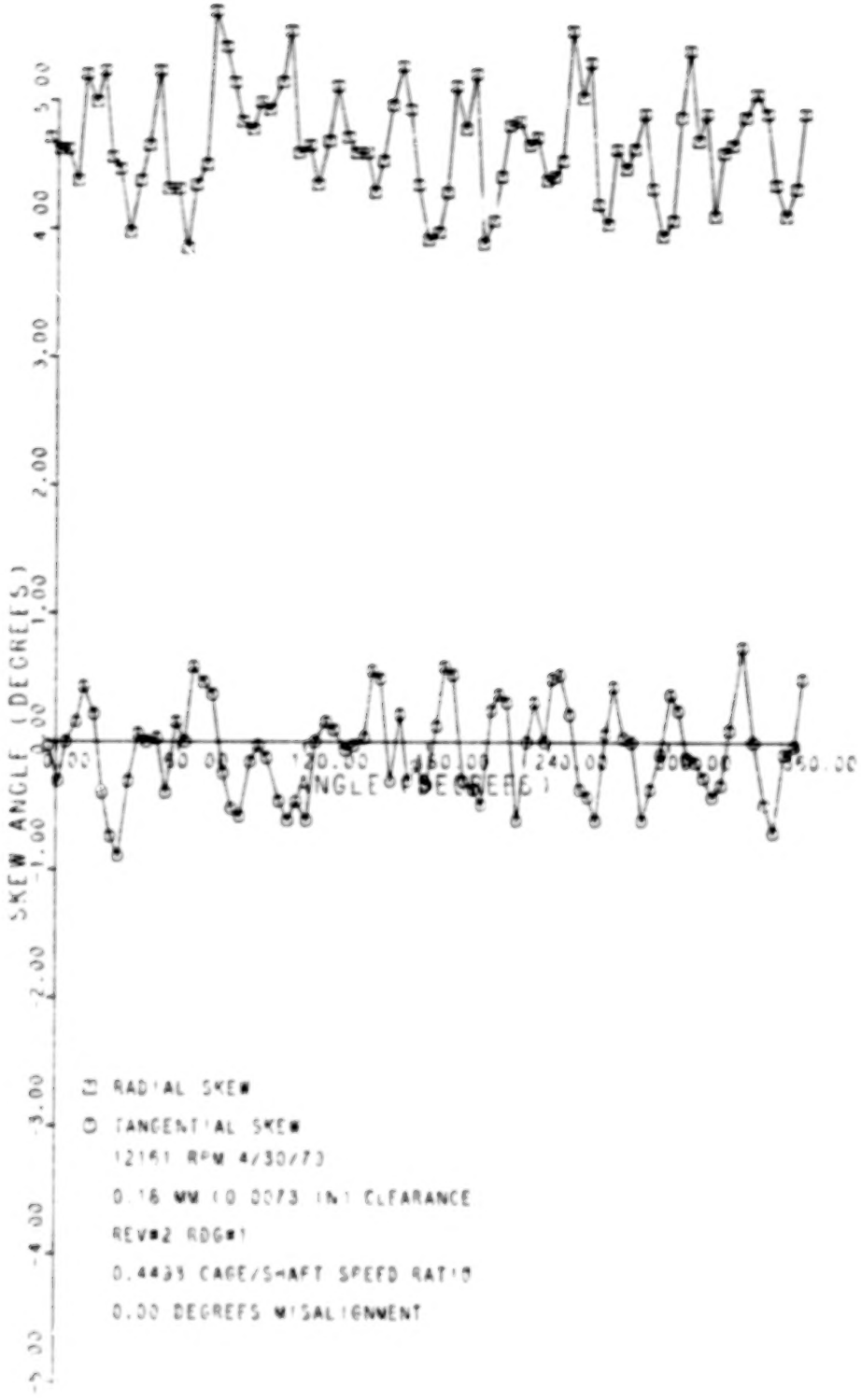

Figure 4c Roller Skew, 0.18 mm Clearance Bearing, 0° Misalignment

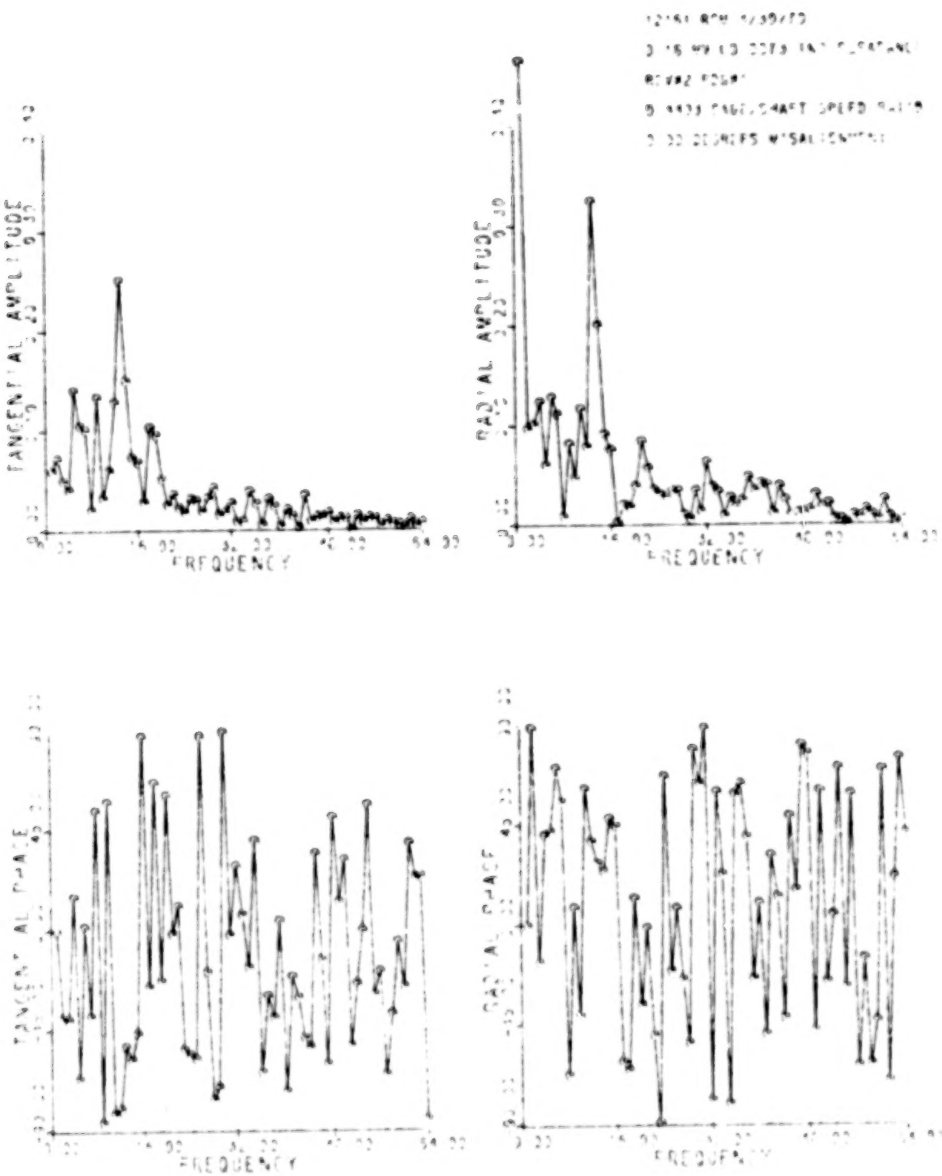

Figure 4cF Fast Fourier Transform of Data in Figure 4c

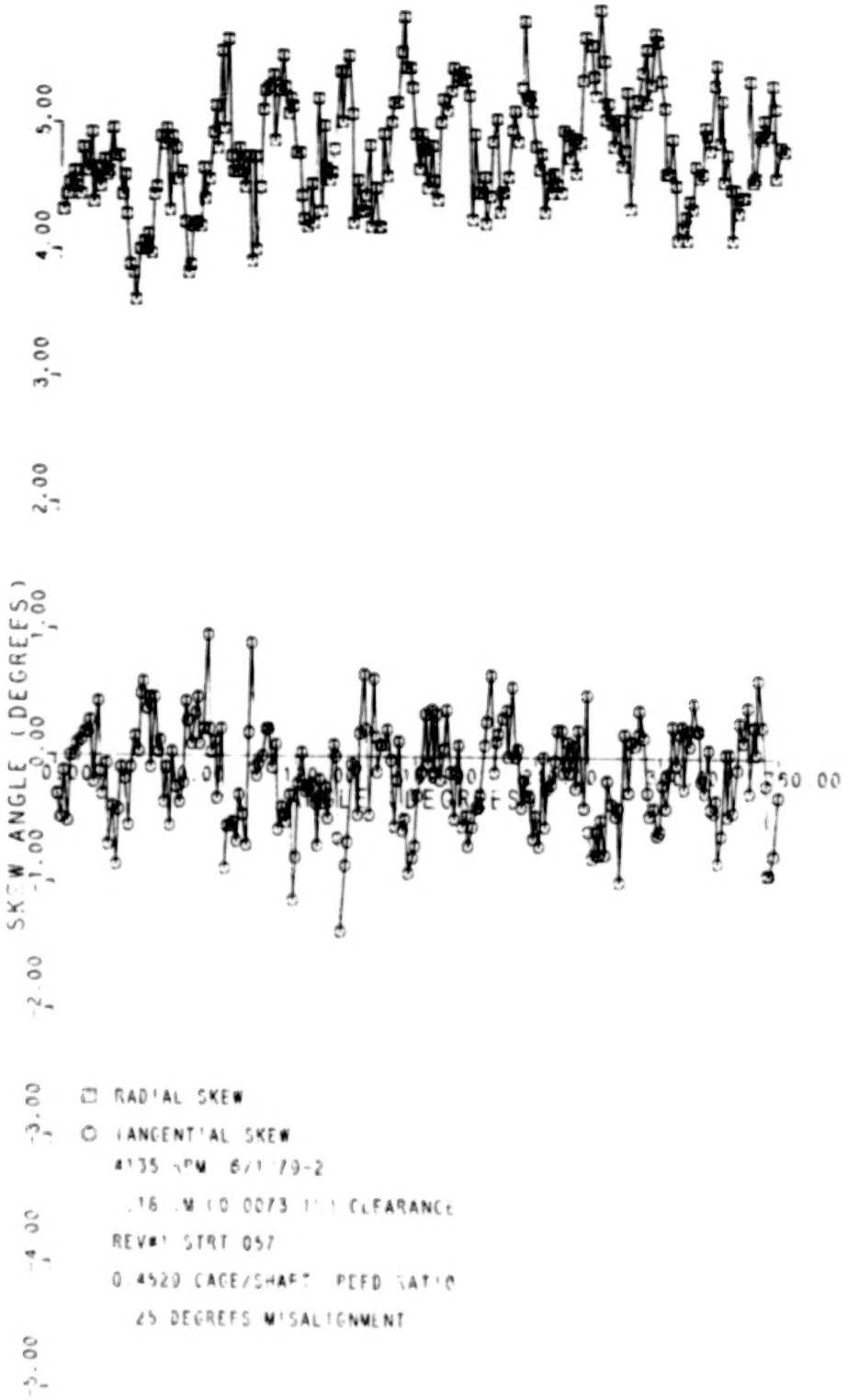

Figure 5a Roller Skew, 0.18 mm Clearance Bearing, 0.25° Misalignment

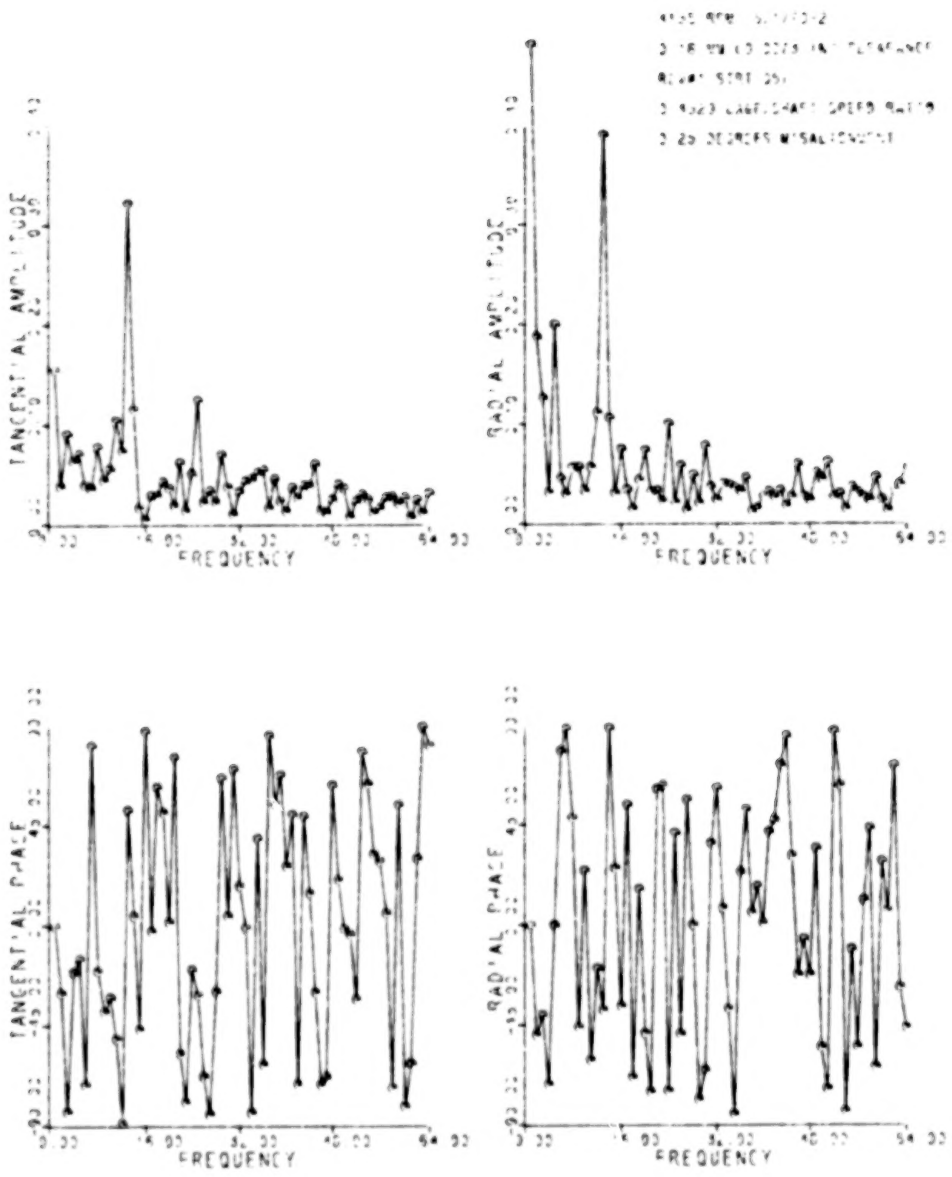

Figure 5aF Fast Fourier Transform of Data in Figure 5a

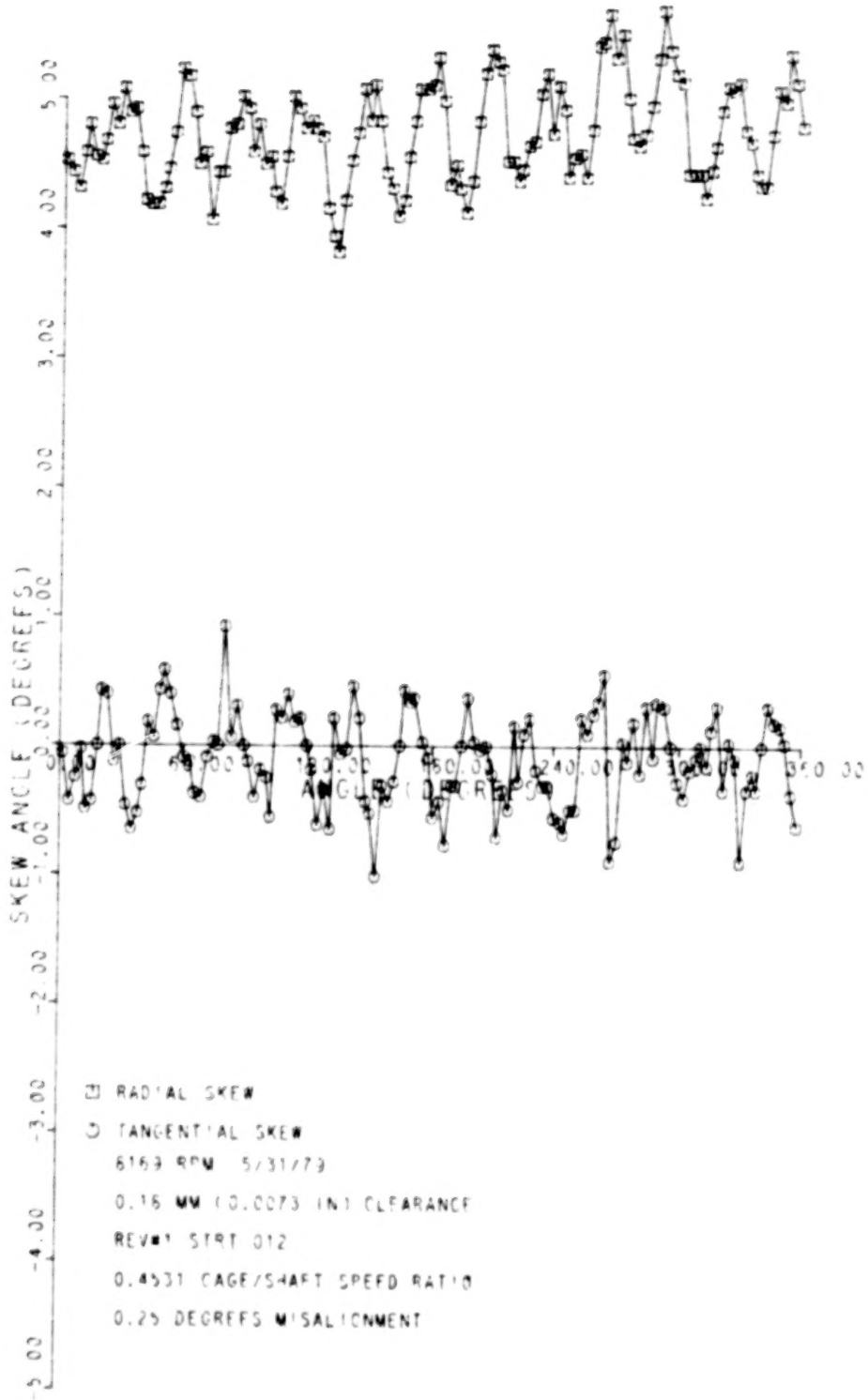

Figure 5b-1 Roller Skew, 0.18 mm Clearance Bearing, 0.25° Misalignment

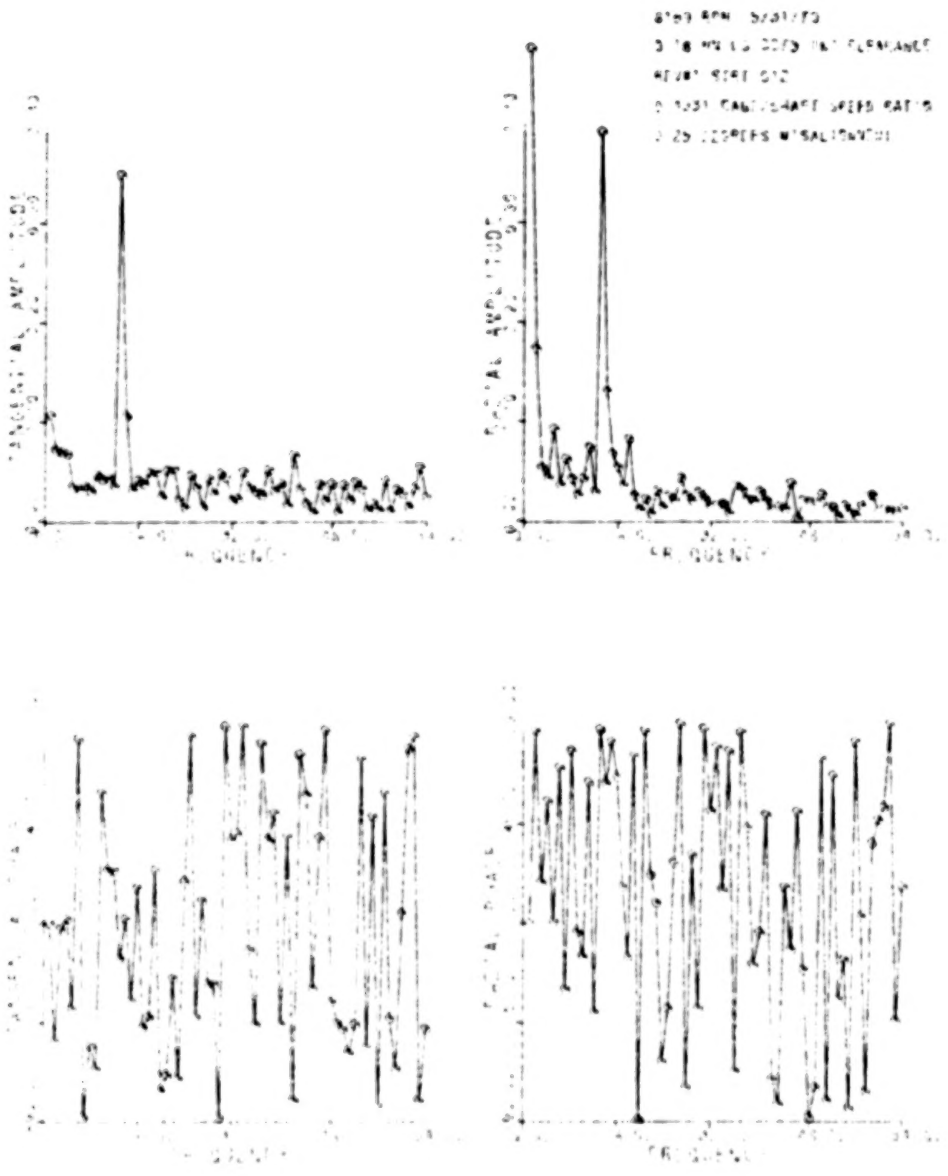

Figure 5b-1F Fast Fourier Transform of Data in Figure 5b-1

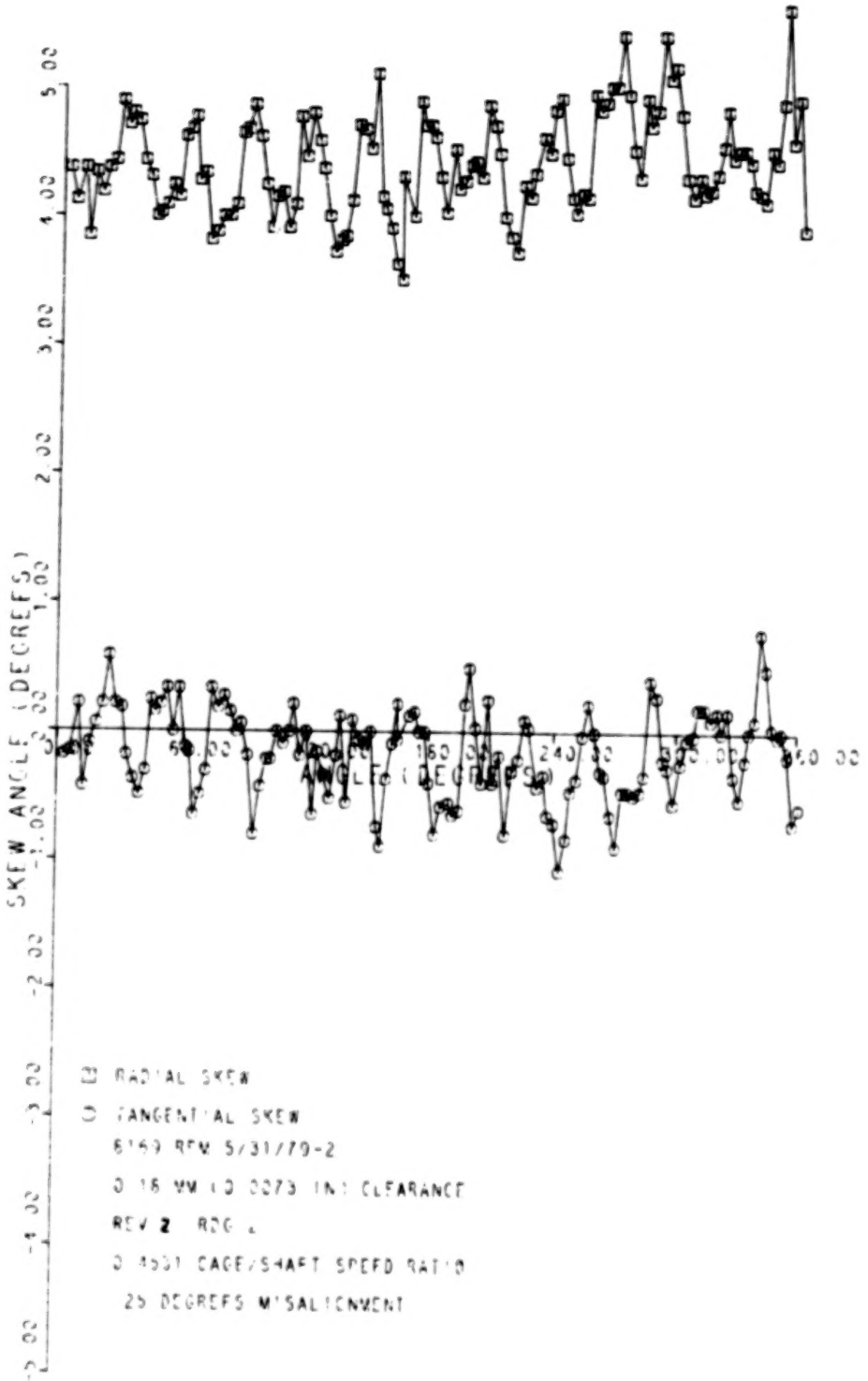

Figure 5b-2 Roller Skew, 0.18 mm Clearance Bearing, 0.25° Misalignment

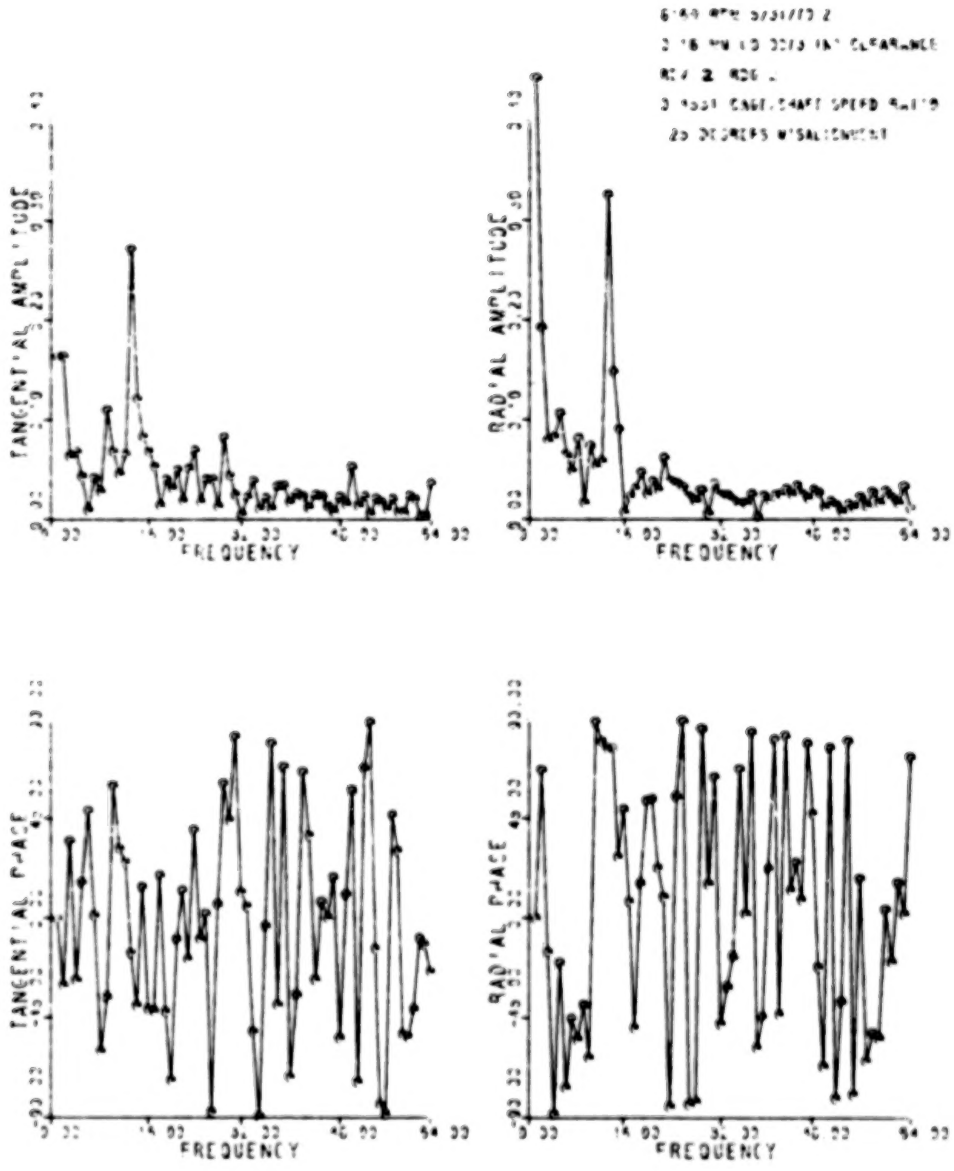

Figure 5b-2F Fast Fourier Transform of Data in Figure 5b-2

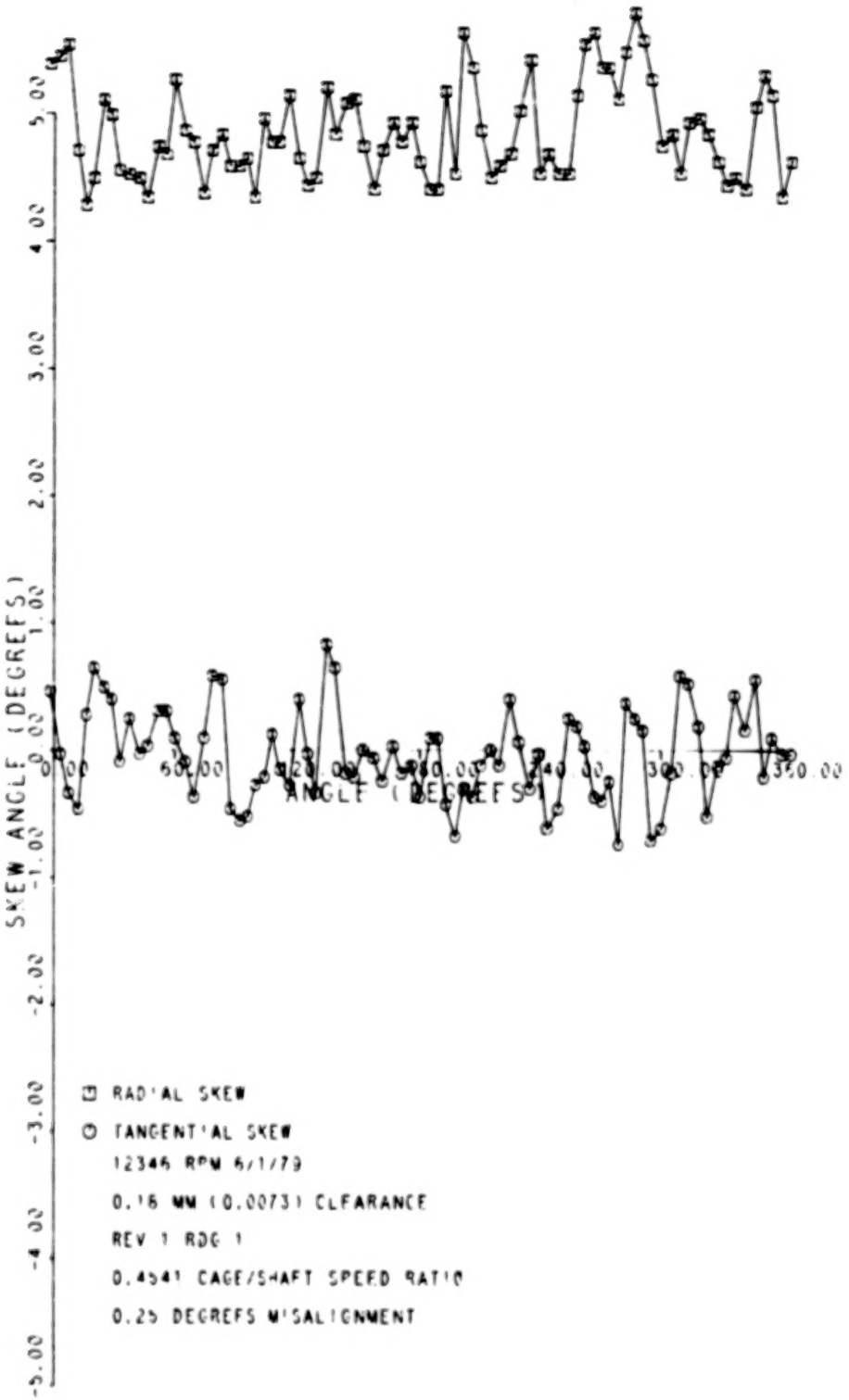

Figure 5c-1 Roller Skew, 0.18 mm Clearance Bearing, 0.25° Misalignment

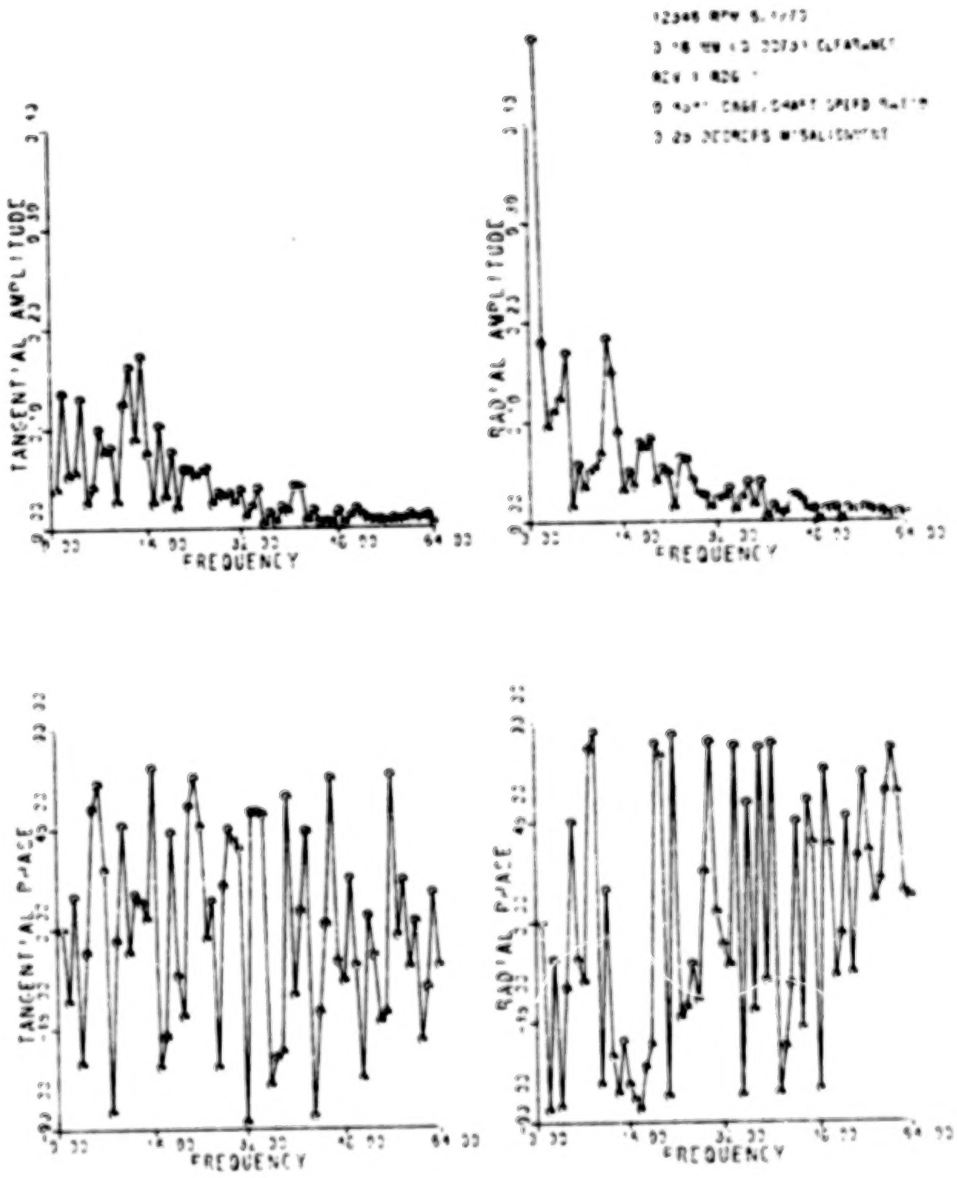

Figure 5c-1F Fast Fourier Transform of Data in Figure 5c-1

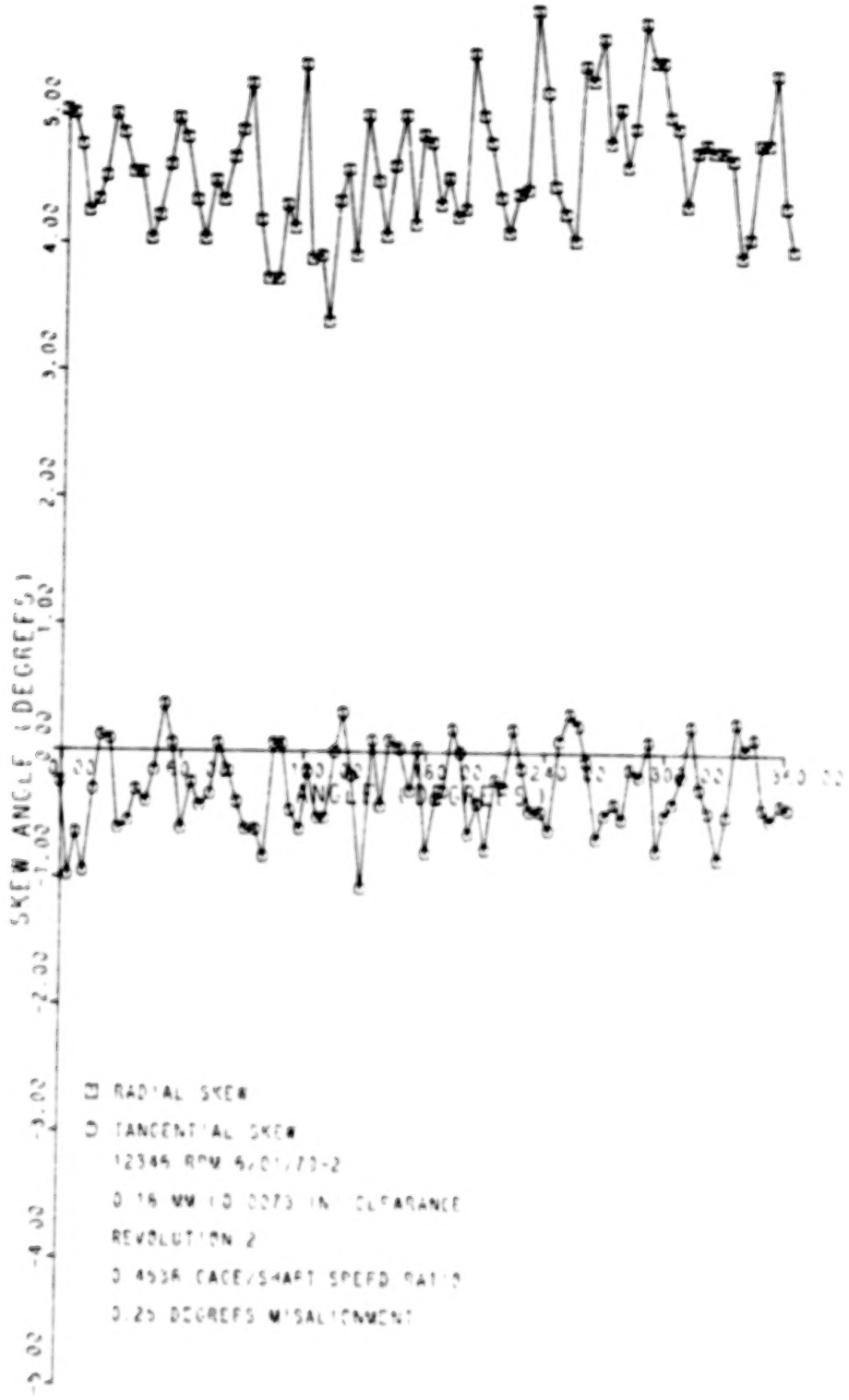

Figure 5c-2 Roller Skew, 0.18 mm Clearance Bearing, 0.25° Misalignment

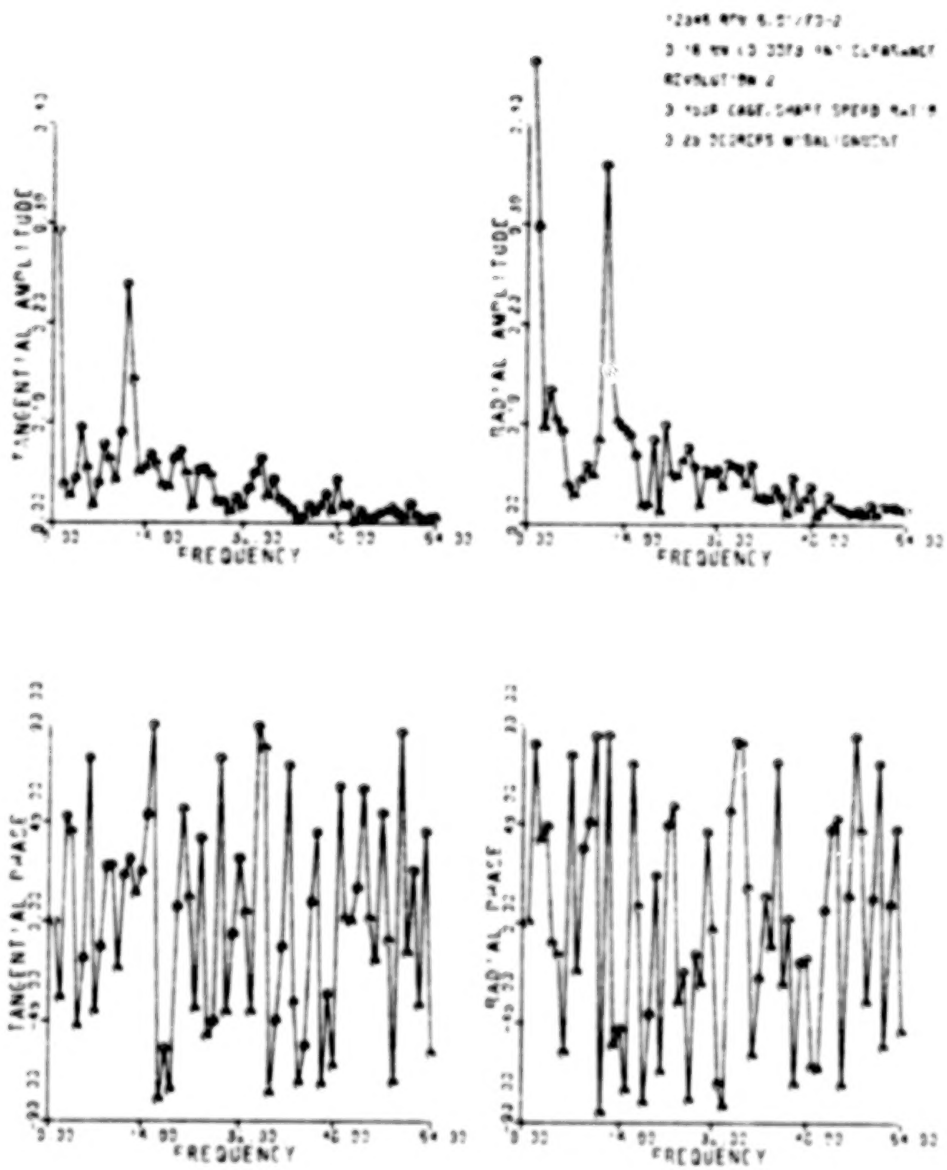

Figure 5c-2F Fast Fourier Transform of Data in Figure 5c-2

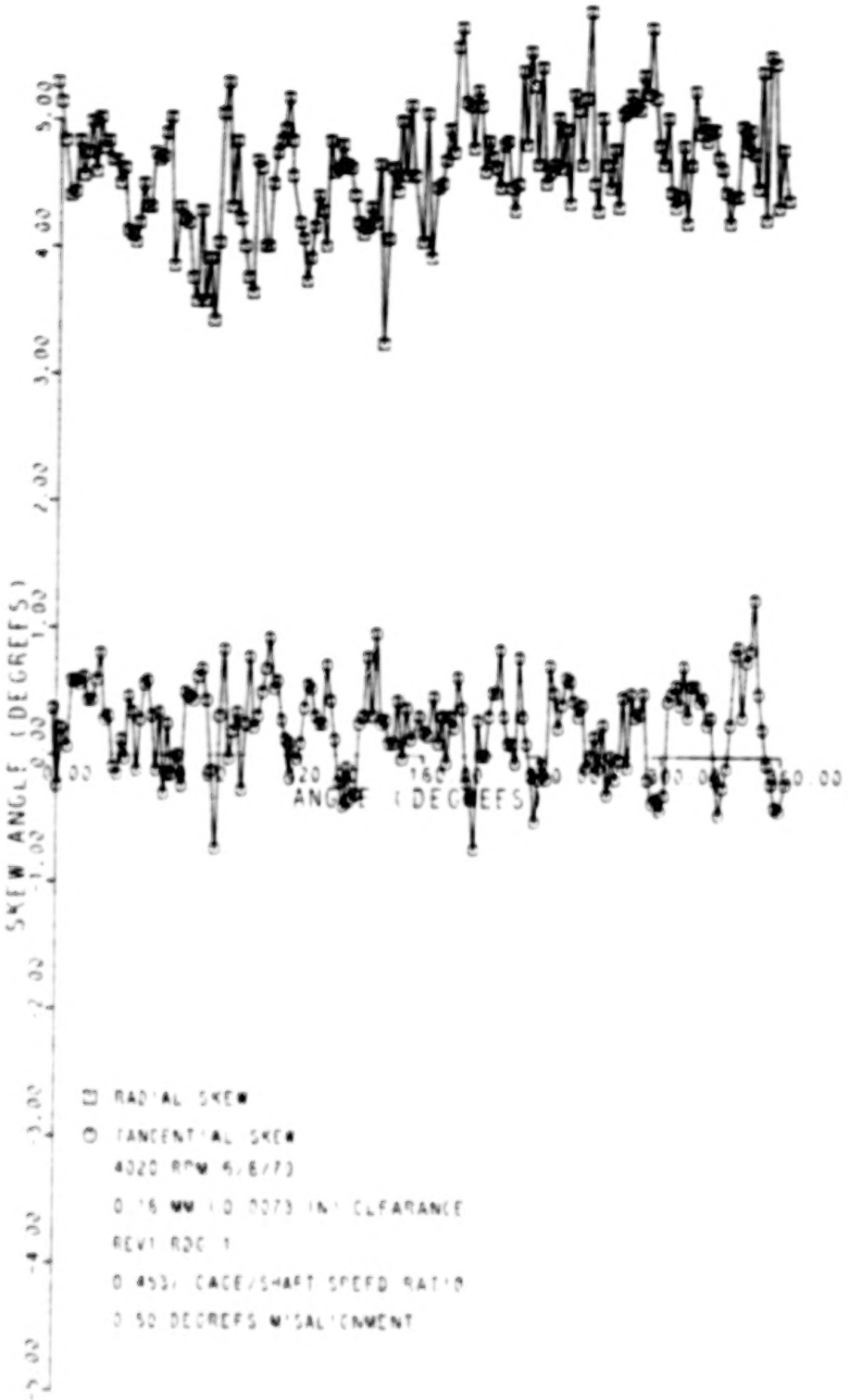

Figure 6a Roller Skew, 0.18 mm Clearance Bearing, 0.50° Misalignment

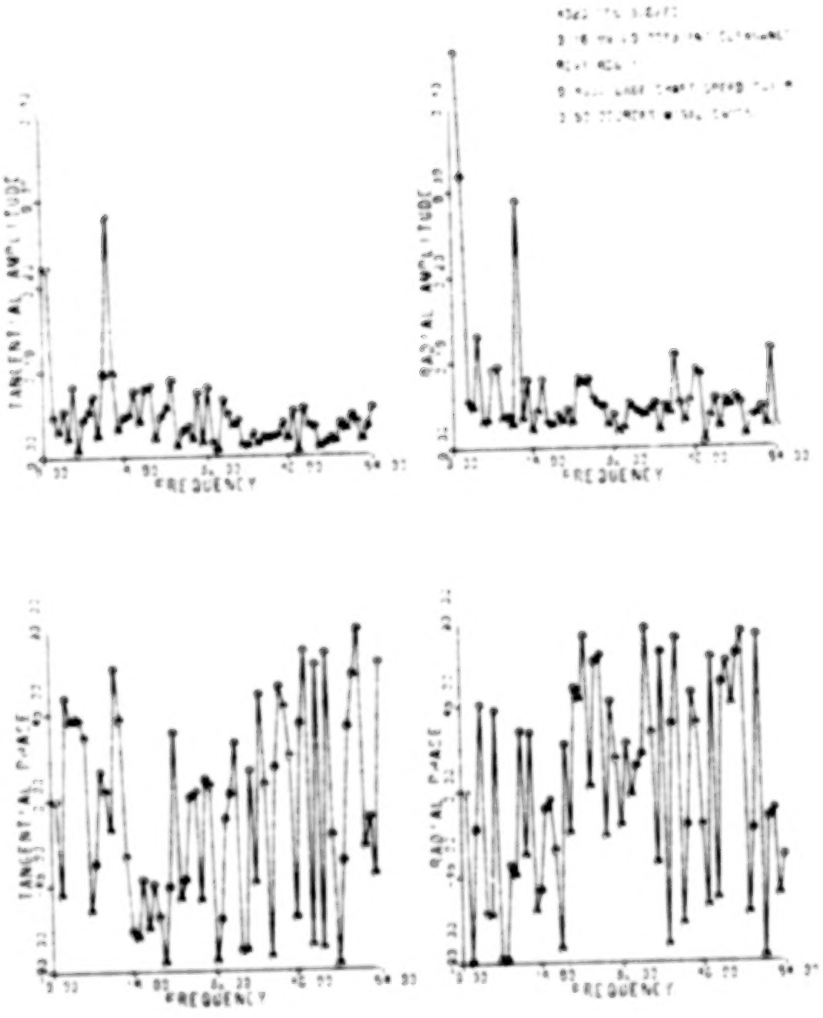

Figure 6aF Fast Fourier Transform of Data in Figure 6a

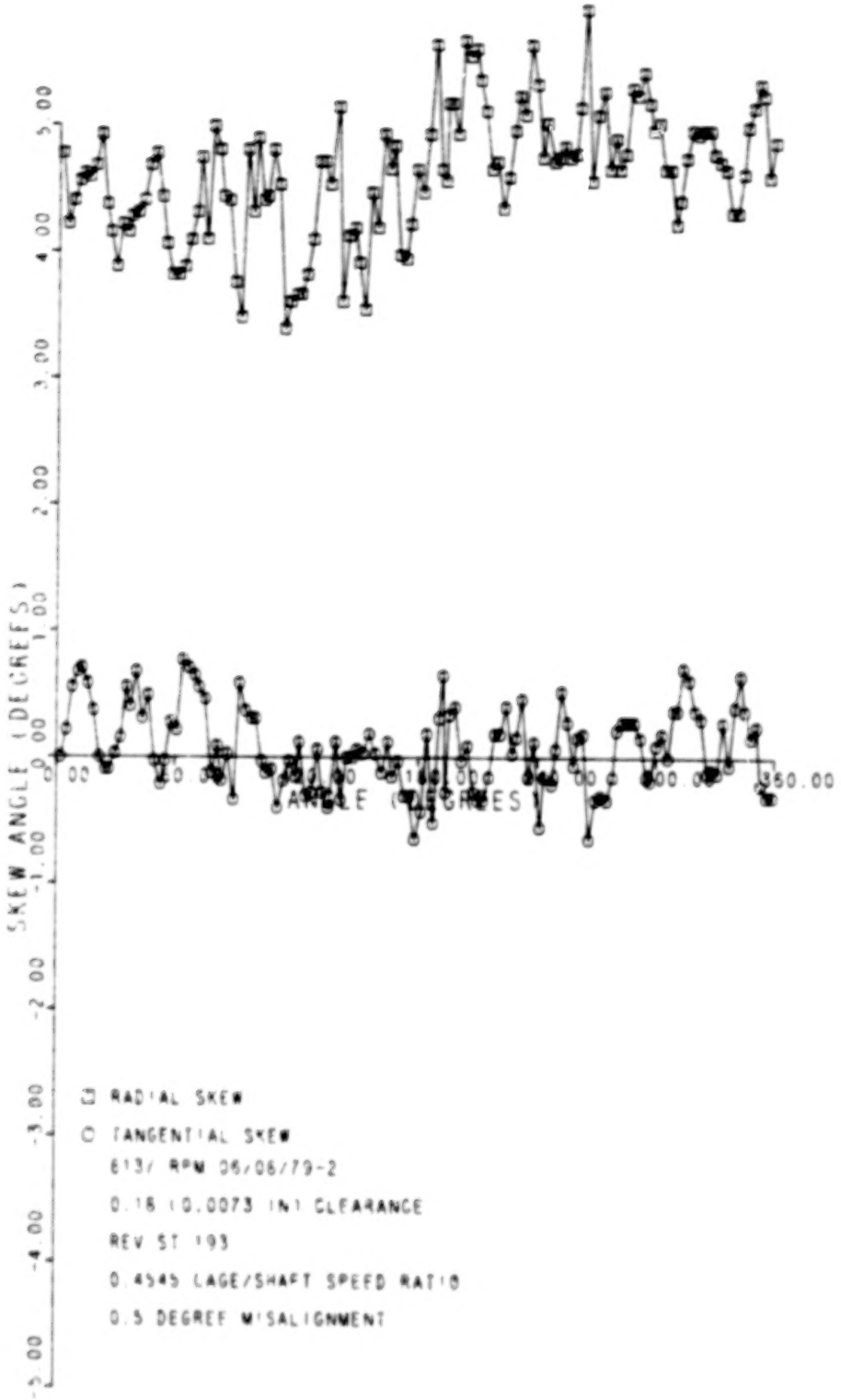

Figure 6b-1 Roller Skew, 0.18 mm Clearance Bearing, 0.50° Misalignment

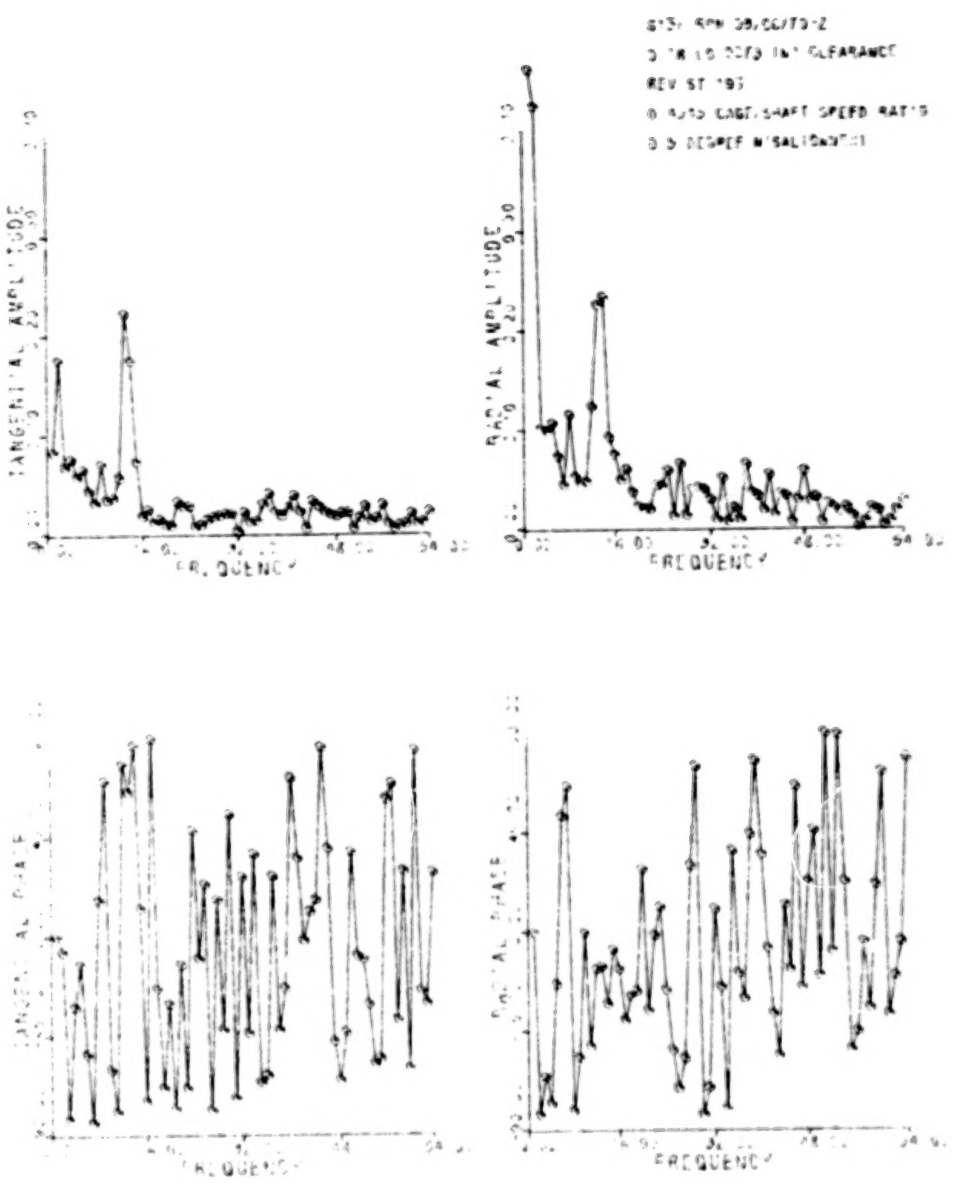

Figure 6b-1F Fast Fourier Transform of Data in Figure 6b-1

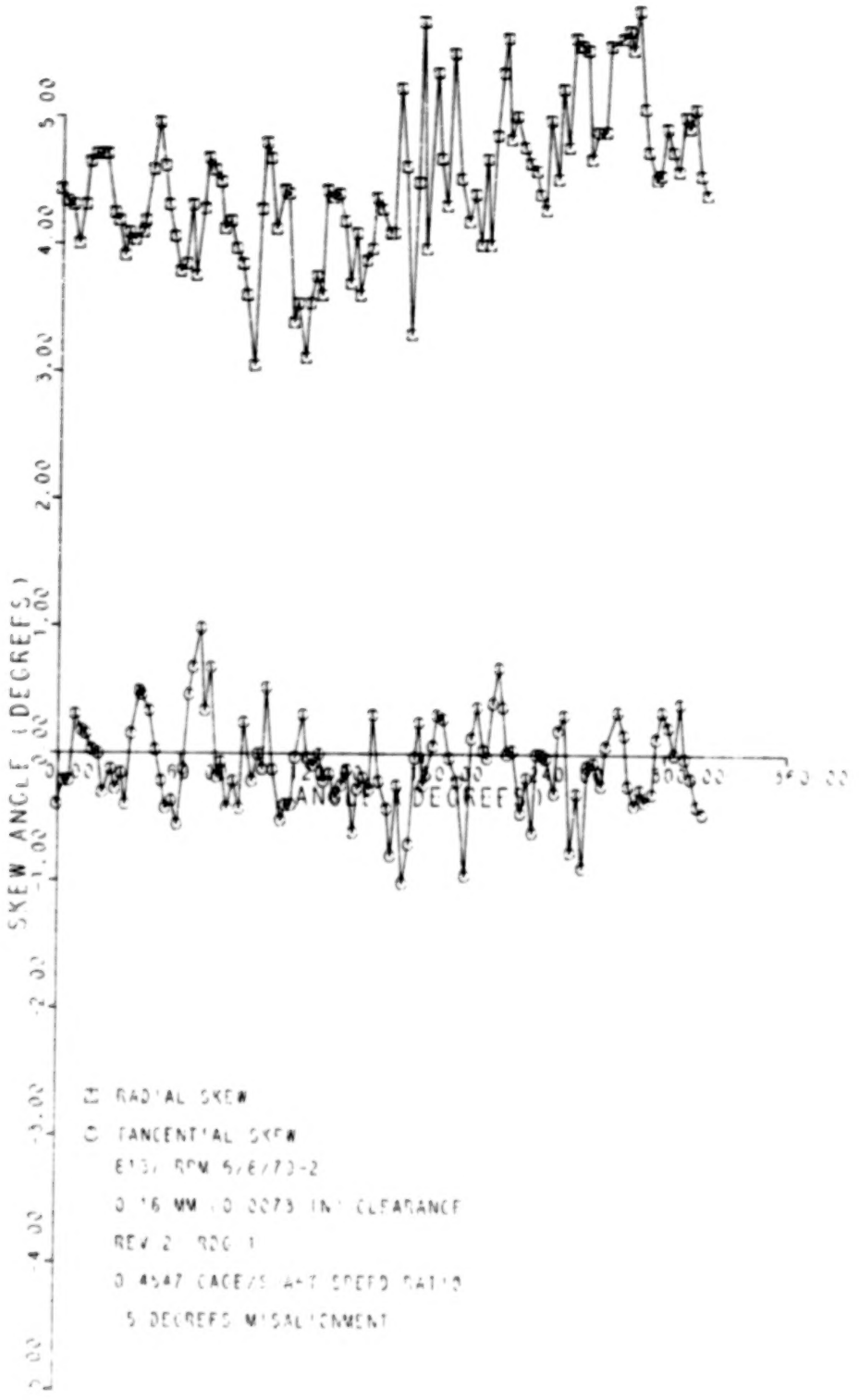

Figure 6b-2 Roller Skew, 0.18 mm Clearance Bearing, 0.50° Misalignment

Fourier Plot not possible as data

does not cover 360^{o}

Figure 6b-2F

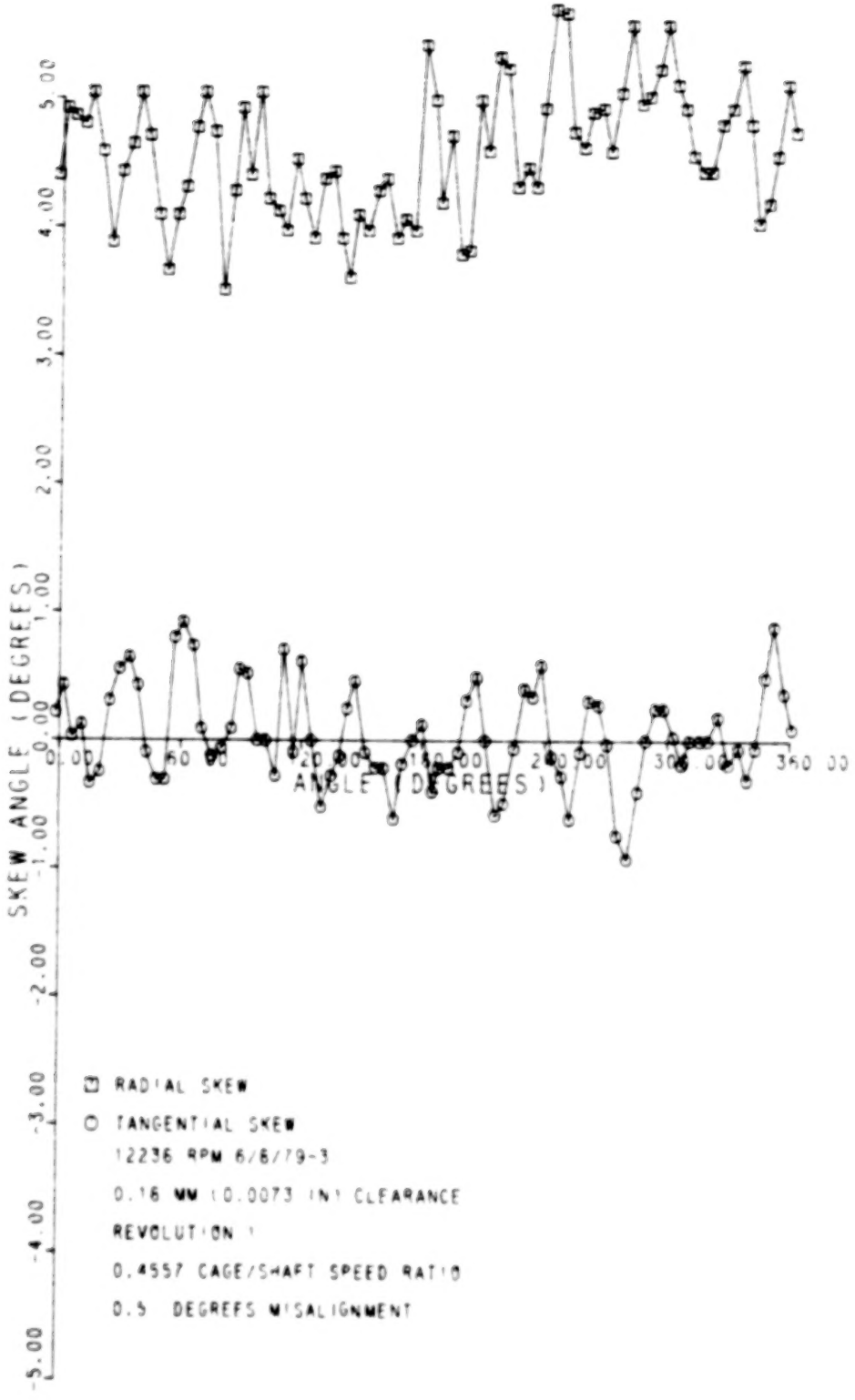

Figure 6c-1 Roller Skew, 0.18 mm Clearance Bearing, 0.50° Misalignment

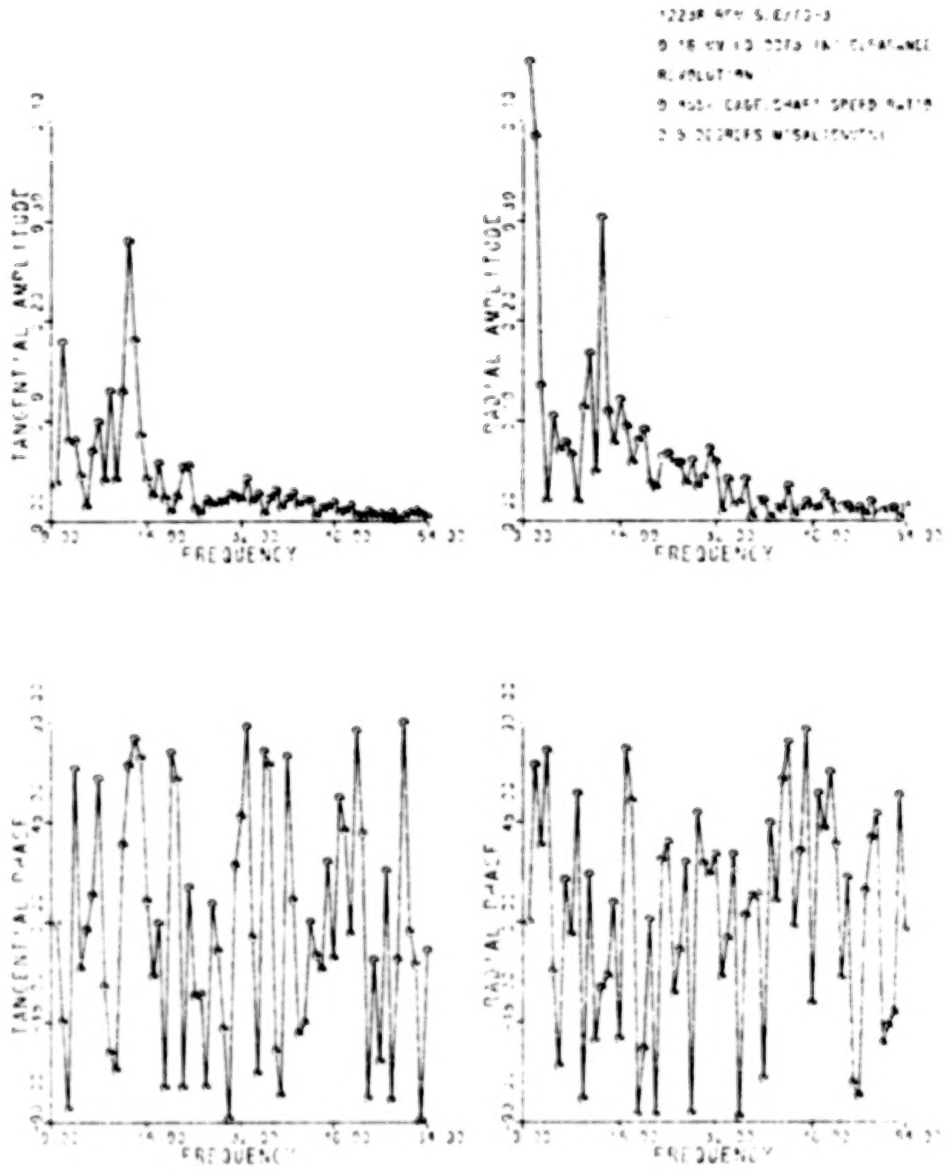

Figure 6c-1F Fast Fourier Transform of Data in Figure 6c-1

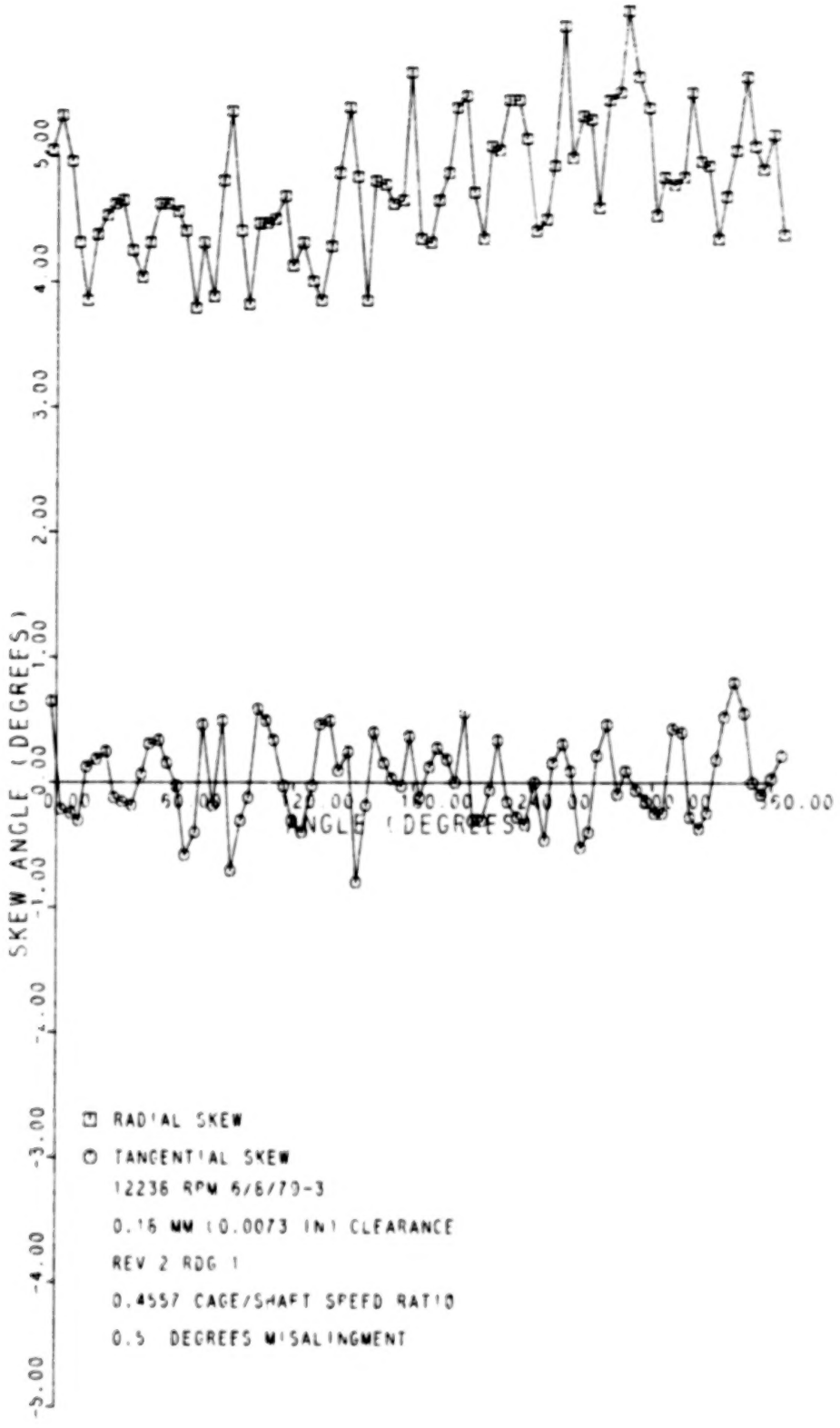

Figure 6c-2 Roller Skew, 0.18 mm Clearance Bearing, 0.50° Misalignment

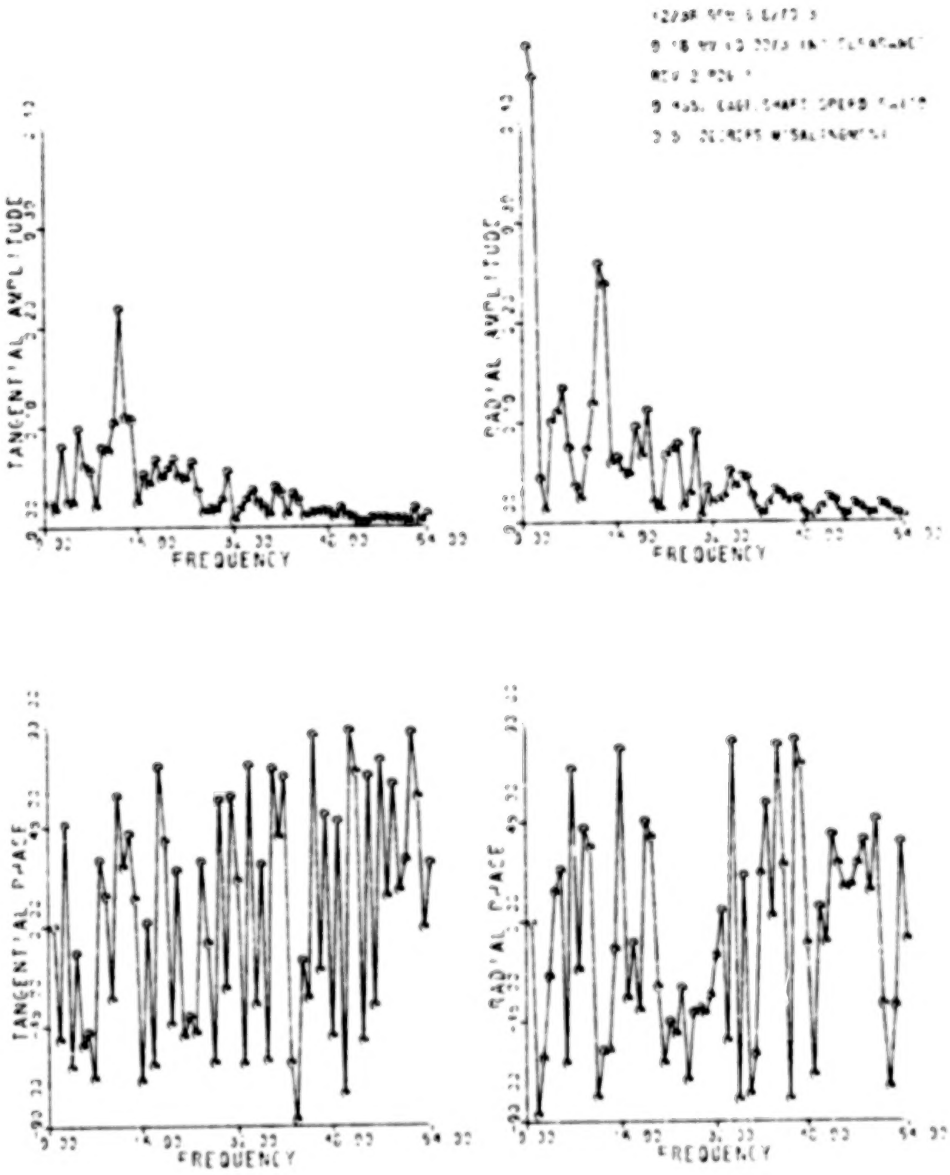

Figure 6c-2F Fast Fourier Transform of Data in Figure 6c-2

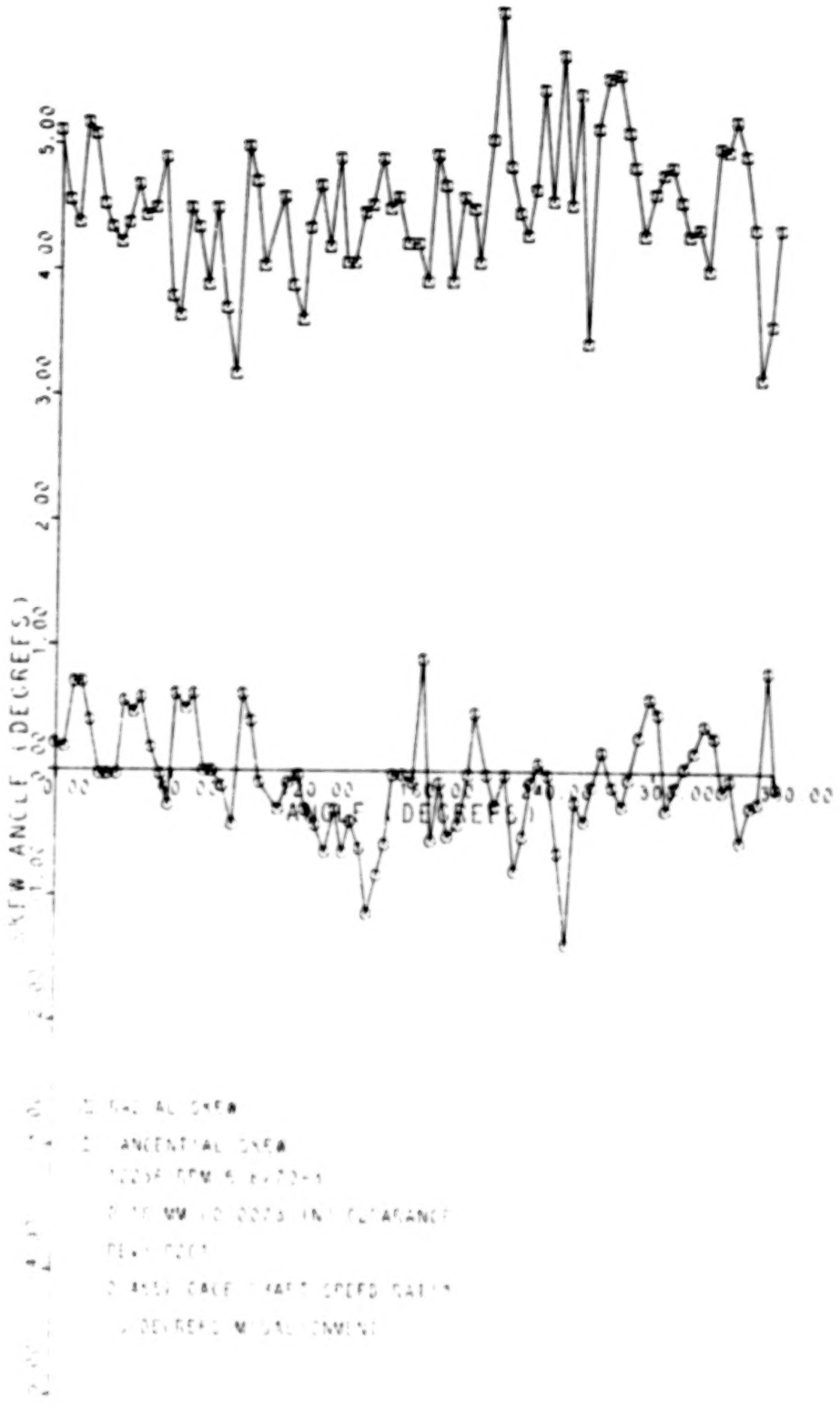

Figure 6c-3 Roller Skew, 0.18 mm Clearance Bearing, 0.50° Misalignment

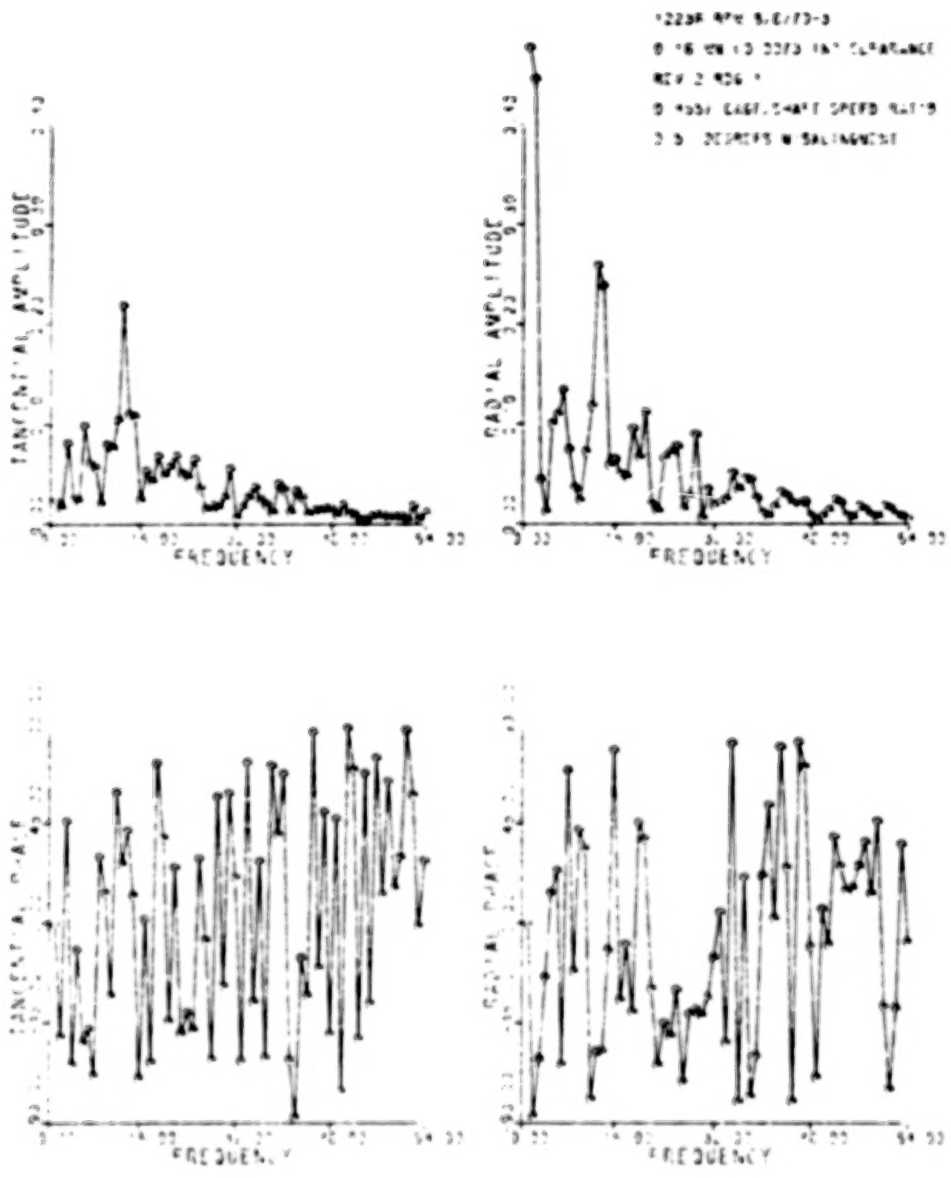

Figure 6c-3F Fast Fourier Transform of Data in Figure 6c-3

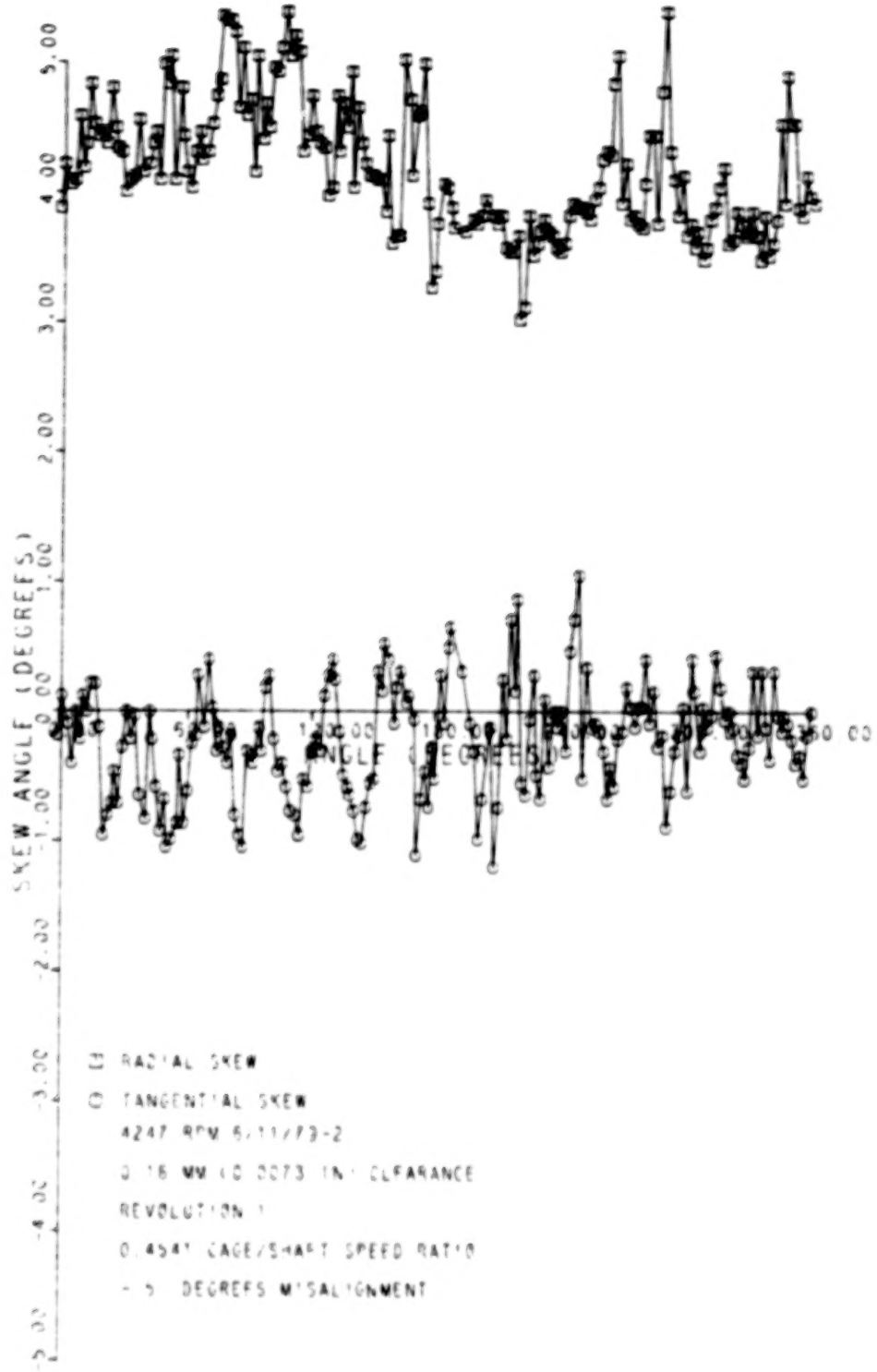

Figure 7a-1 Roller Skew, 0.18 mm Clearance Bearing, -0.50 Misalignment

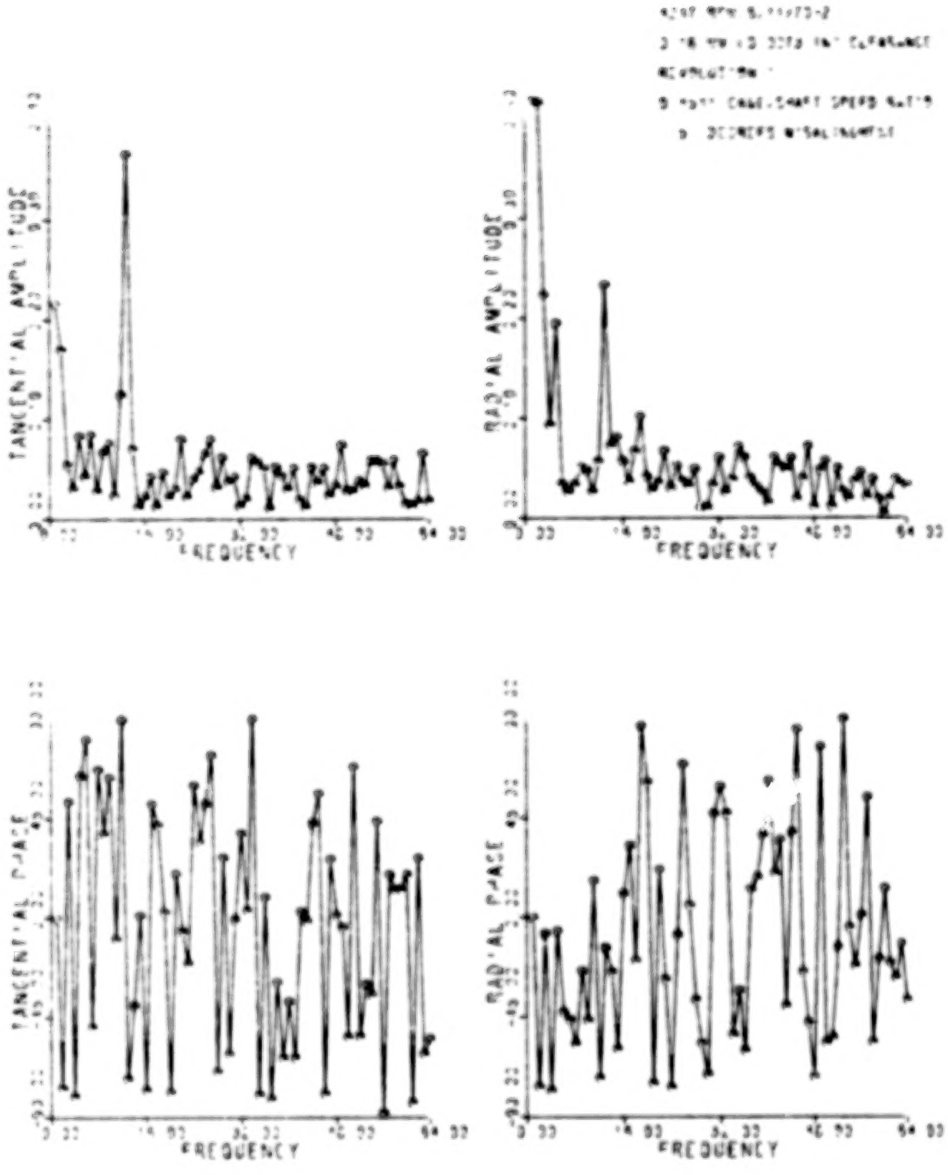

Figure 7a-1F Fast Fourier Transform of Data in Figure 7a-1

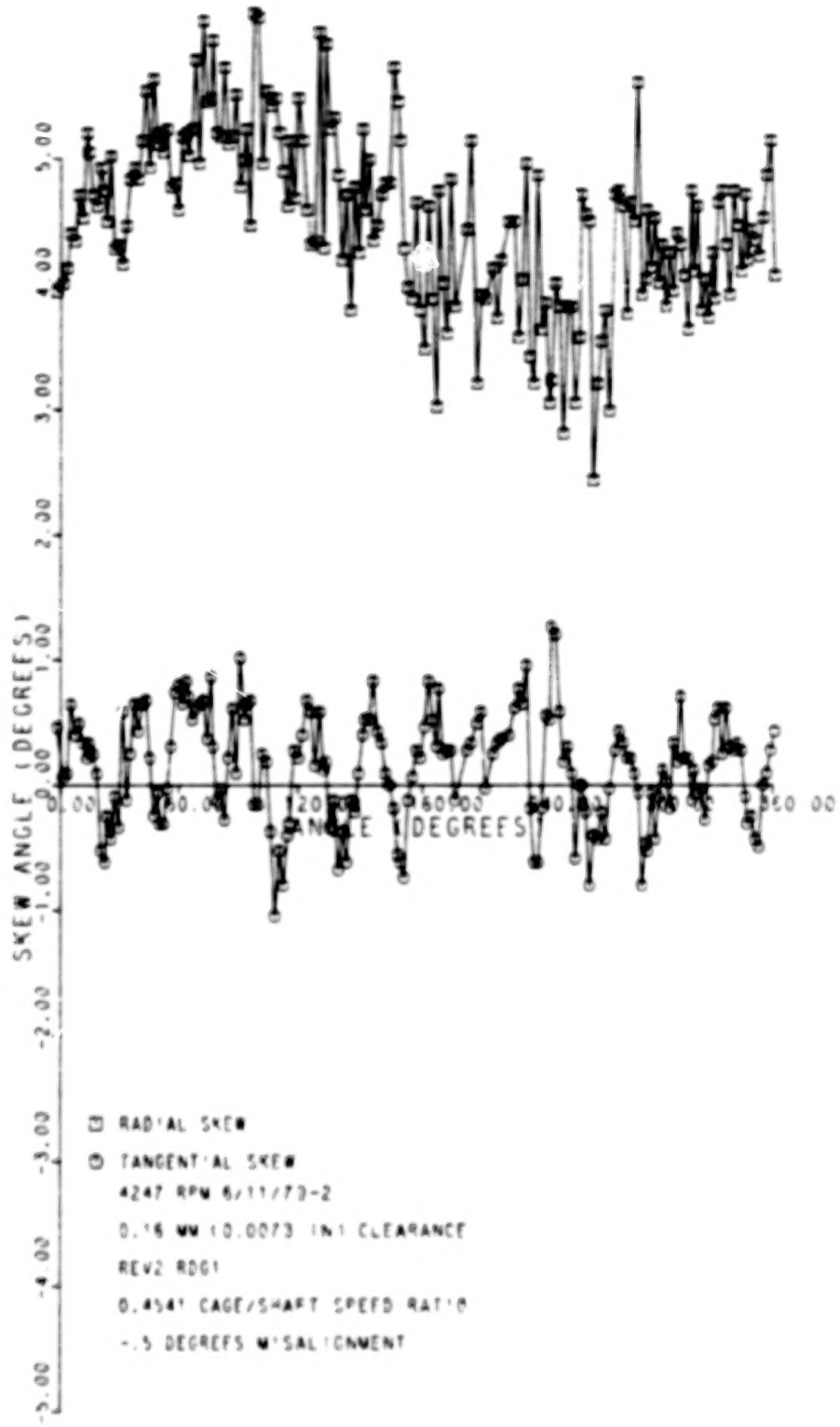

Figure 7a-2 Roller Skew, 0.18 mm Clearance Bearing, -0.50 Misalignment

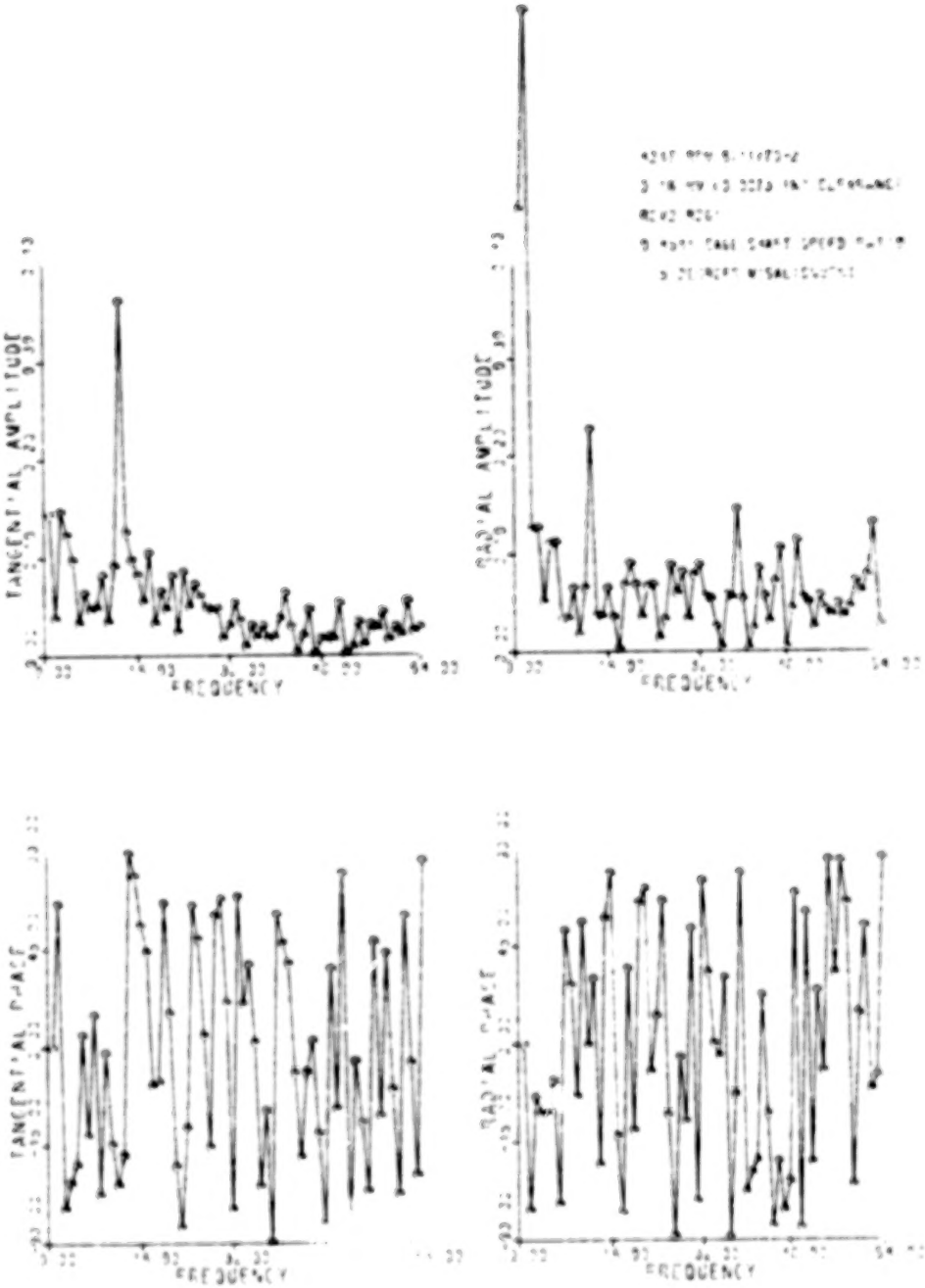

Figure 7a-2F Fast Fourier Transform of Data in Figure 7a-2

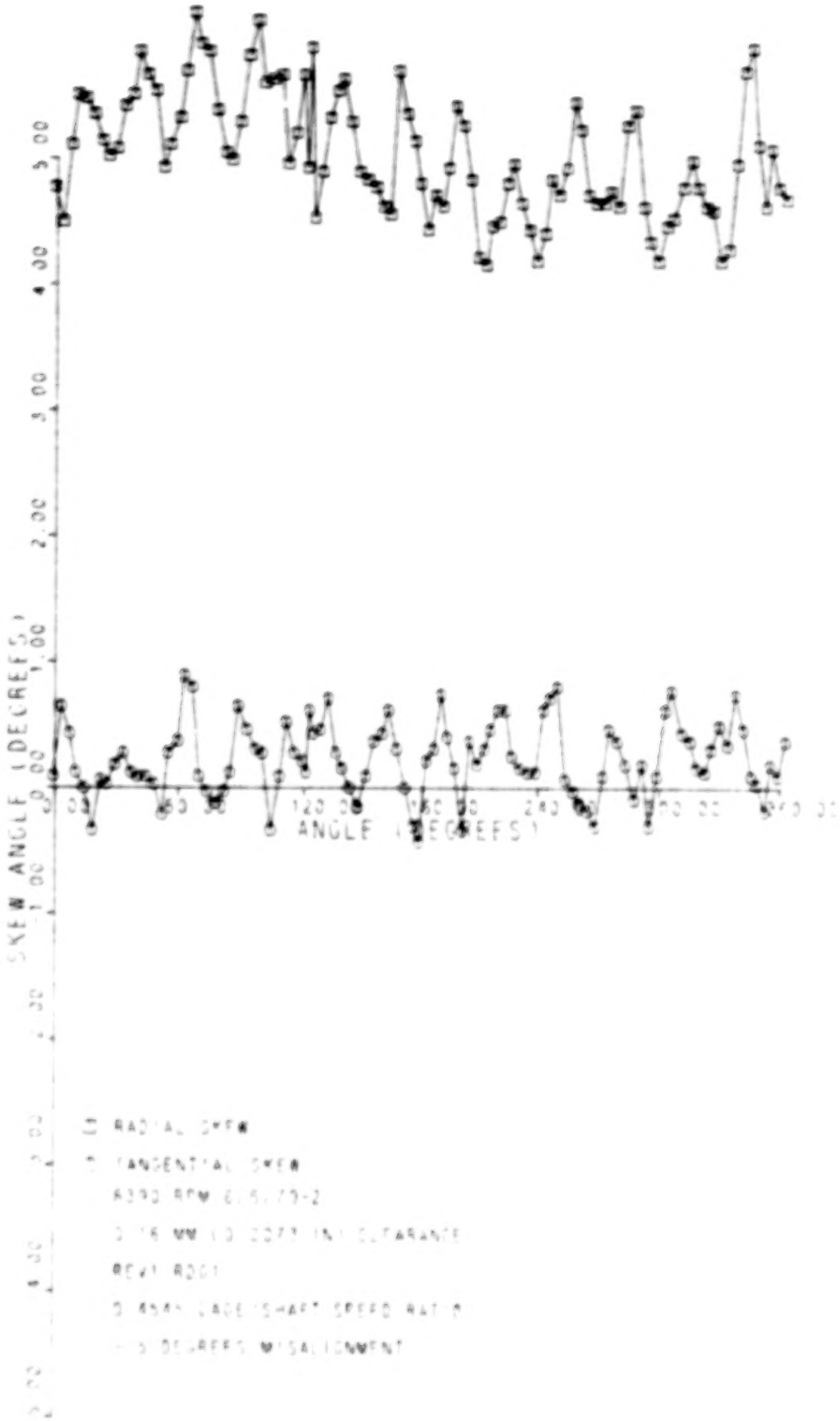

Figure 7b-1 Roller Skew, 0.18 mm Clearance Bearing, -0.50 Misalignment

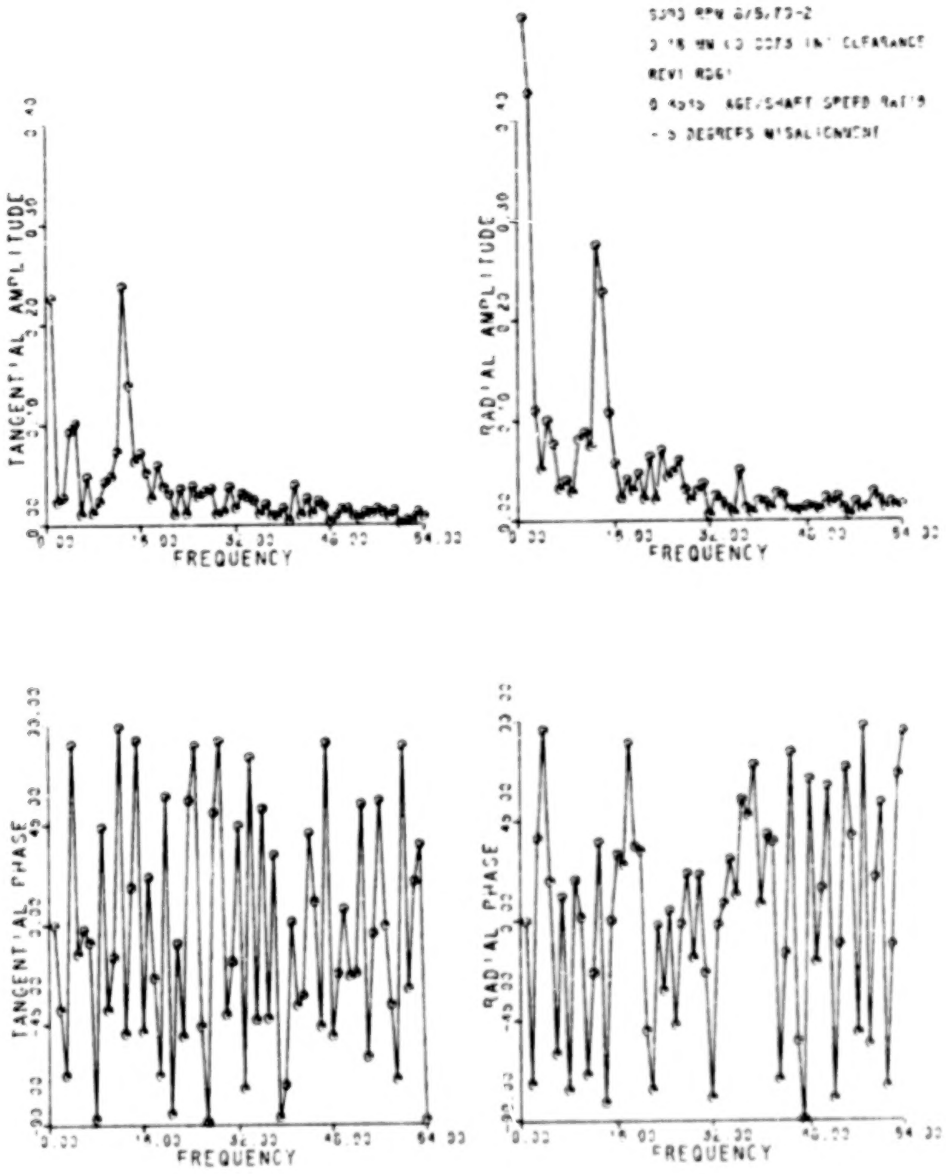

Figure 7b-1F Fast Fourier Transform of Data in Figure 7b-1

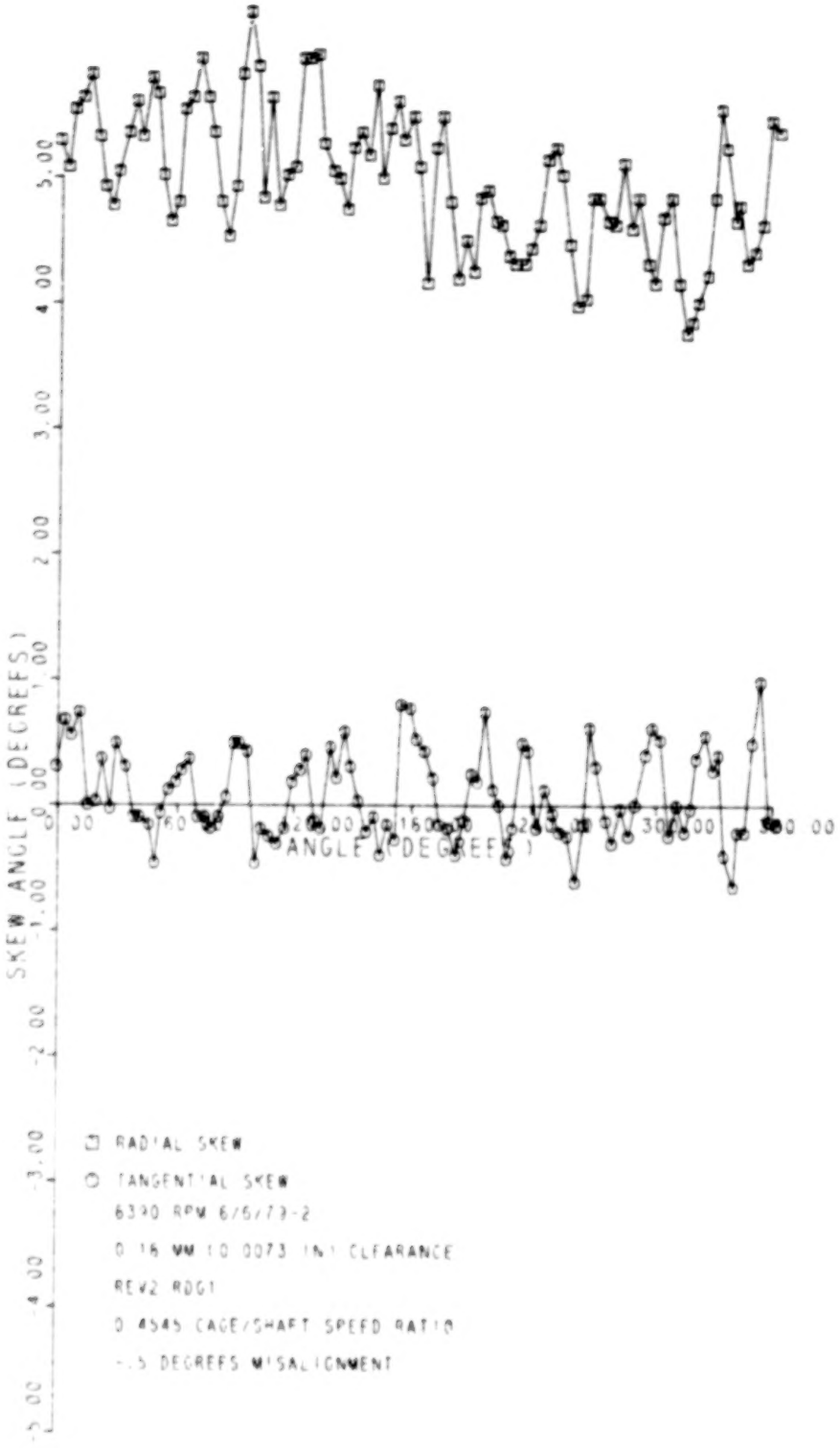

Figure 7b-2 Roller Skew, 0.18 mm Clearance Bearing, -0.50 Misalignment

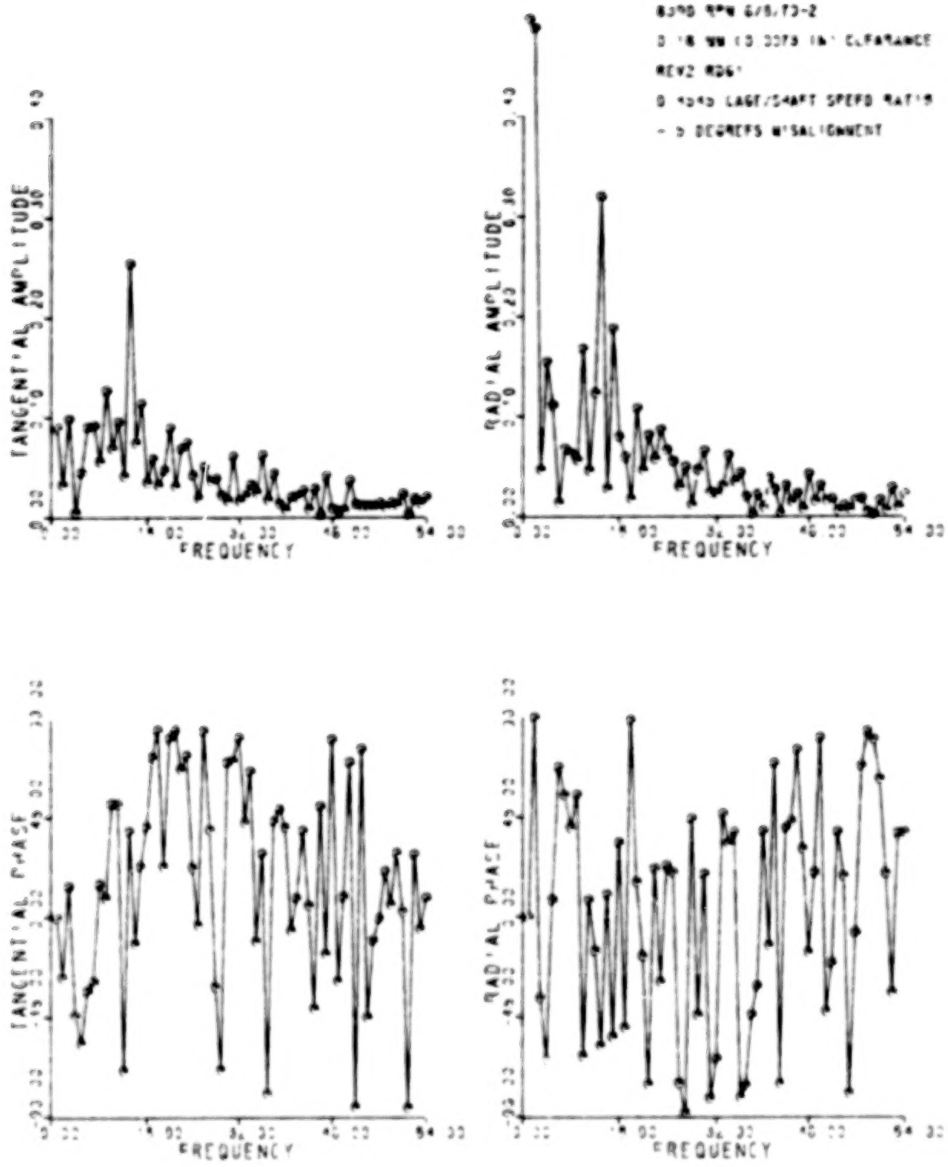

Figure 7b-2F Fast Fourier Transform of Data in Figure 7b-2

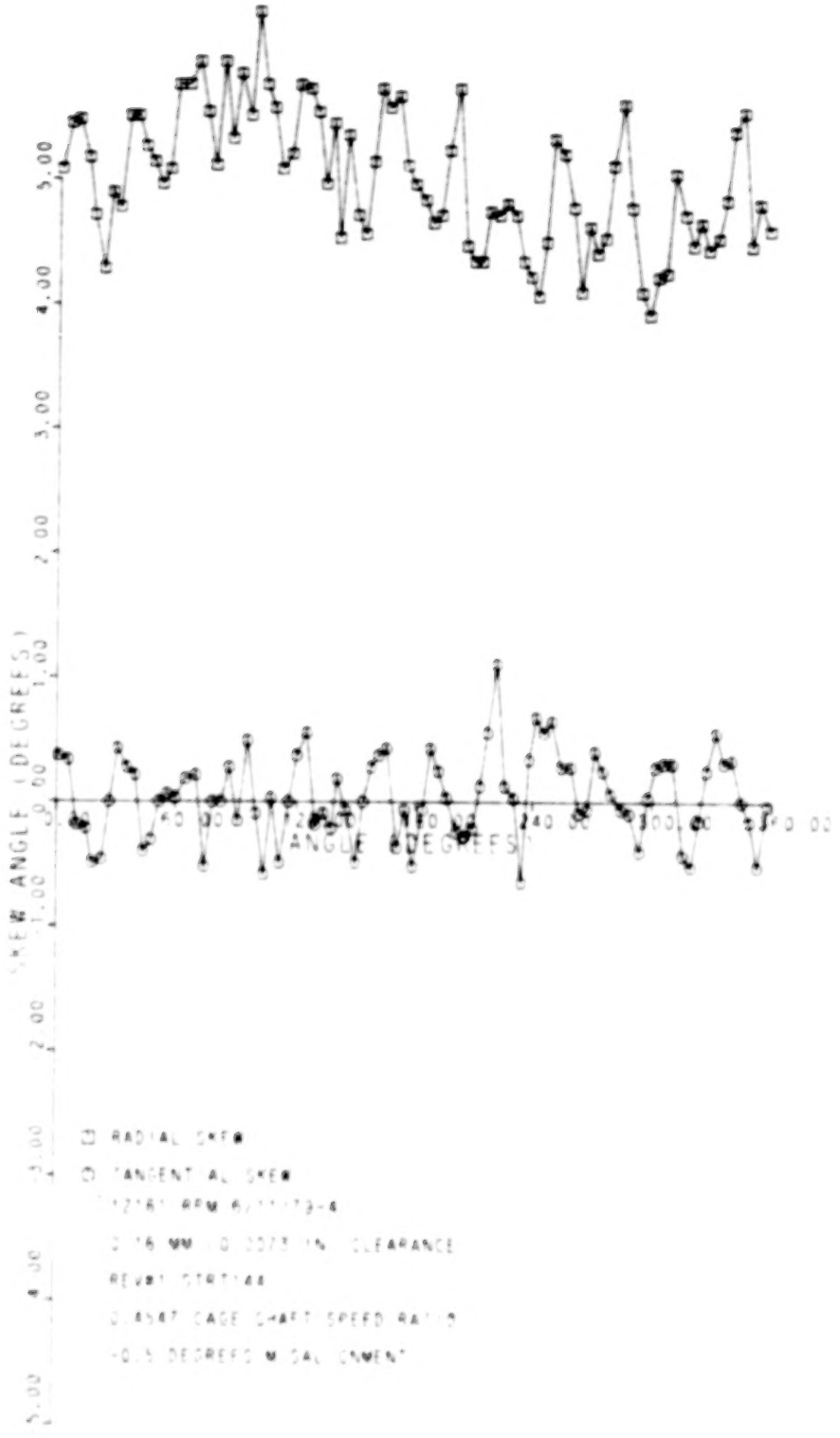

Figure 7c-1 Roller Skew, 0.18 mm Clearance Bearing, -0.50 Misalignment

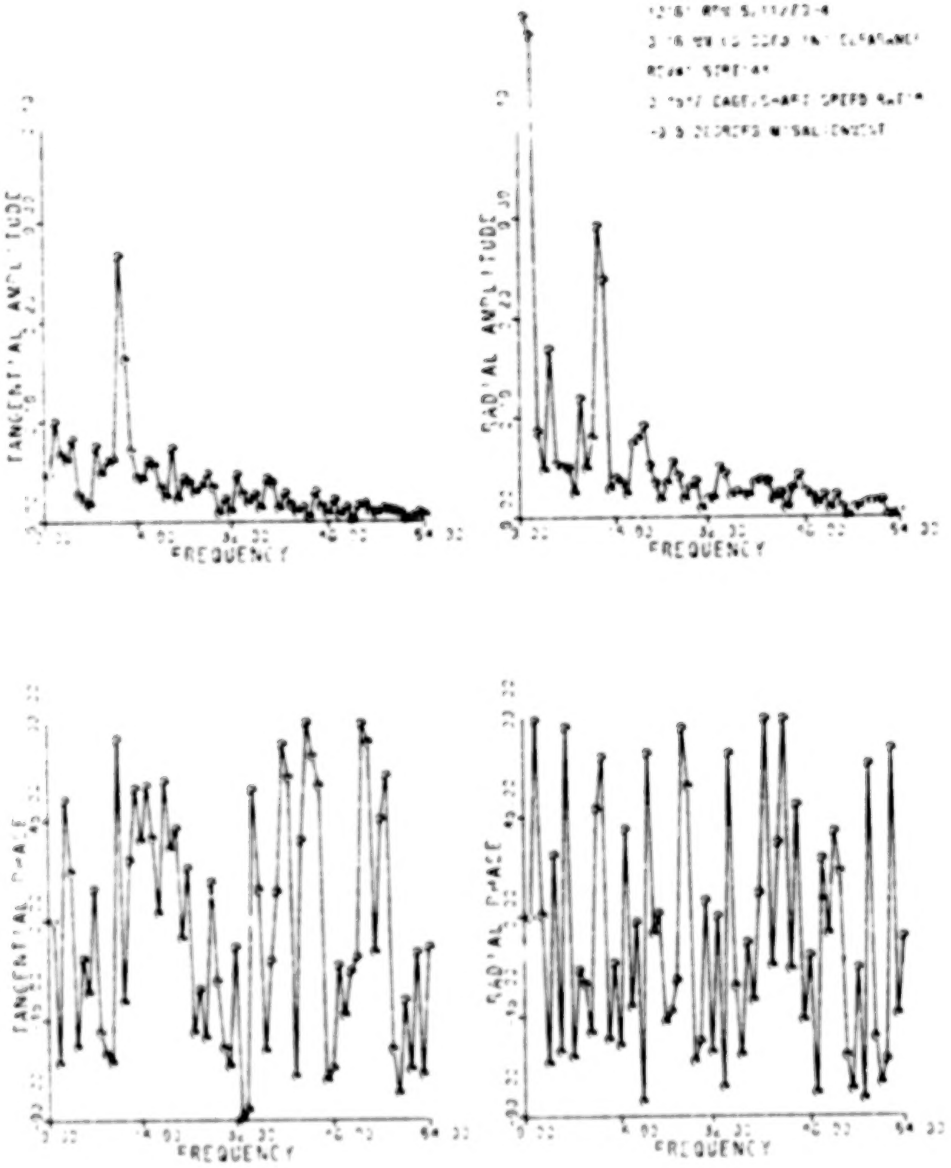

Figure 7c-1F Fast Fourier Transform of Data in Figure 7c-1

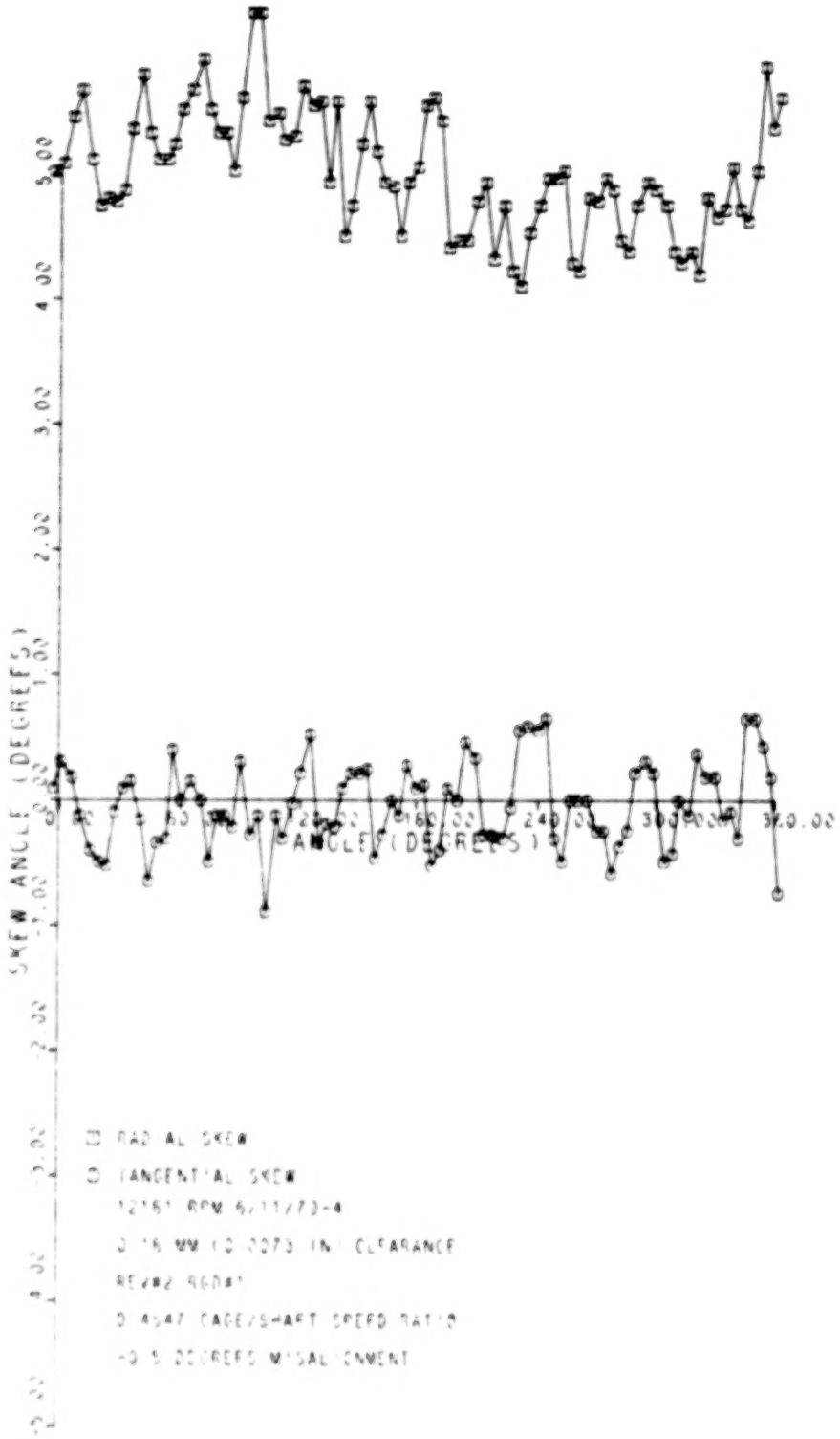

Figure 7c-2 Roller Skew, 0.18 mm Clearance Bearing, -0.50 Misalignment

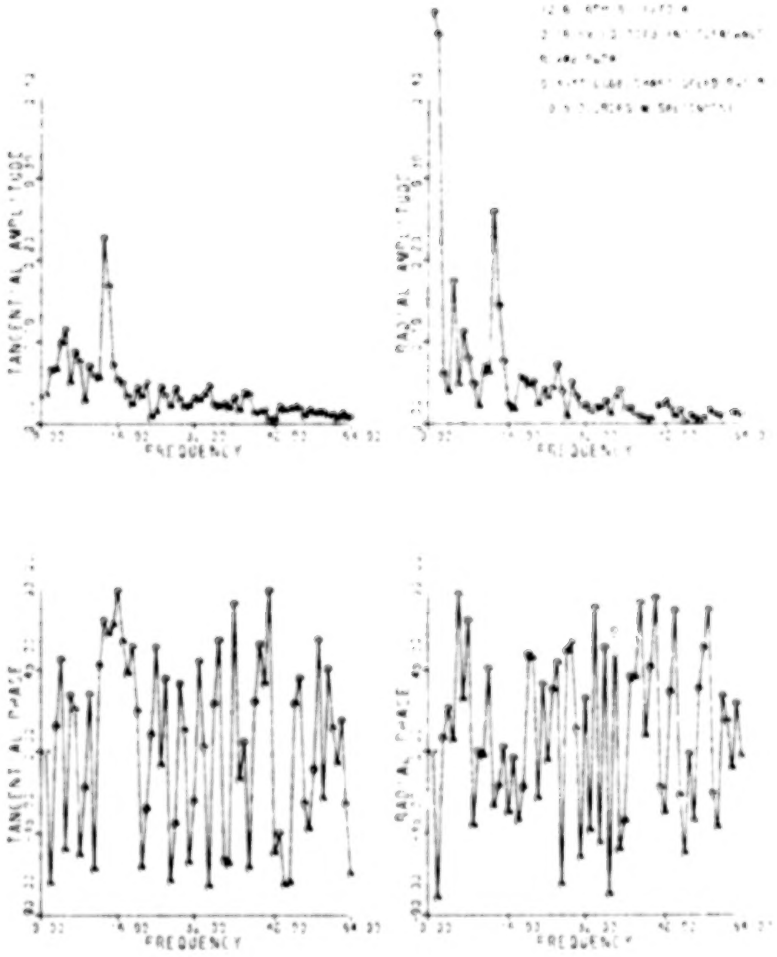

Figure 7c-2F Fast Fourier Transform of Data in Figure 7c-2

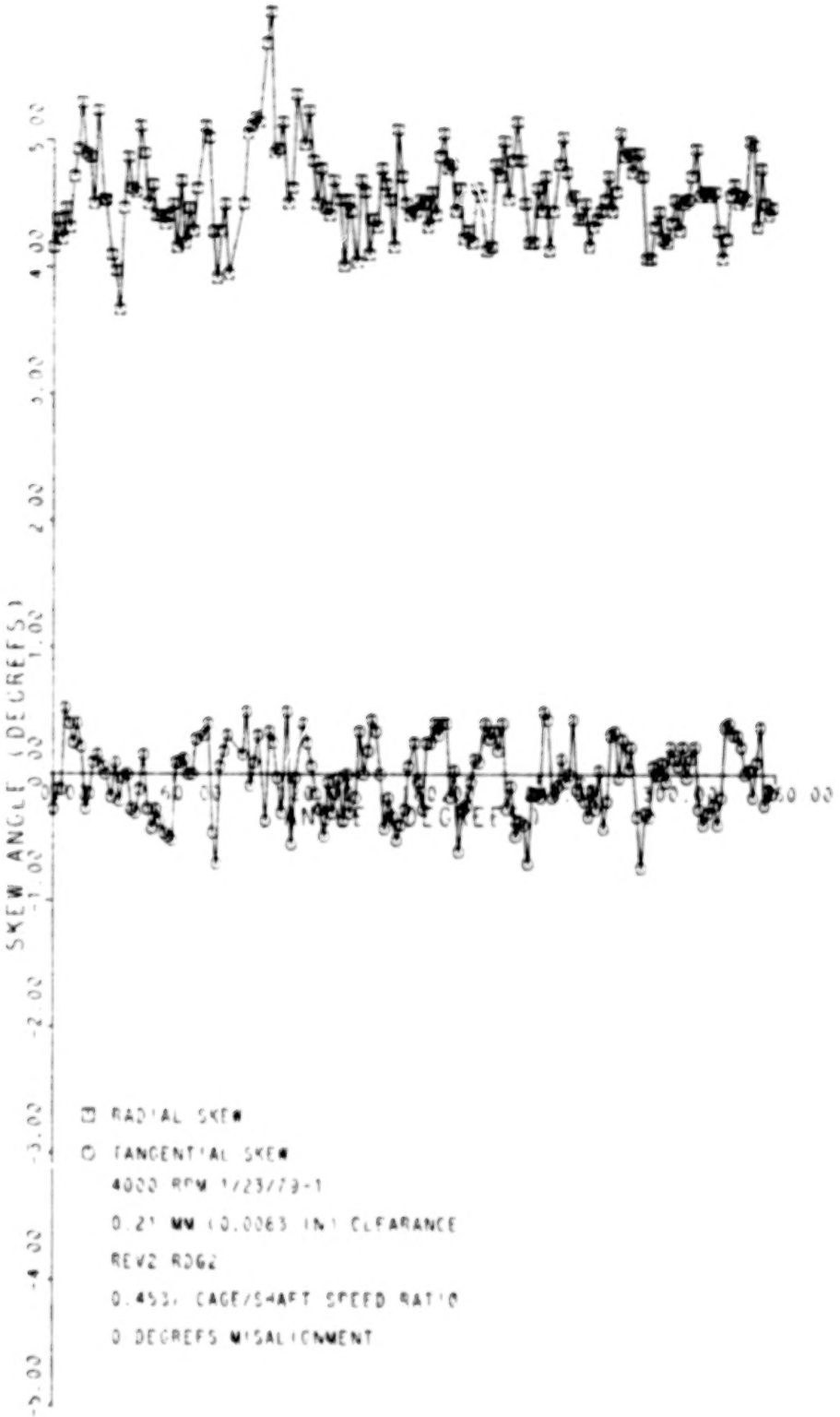

Figure 8a Roller Skew, 0.21 mm Clearance Bearing, 0° Misalignment

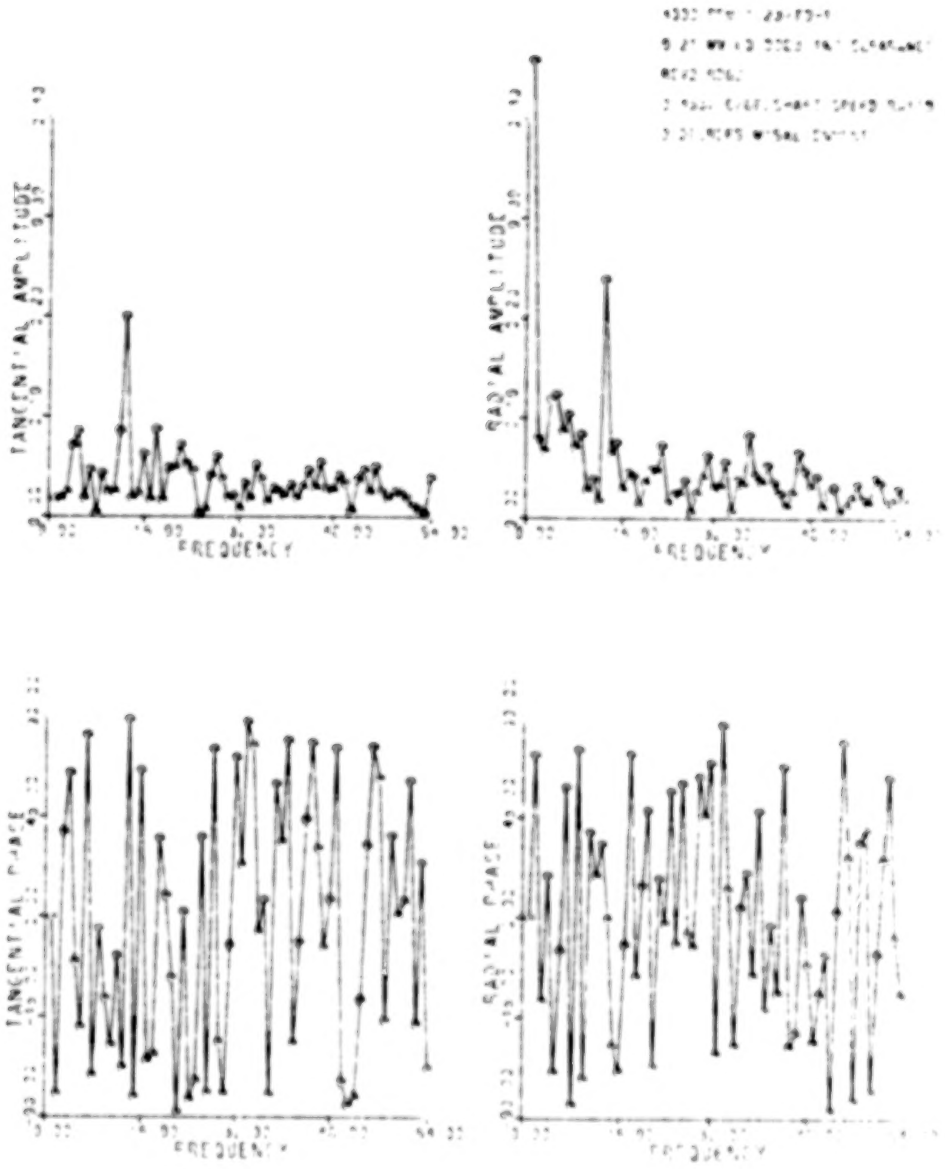

Figure 8aF Fast Fourier Transform of Data in Figure 8a

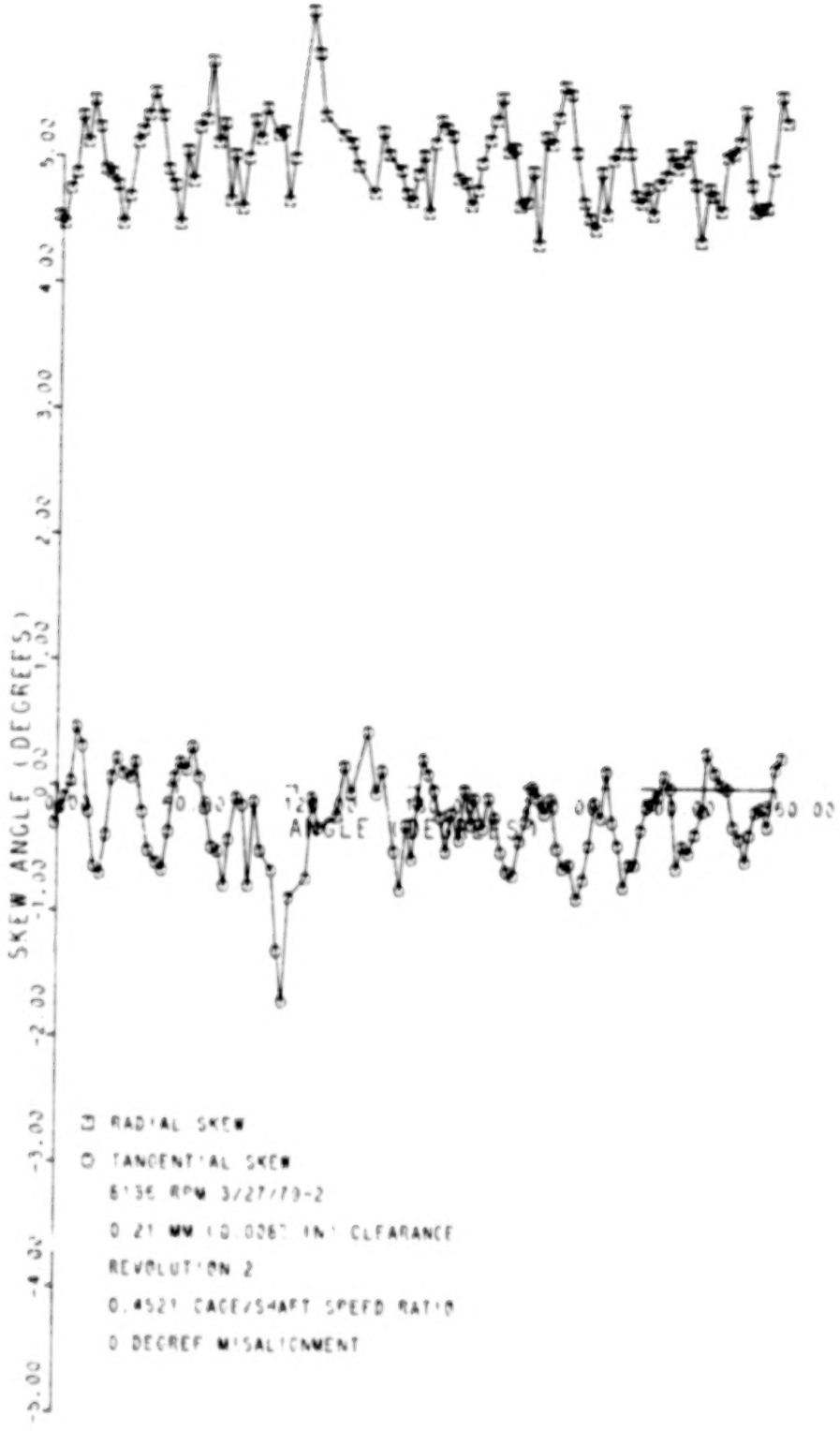

Figure 8b Roller Skew, 0.21 mm Clearance Bearing, 0° Misalignment

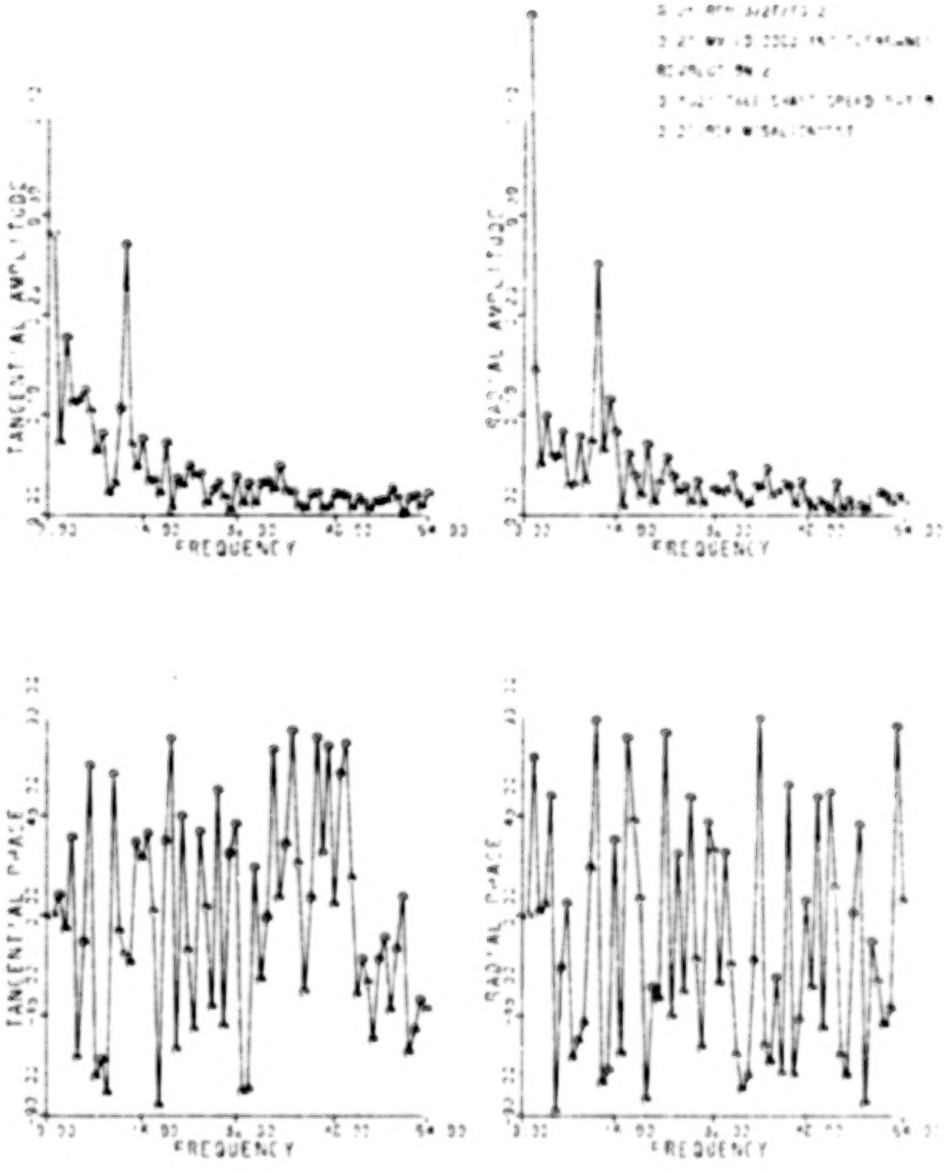

Figure 8bF Fast Fourier Transform of Data in Figure 8b

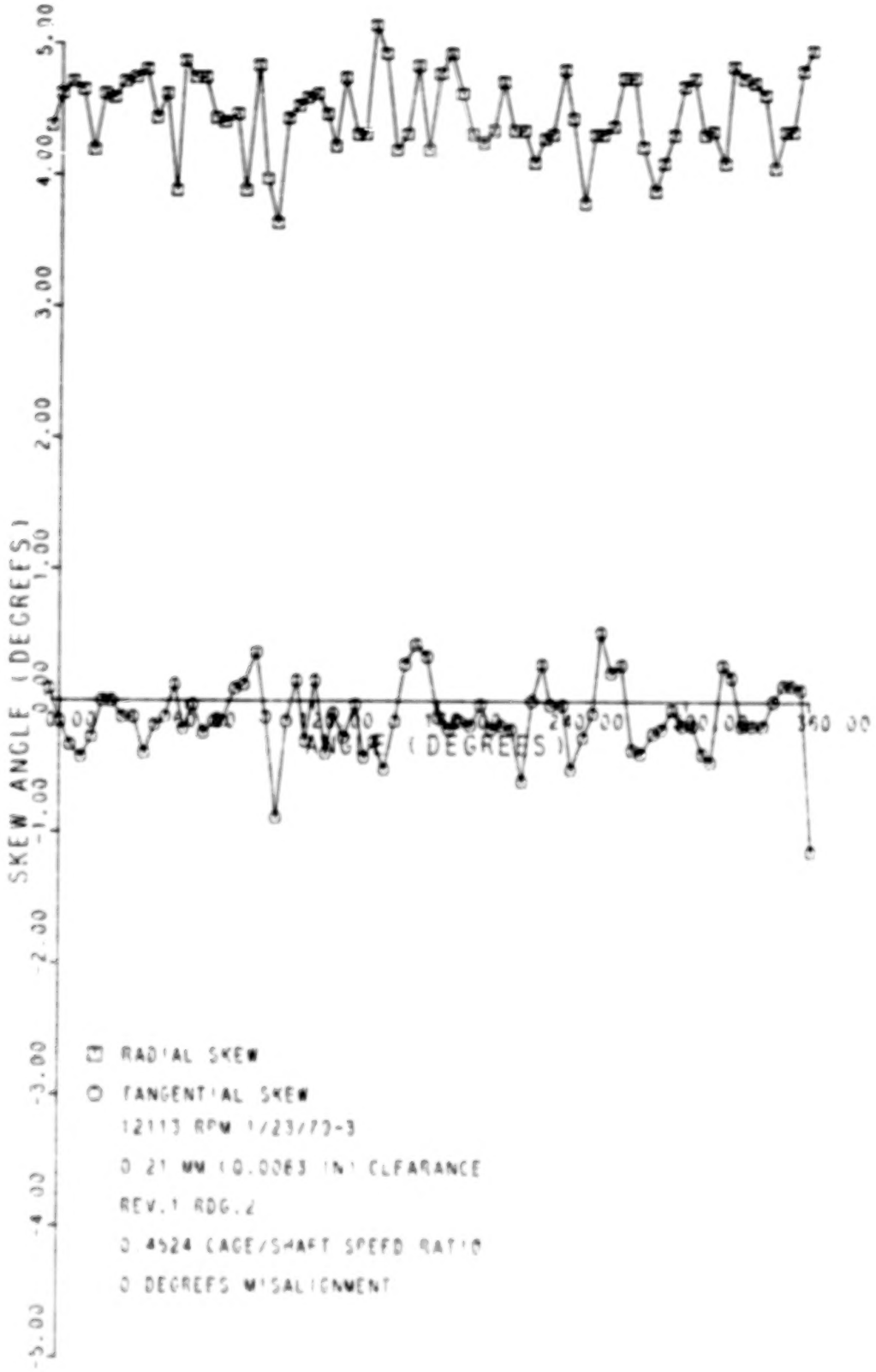

Figure 8c Roller Skew, 0.21 mm Clearance Bearing, 0^{o} Misalignment

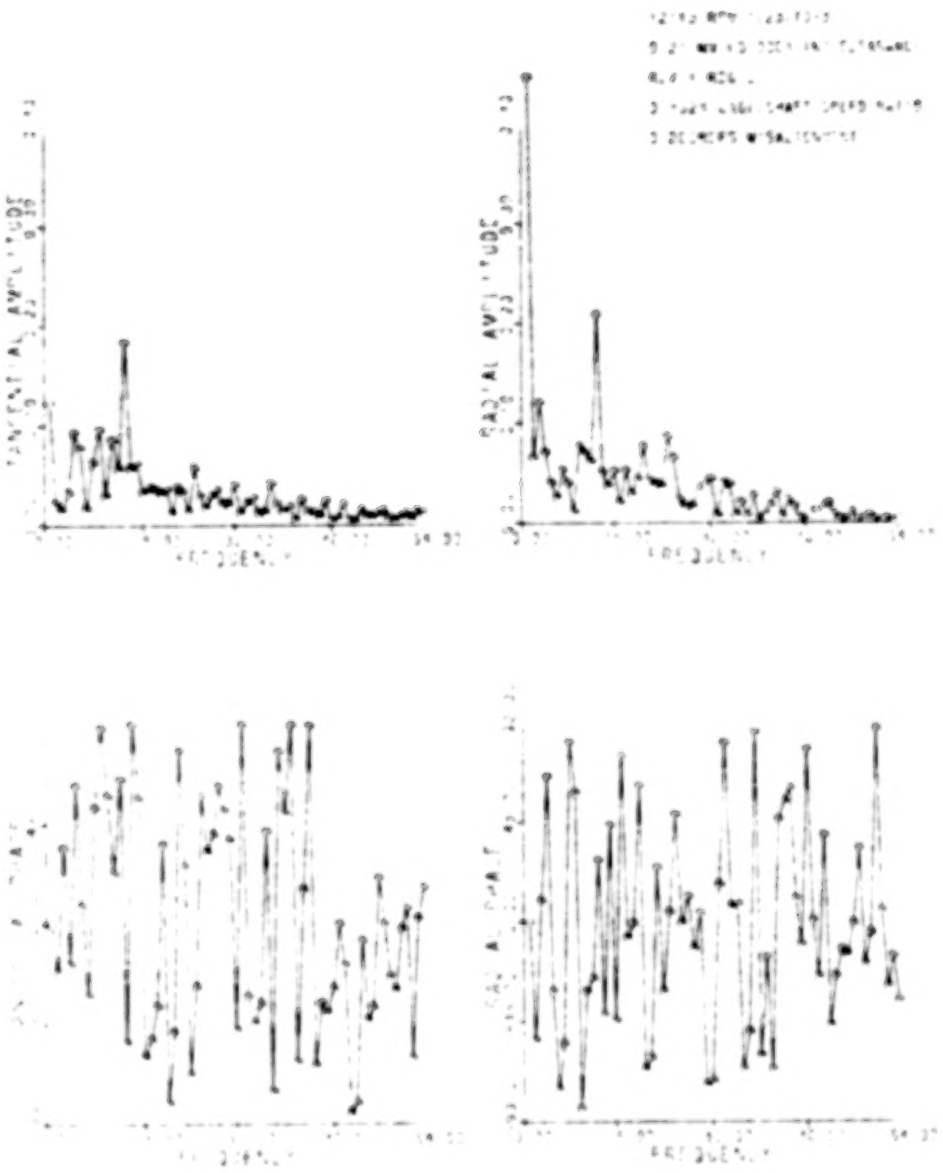

Figure 8cF Fast Fourier Transform of Data in Figure 8c

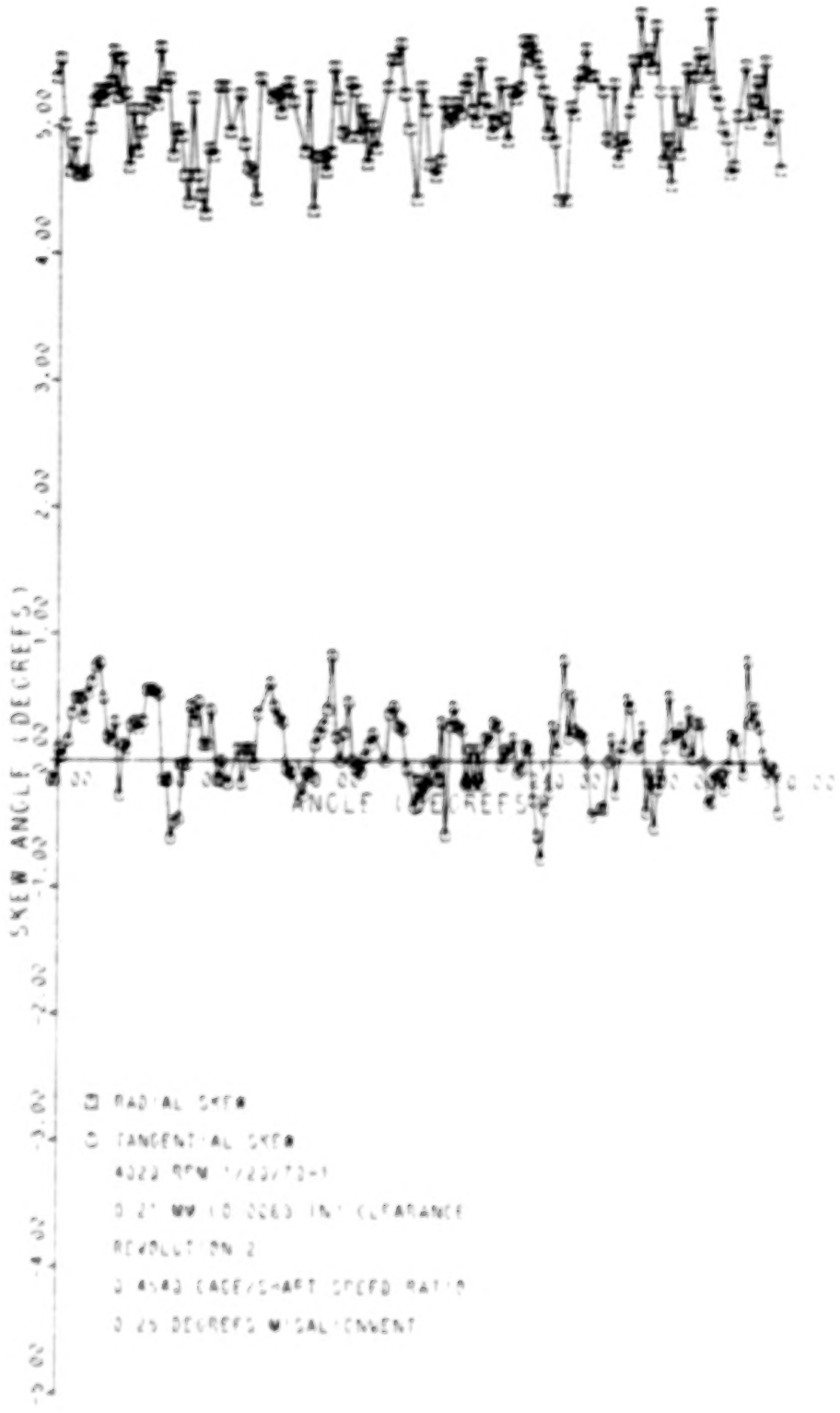

Figure 9a Roller Skew, 0.21 mm Clearance Bearing, 0.25° Misalignment

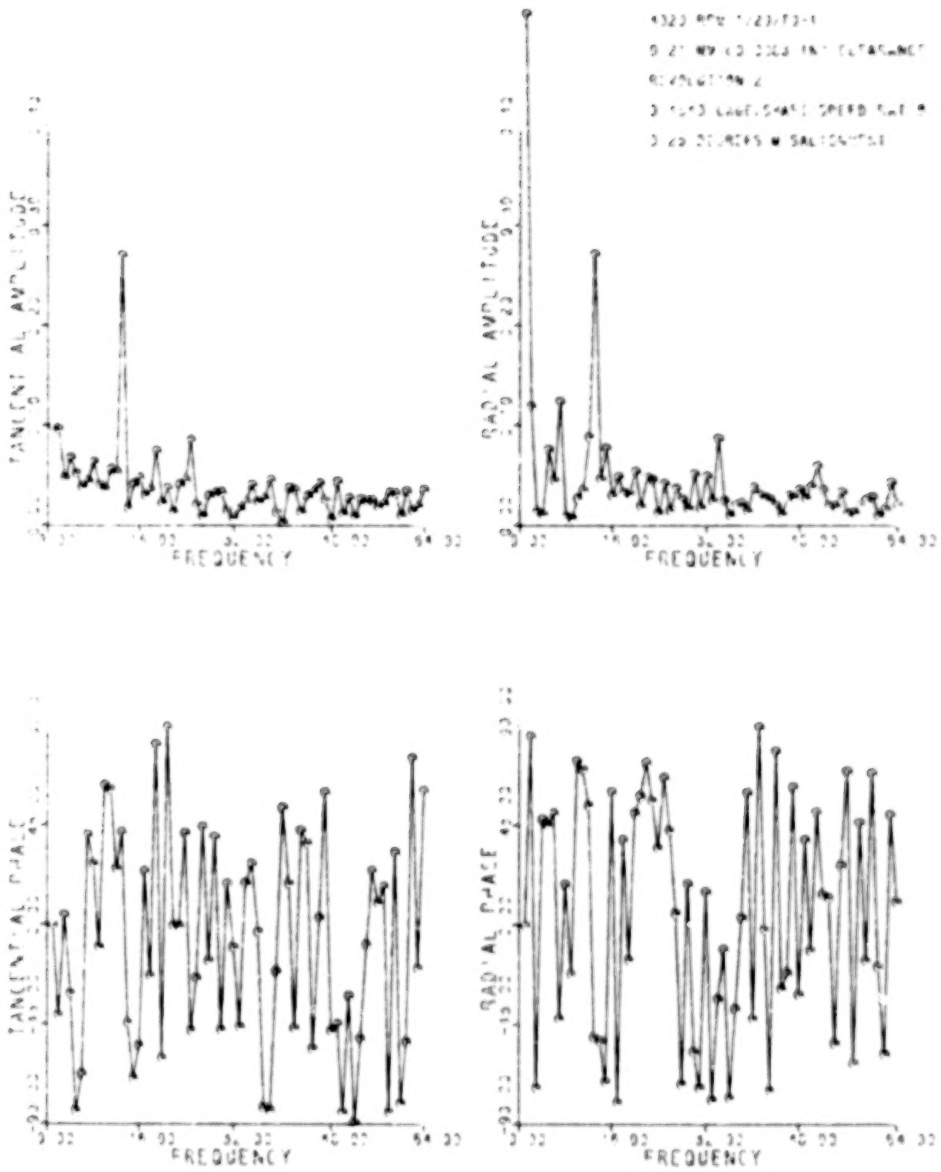

Figure 9aF Fast Fourier Transform of Data in Figure 9a

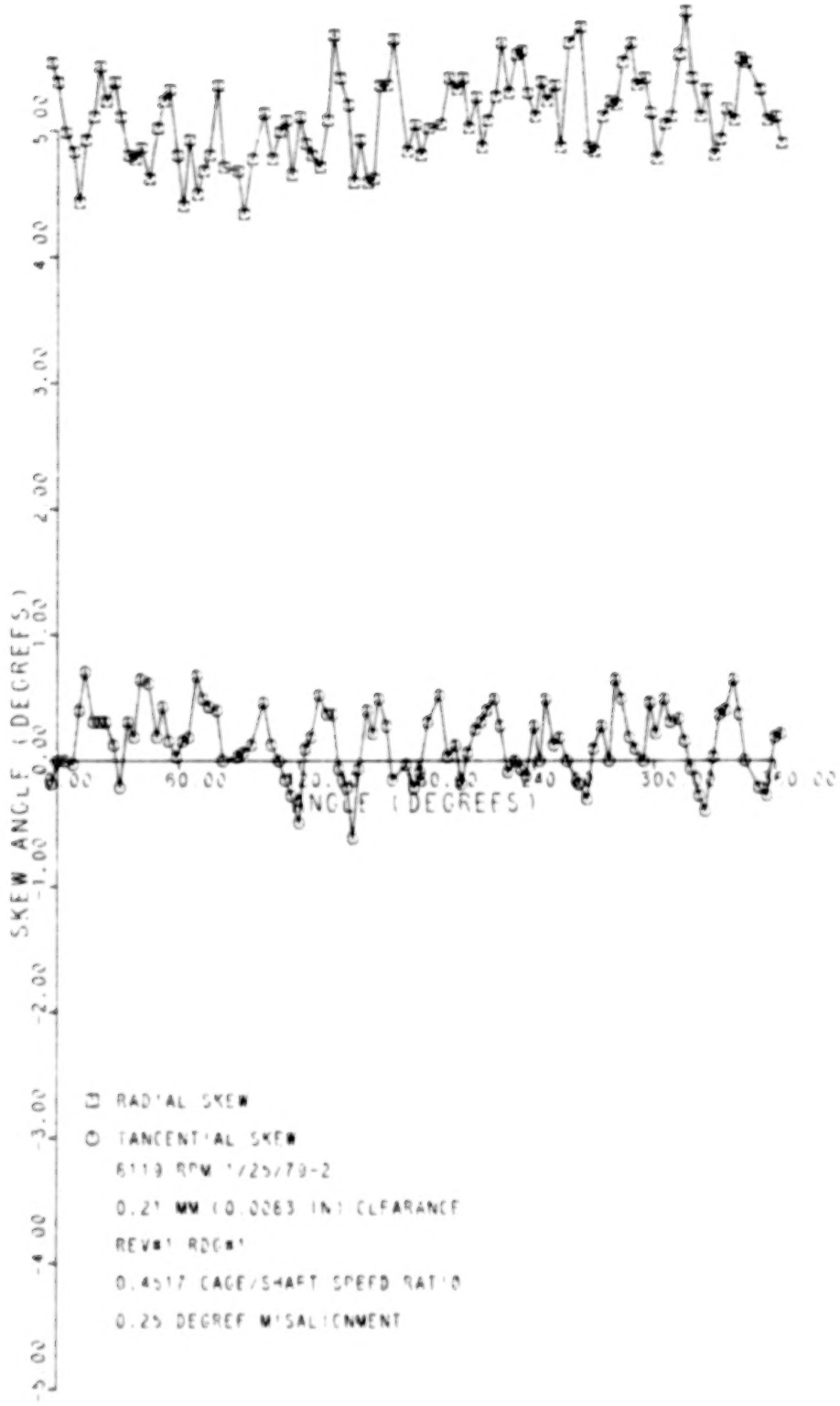

Figure 9b Roller Skew, 0.21 mm Clearance Bearing, 0.25° Misalignment

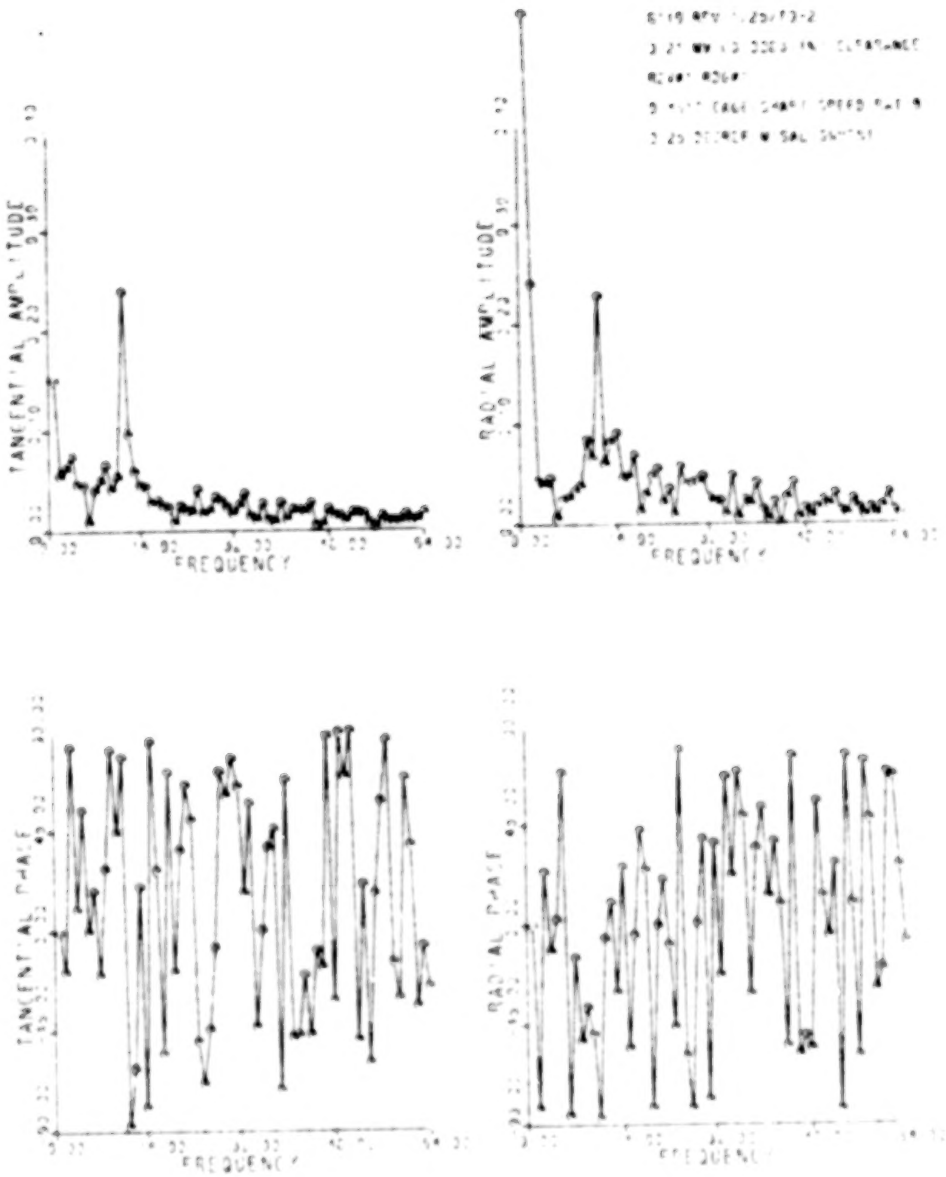

Figure 9bF Fast Fourier Transform of Data in Figure 9b

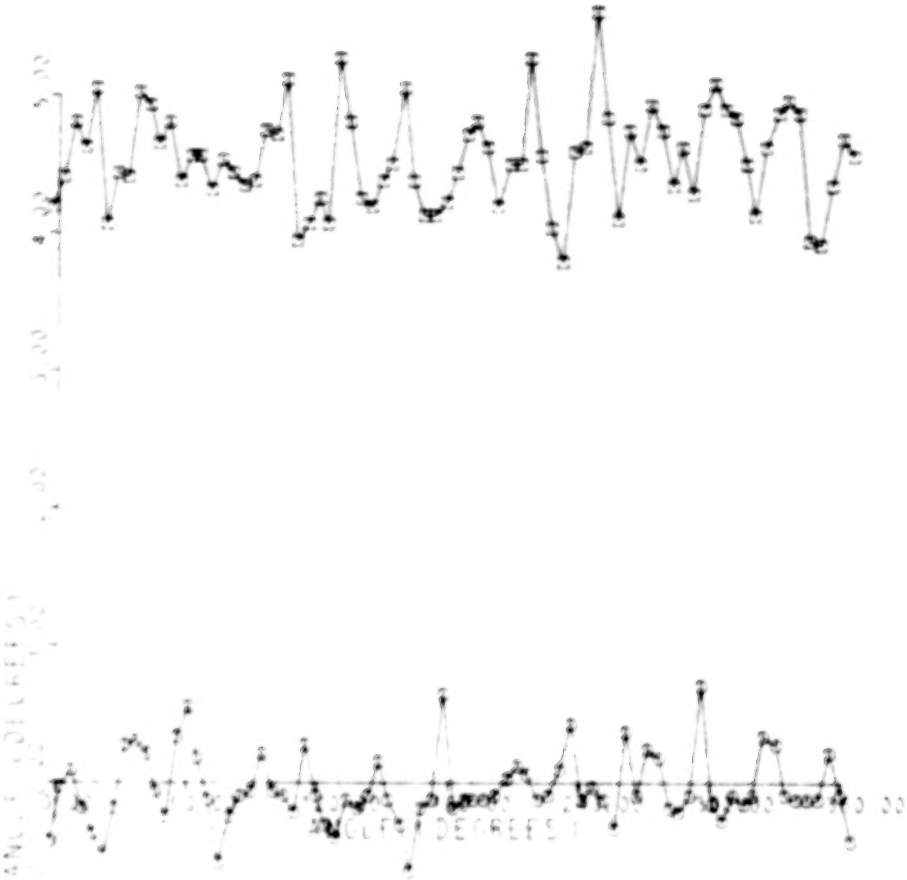

Figure 9c Roller Skew, 0.21 mm Clearance Bearing, 0.25° Misalignment

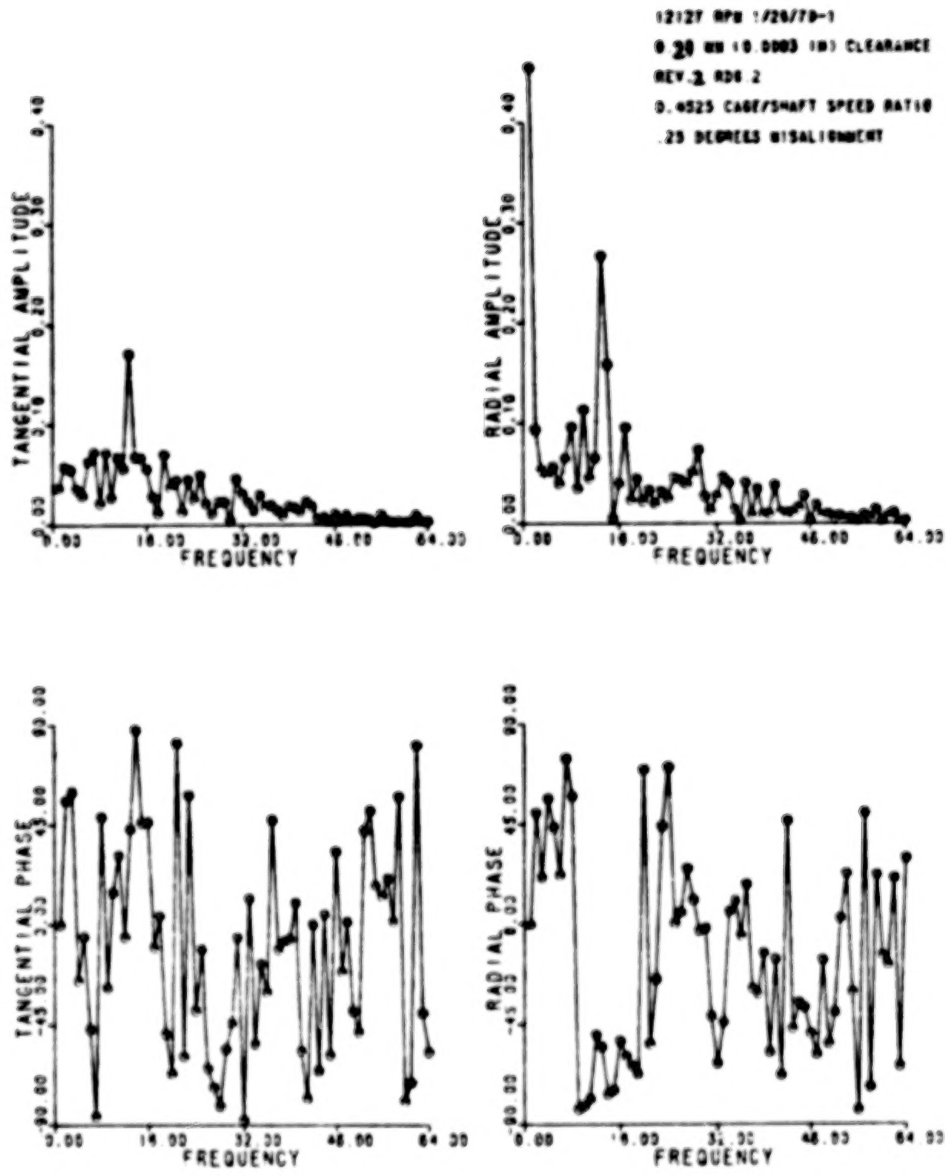

Figure 9cF Fast Fourier Transform of Data in Figure 9c

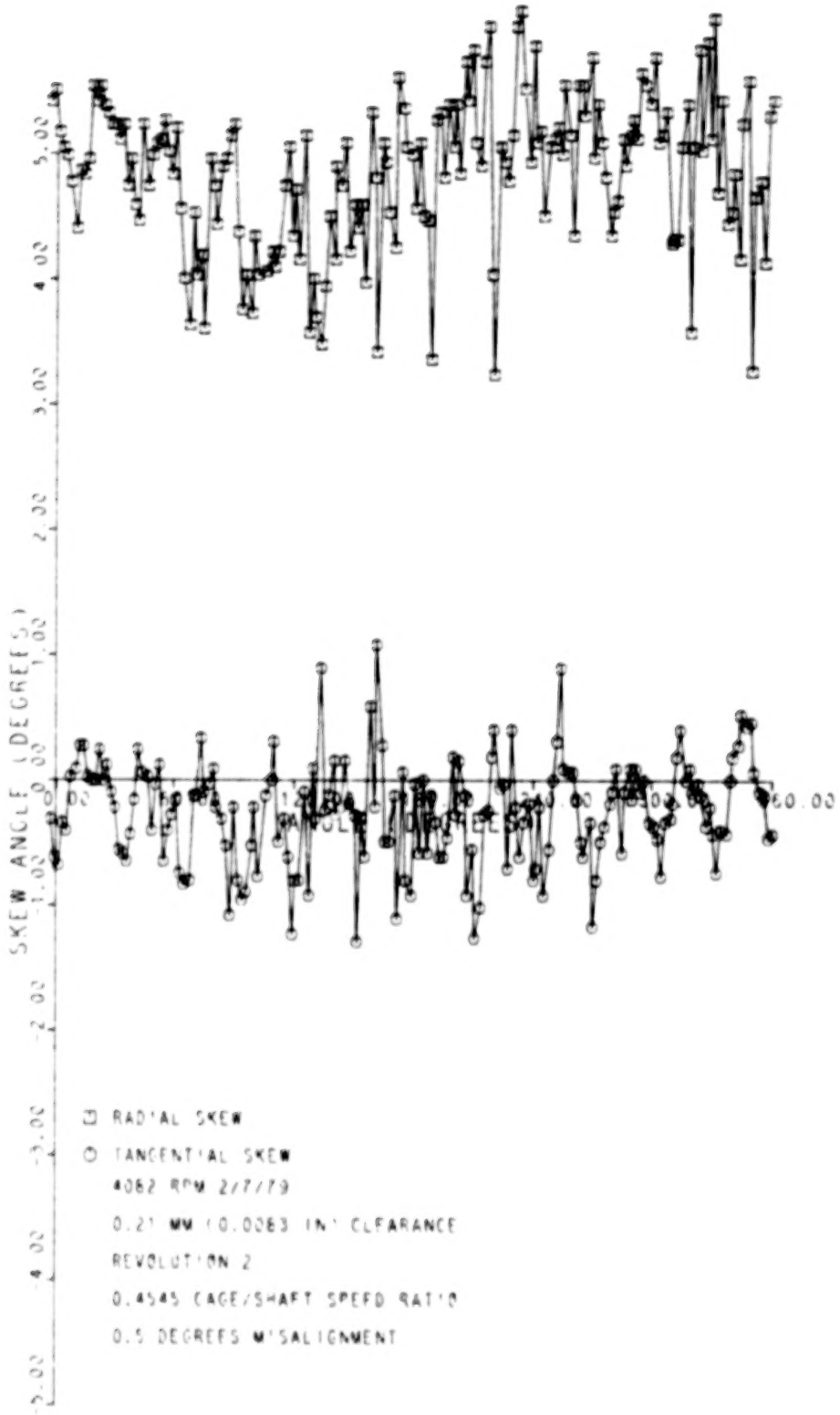

Figure 10a Roller Skew, 0.21 mm Clearance Bearing, 0.50° Misalignment

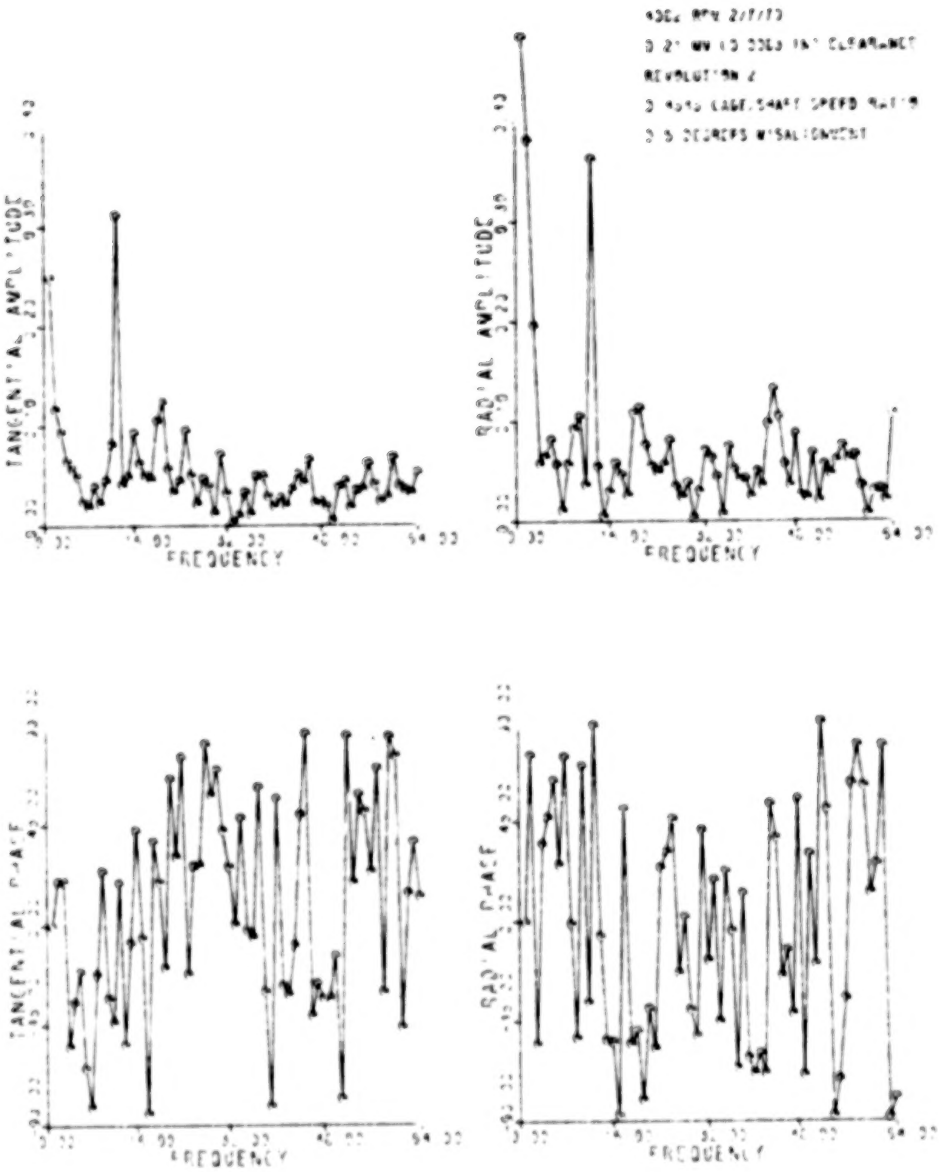

Figure 10aF Fast Fourier Transform of Data in Figure 10a

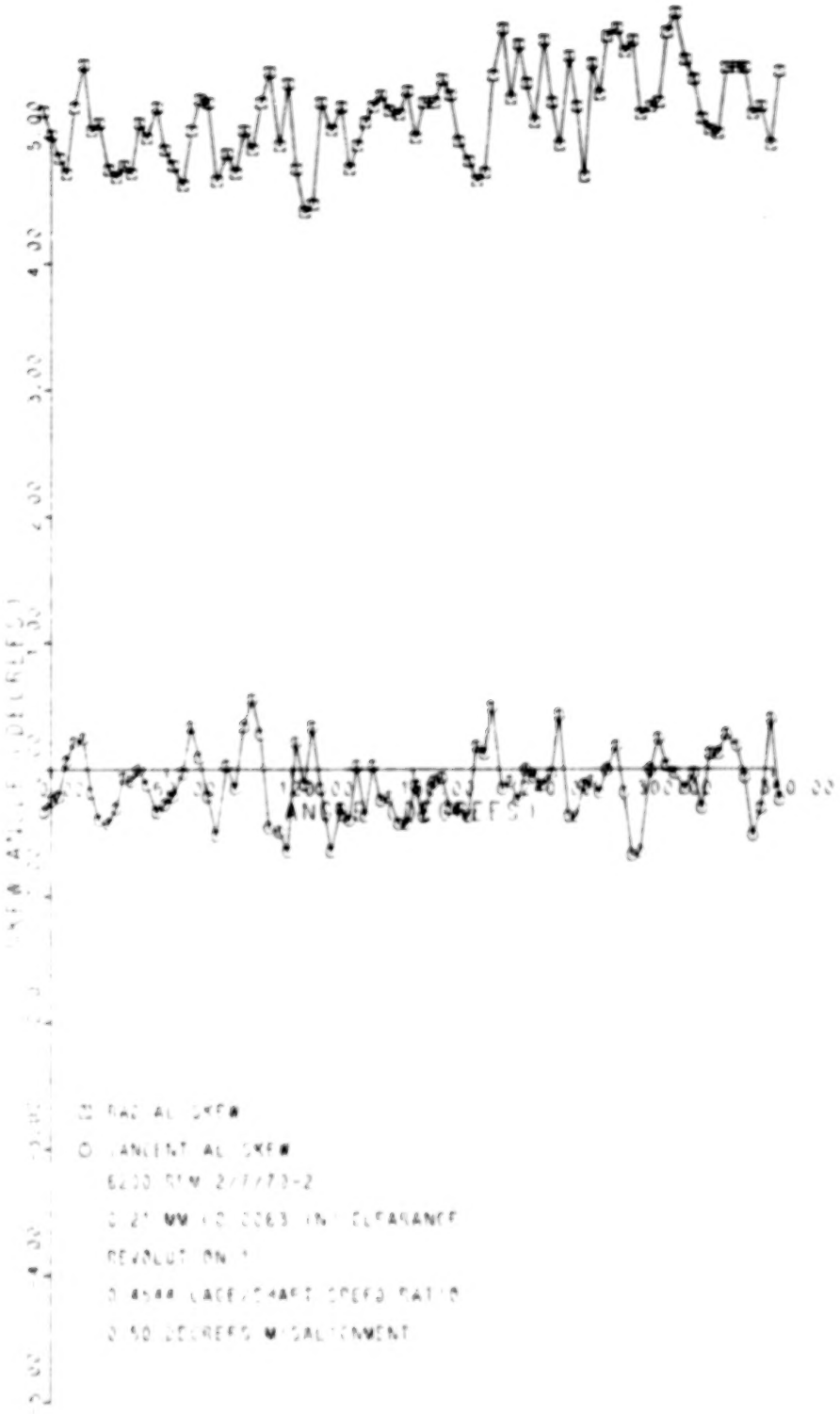

Figure 10b-1 Roller Skew, 0.21 mm Clearance Bearing, 0.50° Misalignment

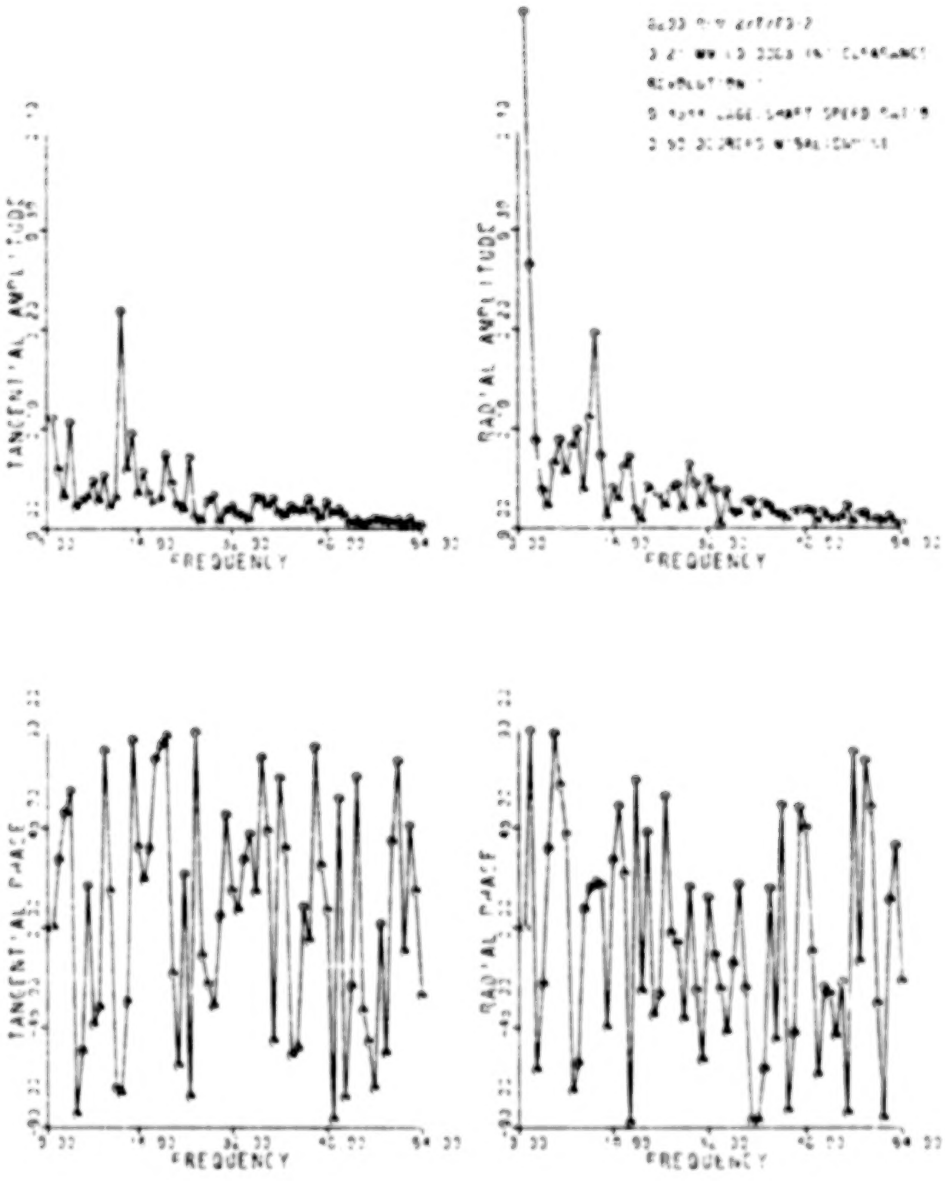

Figure 10b-1F Fast Fourier Transform of Data in Figure 10b-1

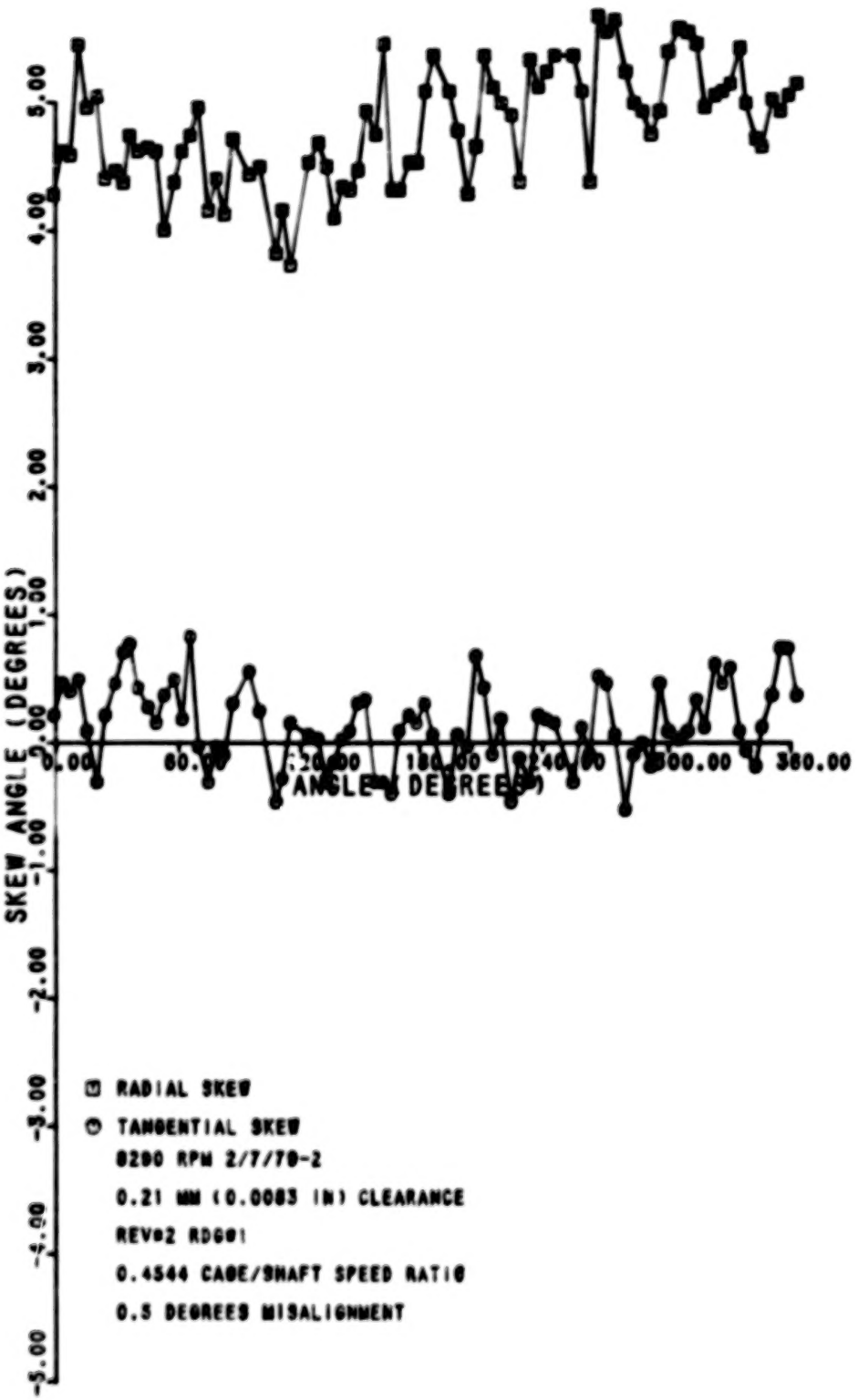

Figure 10b-2 Roller Skew, 0.21 mm Clearance Bearing, 0.50° Misalignment

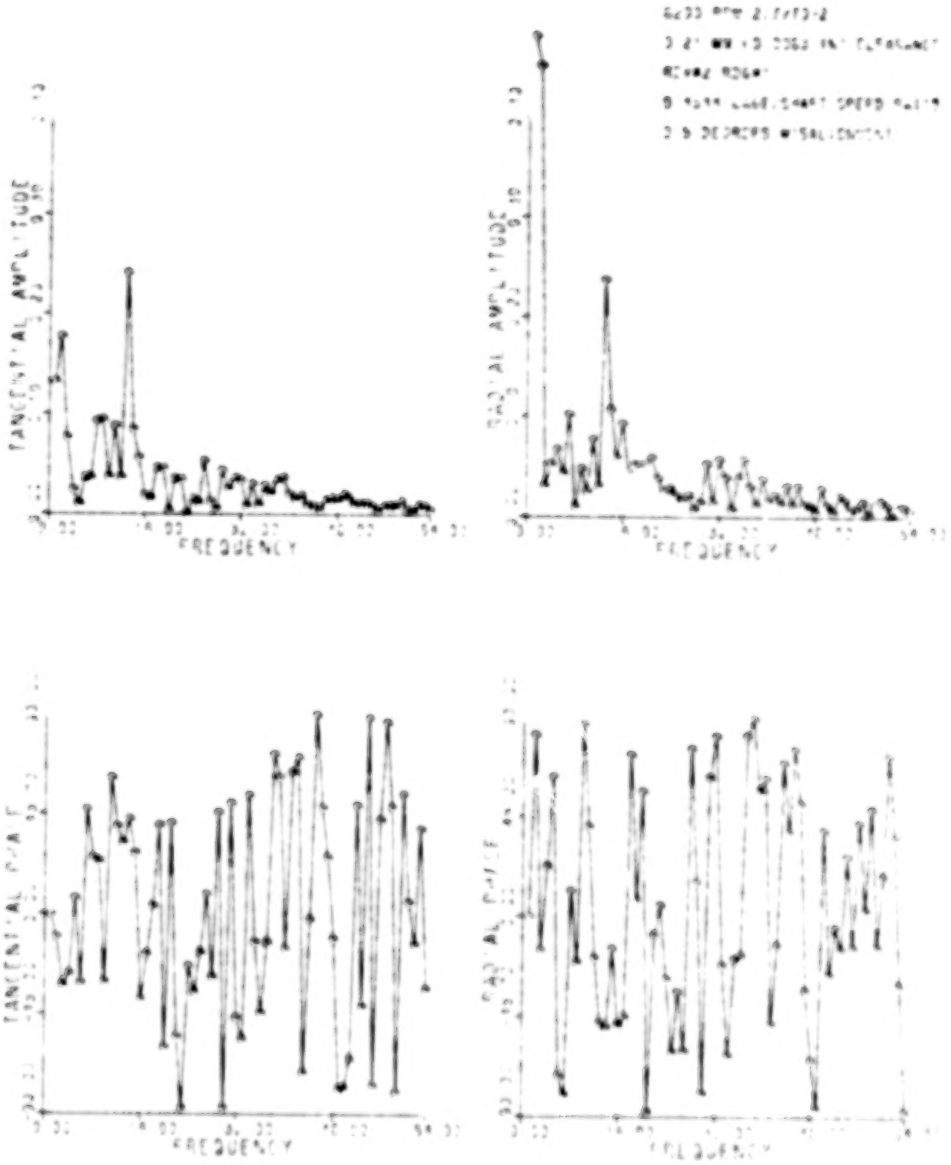

Figure 10b-2F Fast Fourier Transform of Data in Figure 10b-2

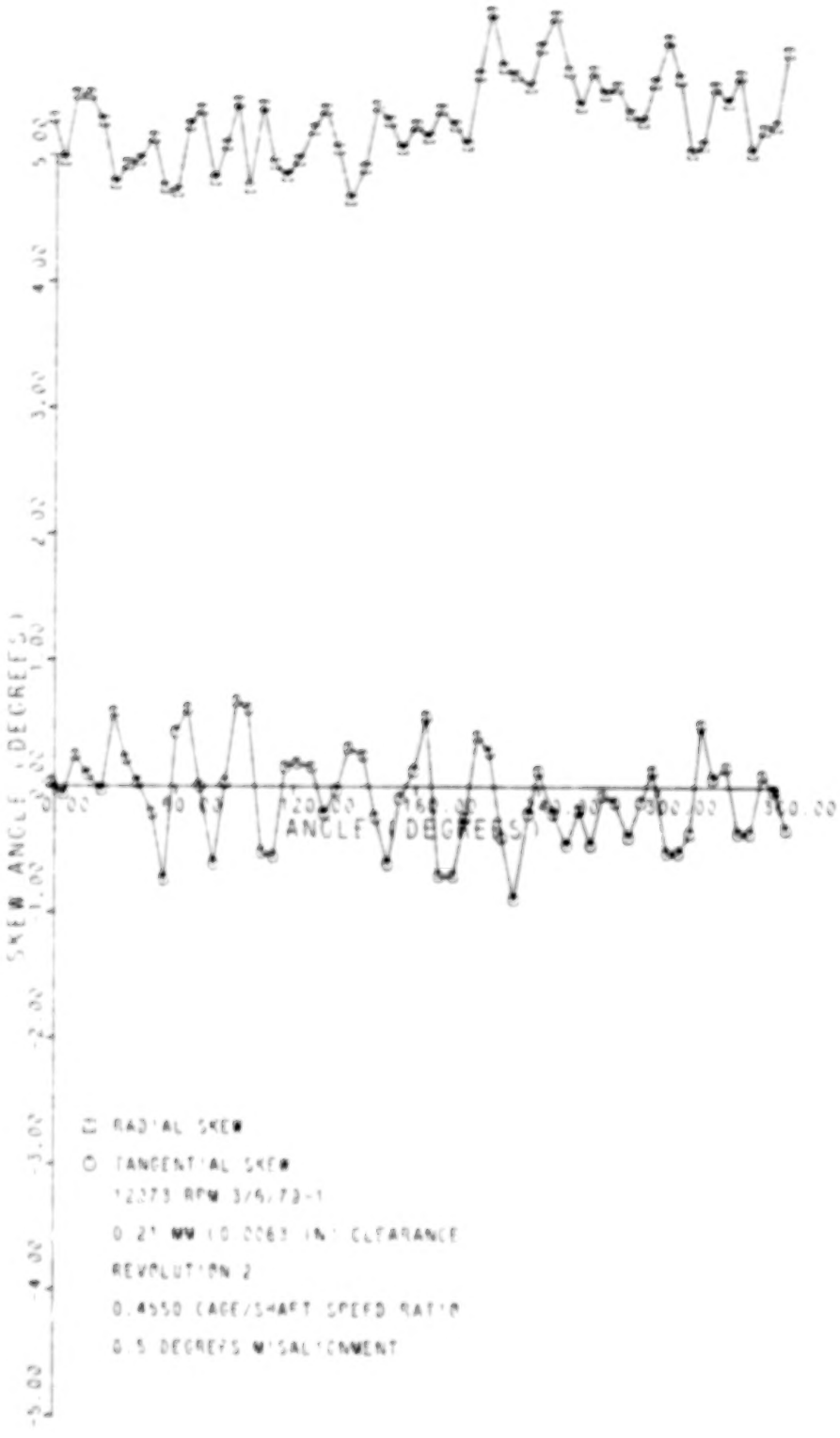

Figure 10c-1 Roller Skew, 0.21 mm Clearance Bearing, 0.50° Misalignment

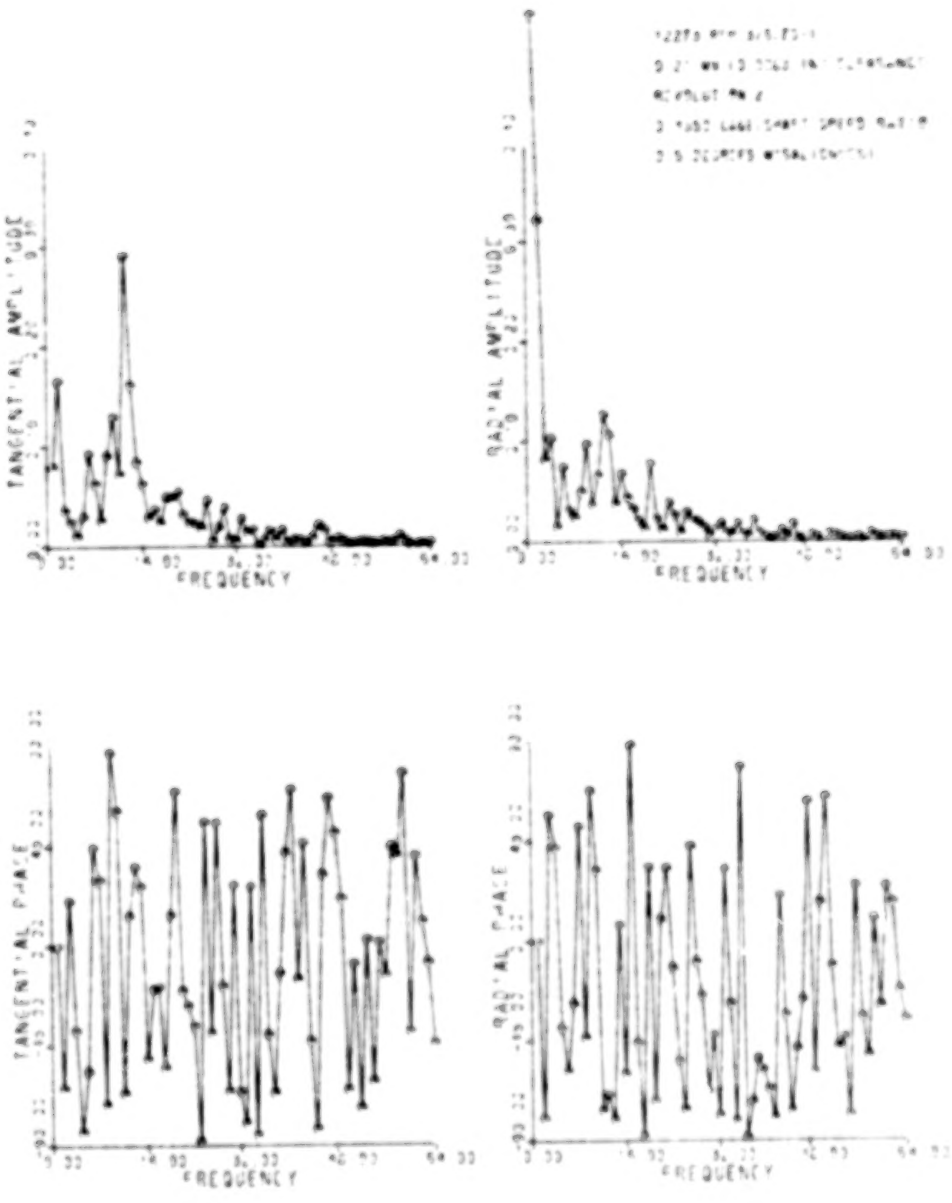

Figure 10c-1F Fast Fourier Transform of Data in Figure 10c-1

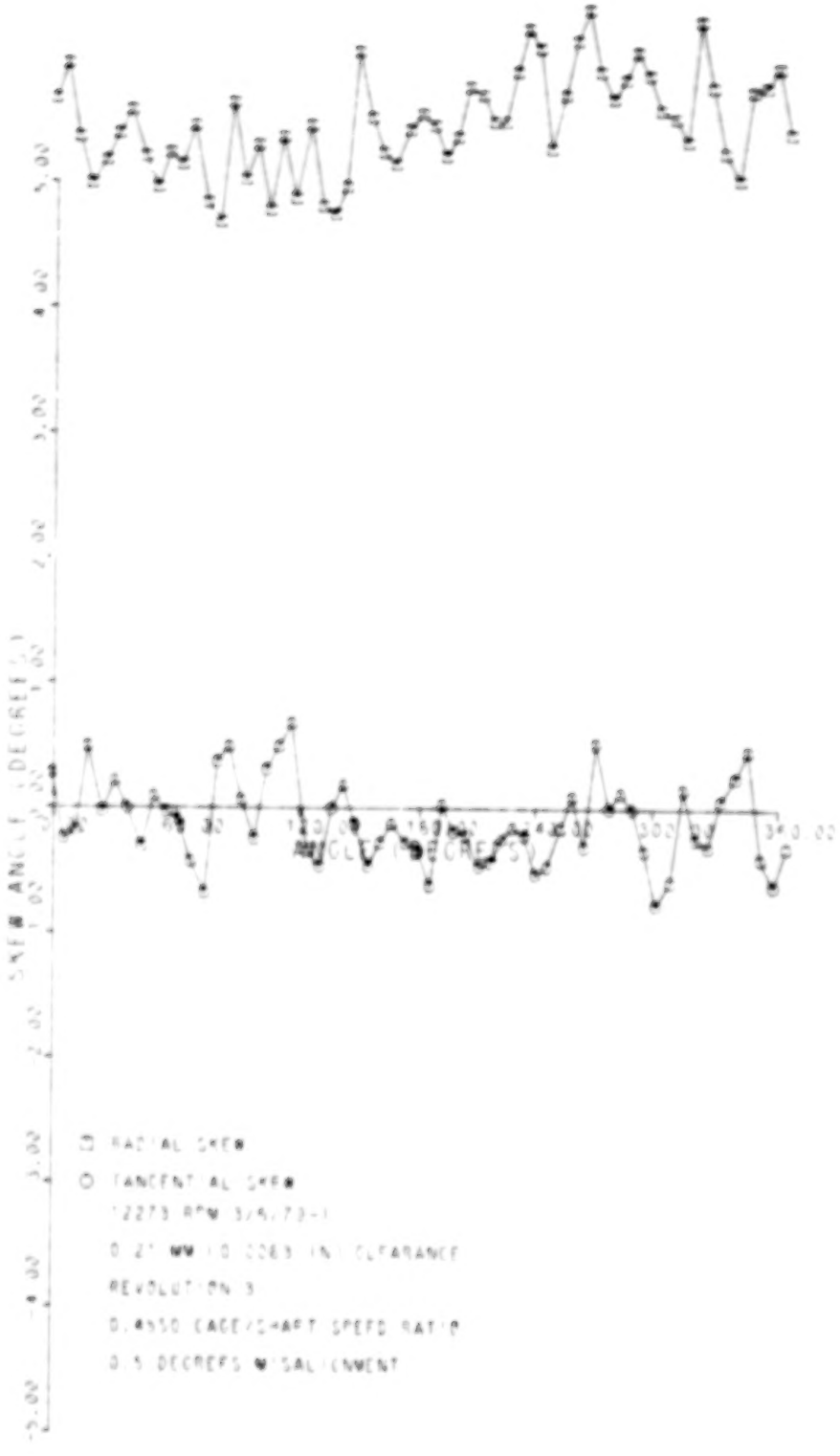

Figure 10c-2 Roller Skew, 0.21 mm Clearance Bearing, 0.50° Misalignment

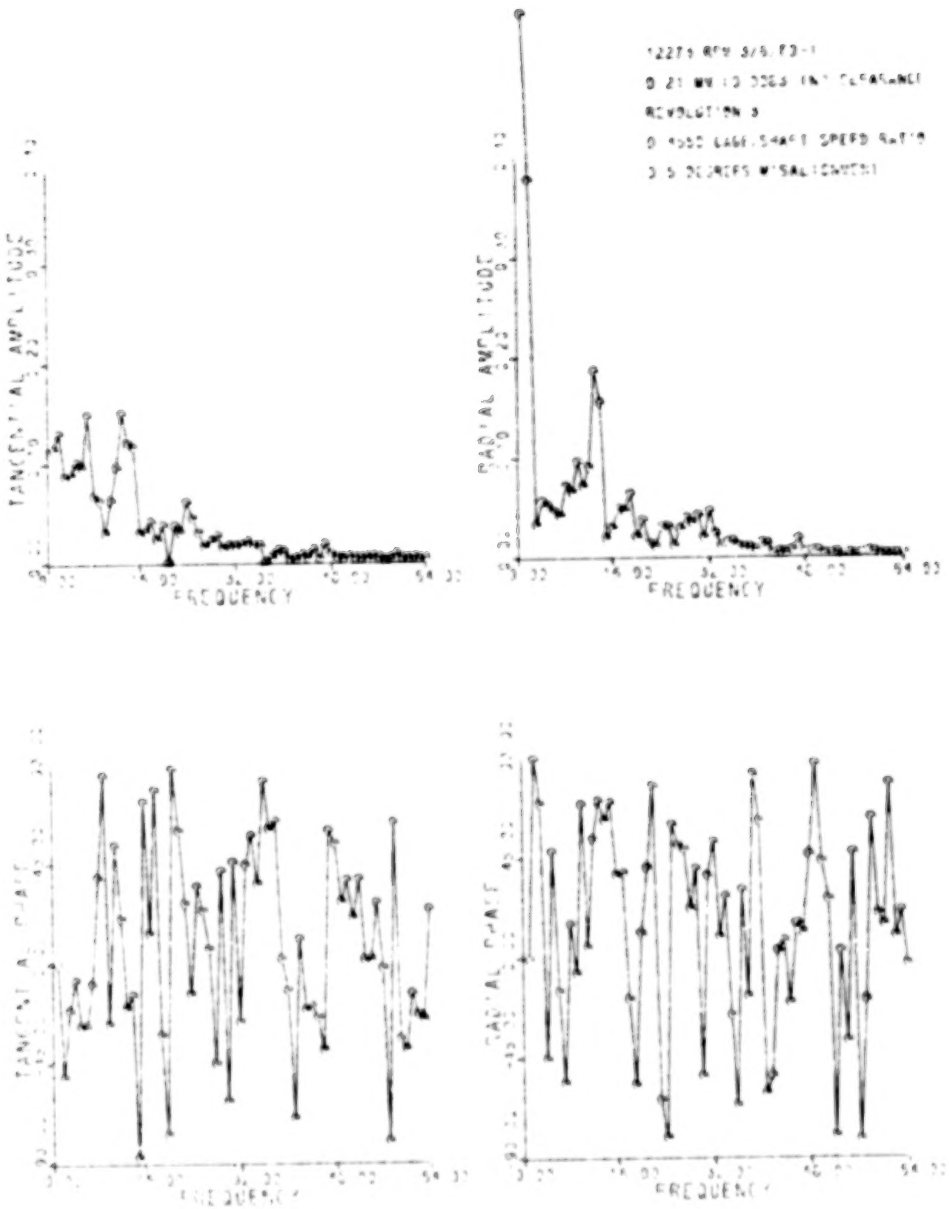

Figure 10c-2F Fast Fourier Transform of Data in Figure 10c-2

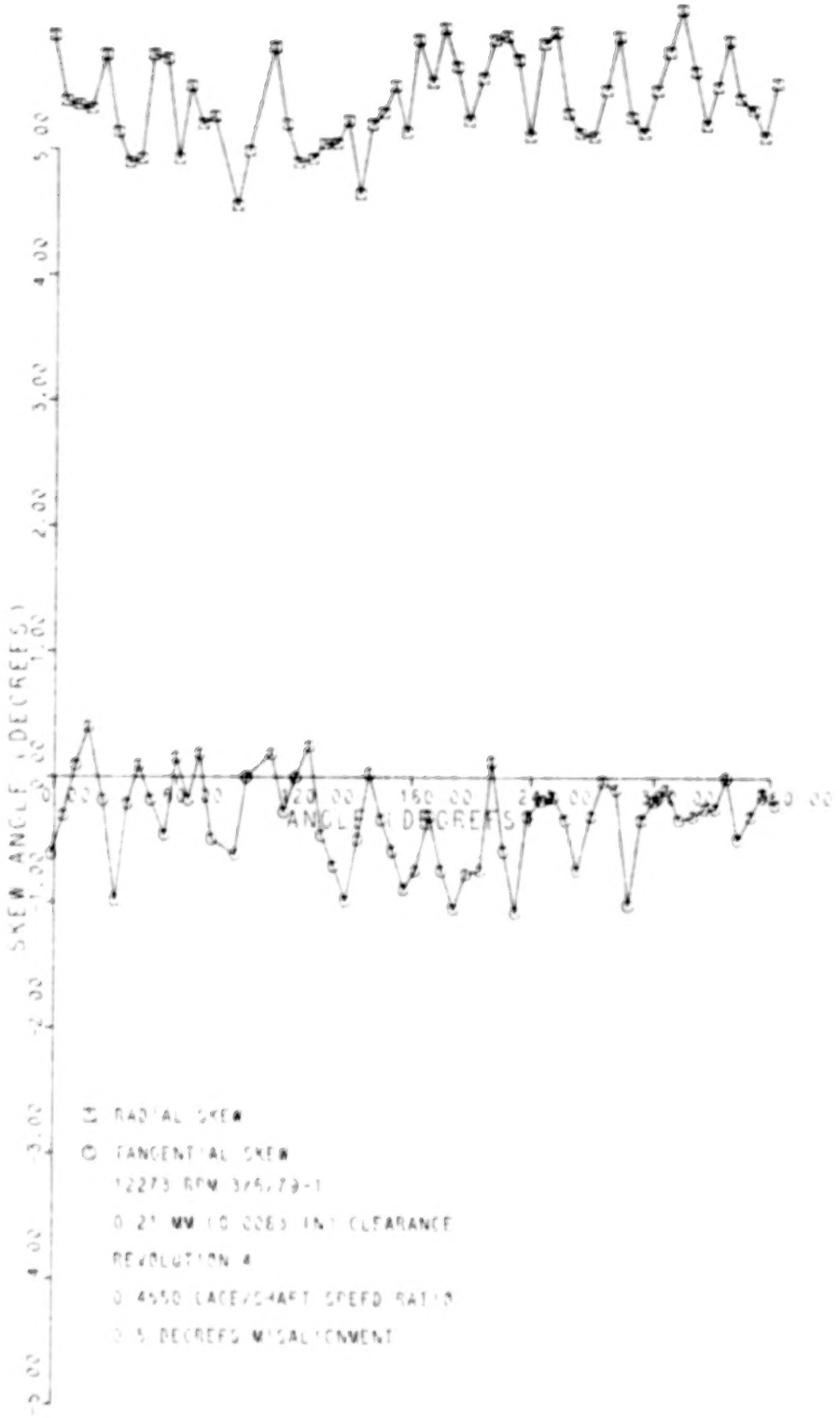

Figure 10c-3 Roller Skew, 0.21 mm Clearance Bearing, 0.50° Misalignment

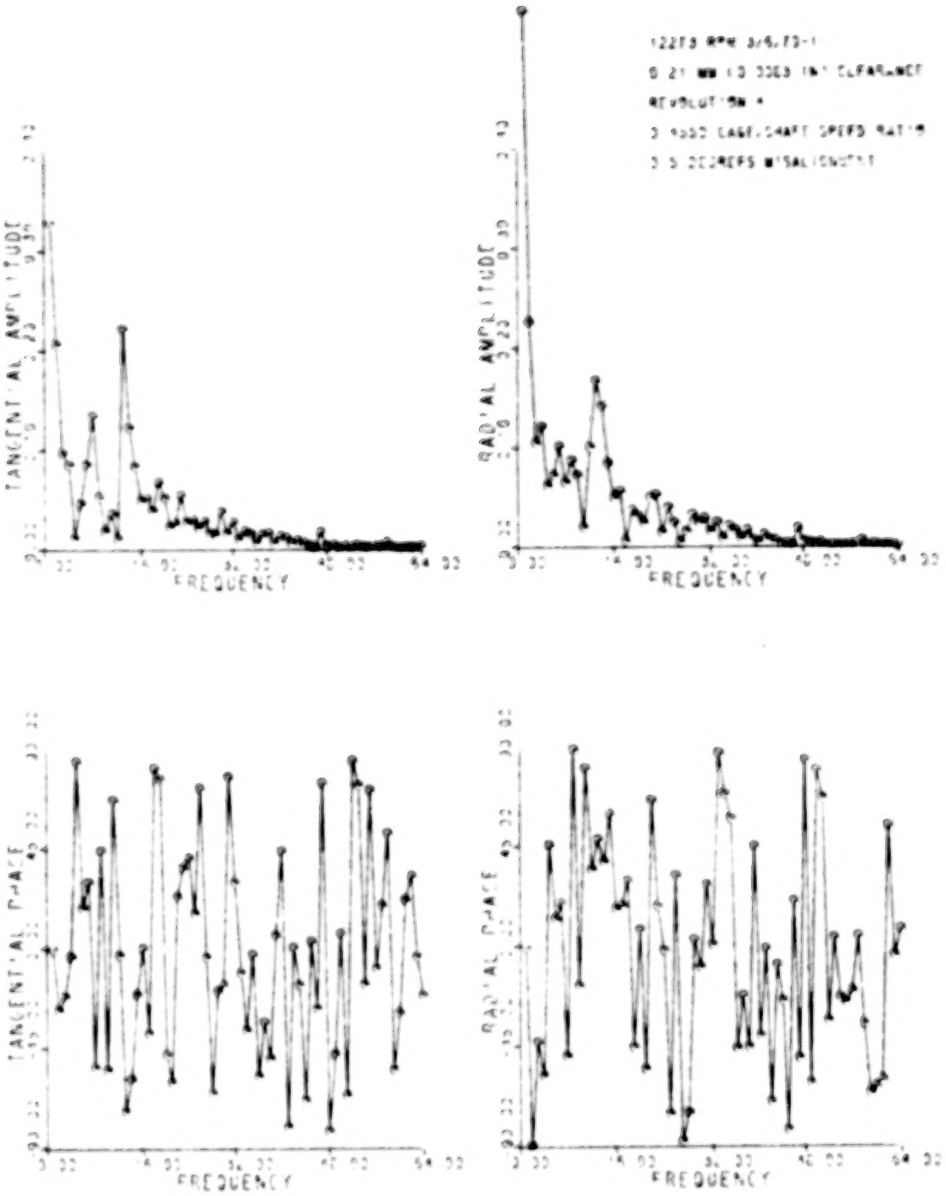

Figure 10c-3F Fast Fourier Transform of Data in Figure 10c-3

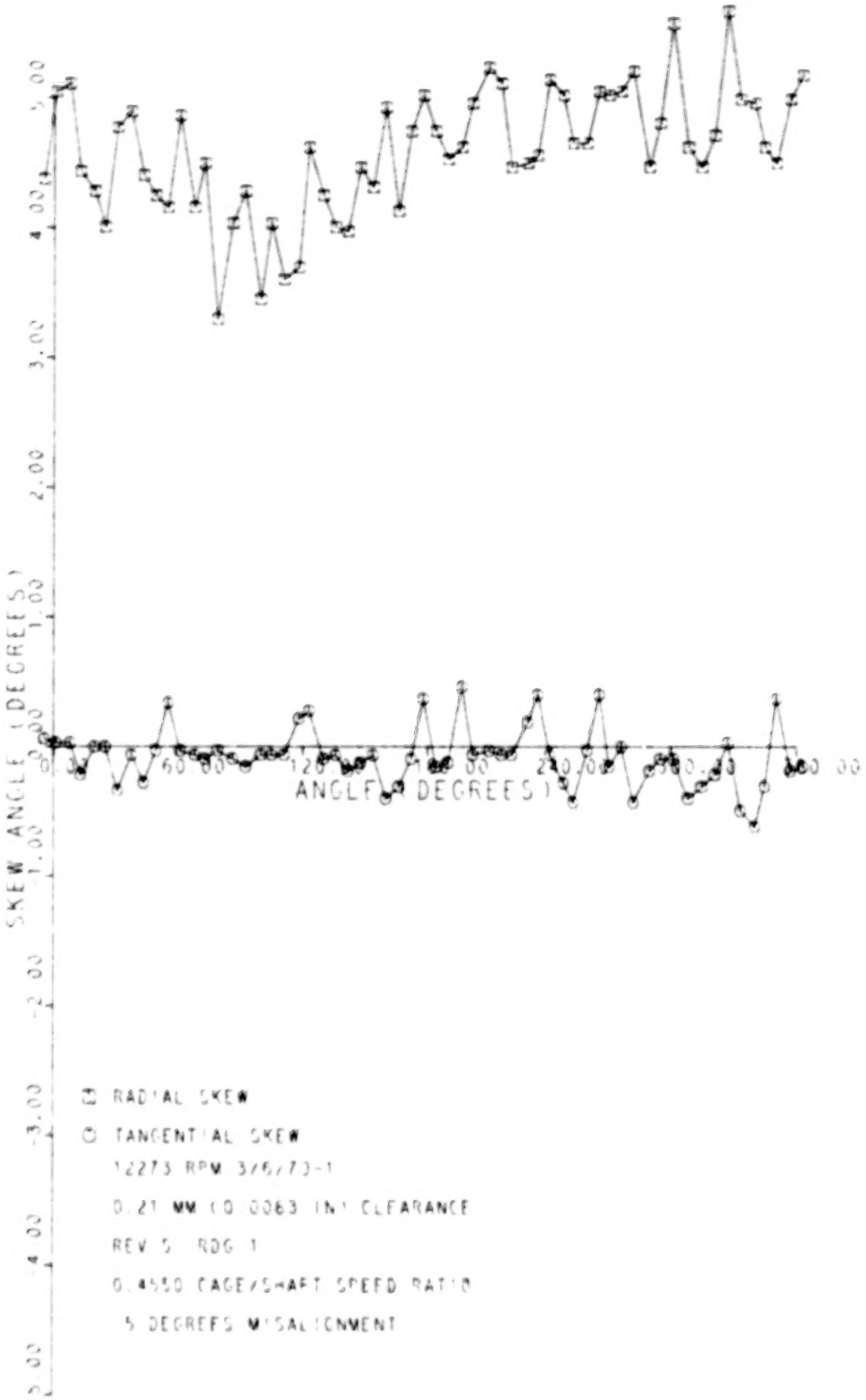

Figure 10c-4 Roller Skew, 0.21 mm Clearance Bearing, 0.50° Misalignment

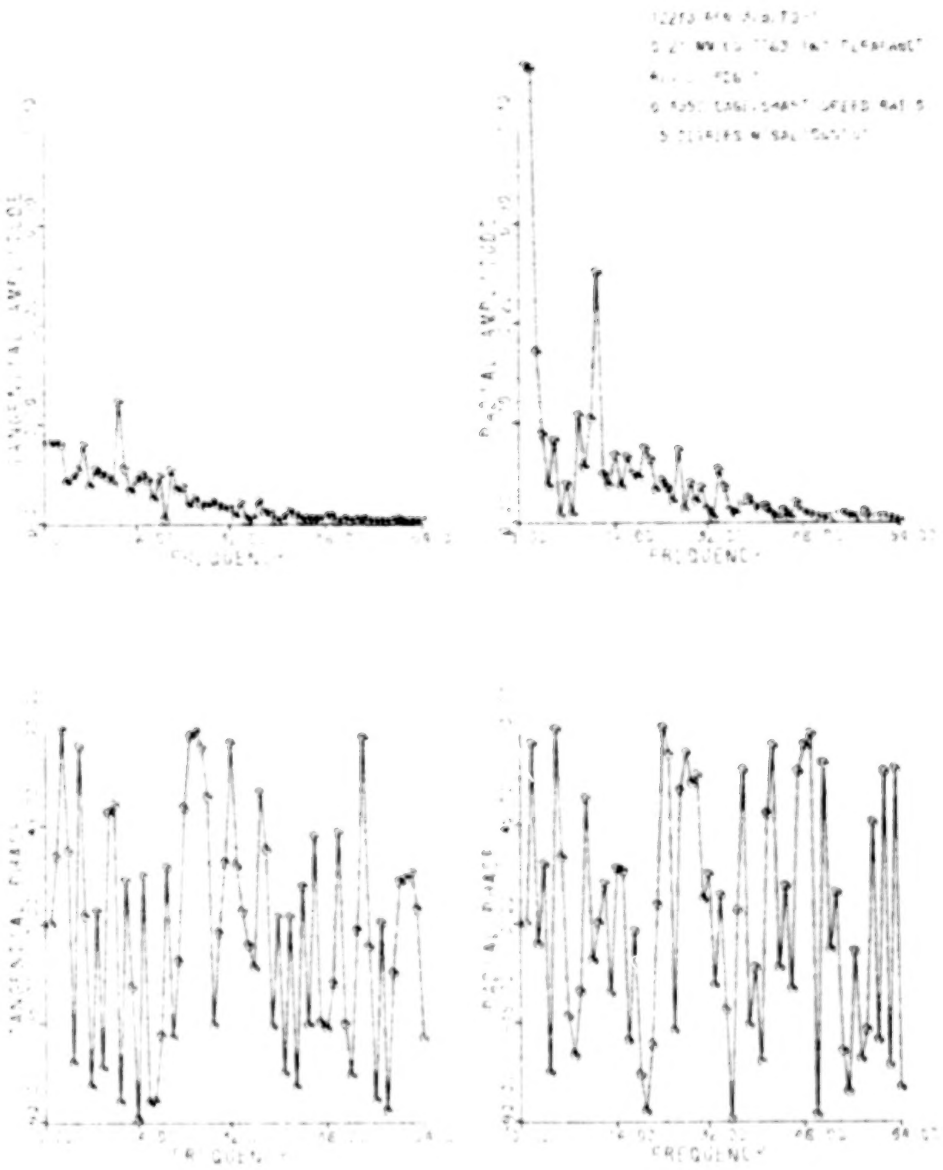

Figure 10c-4F Fast Fourier Transform of Data in Figure 10c-4

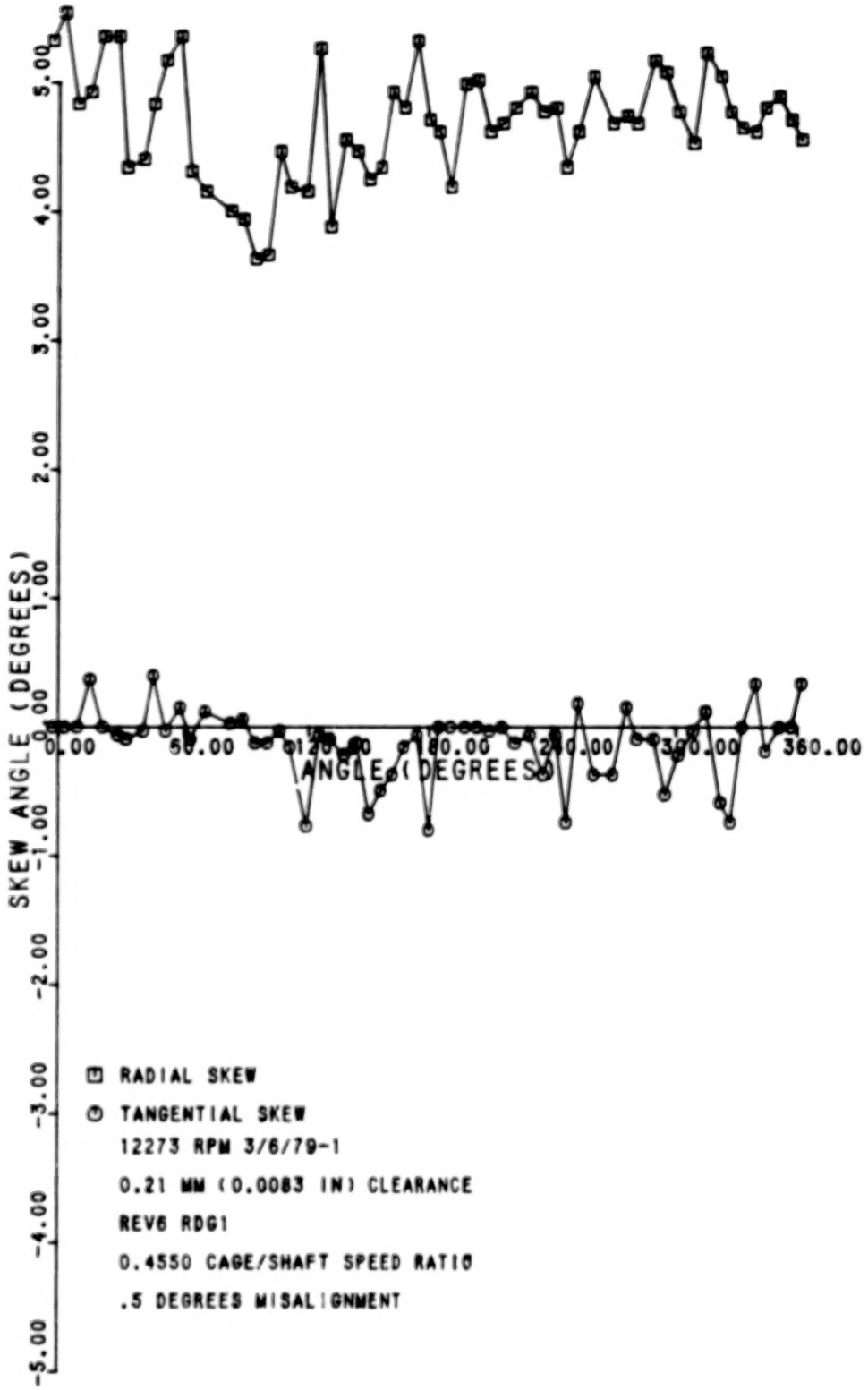

Figure 10c-5 Roller Skew, 0.21 mm Clearance Bearing, 0.50° Misalignment

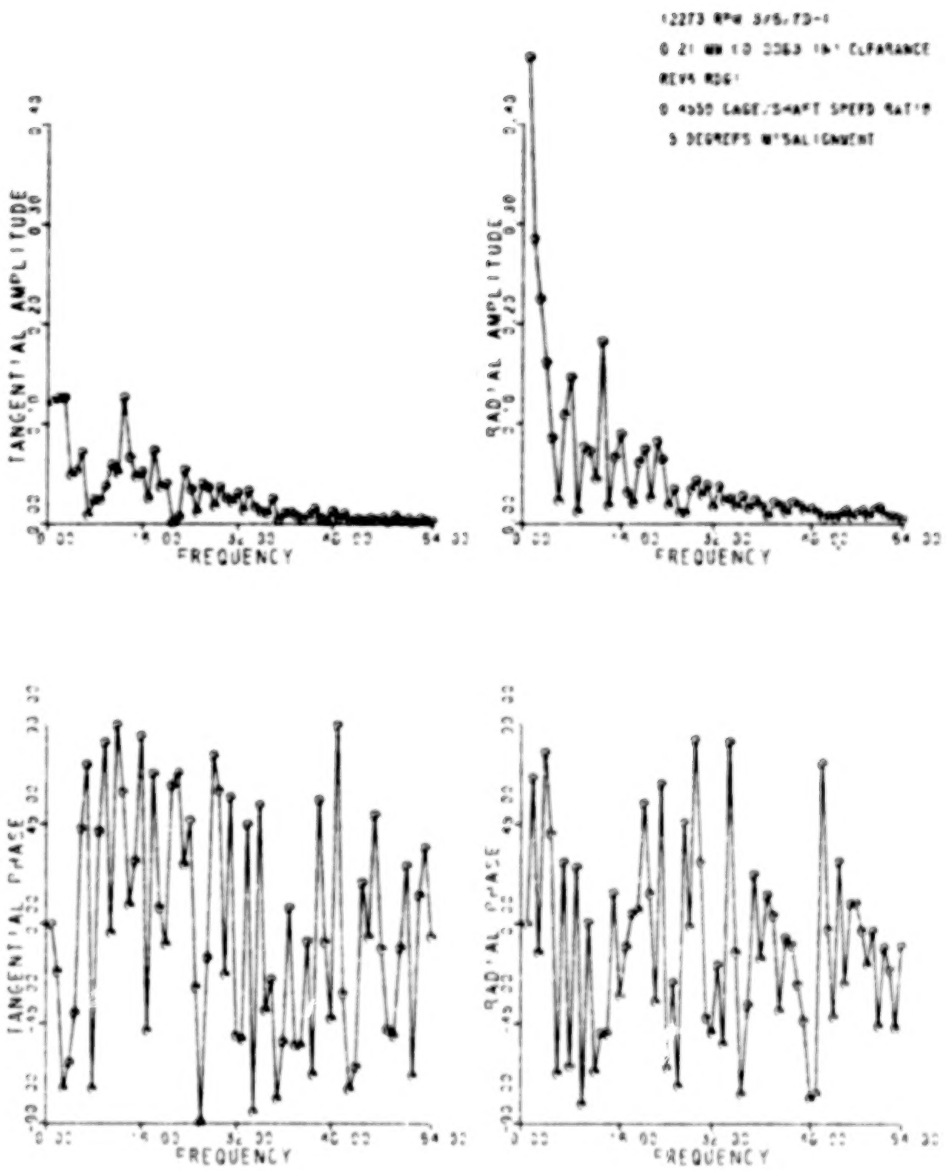

Figure 10c-5F Fast Fourier Transform of Data in Figure 10c-5

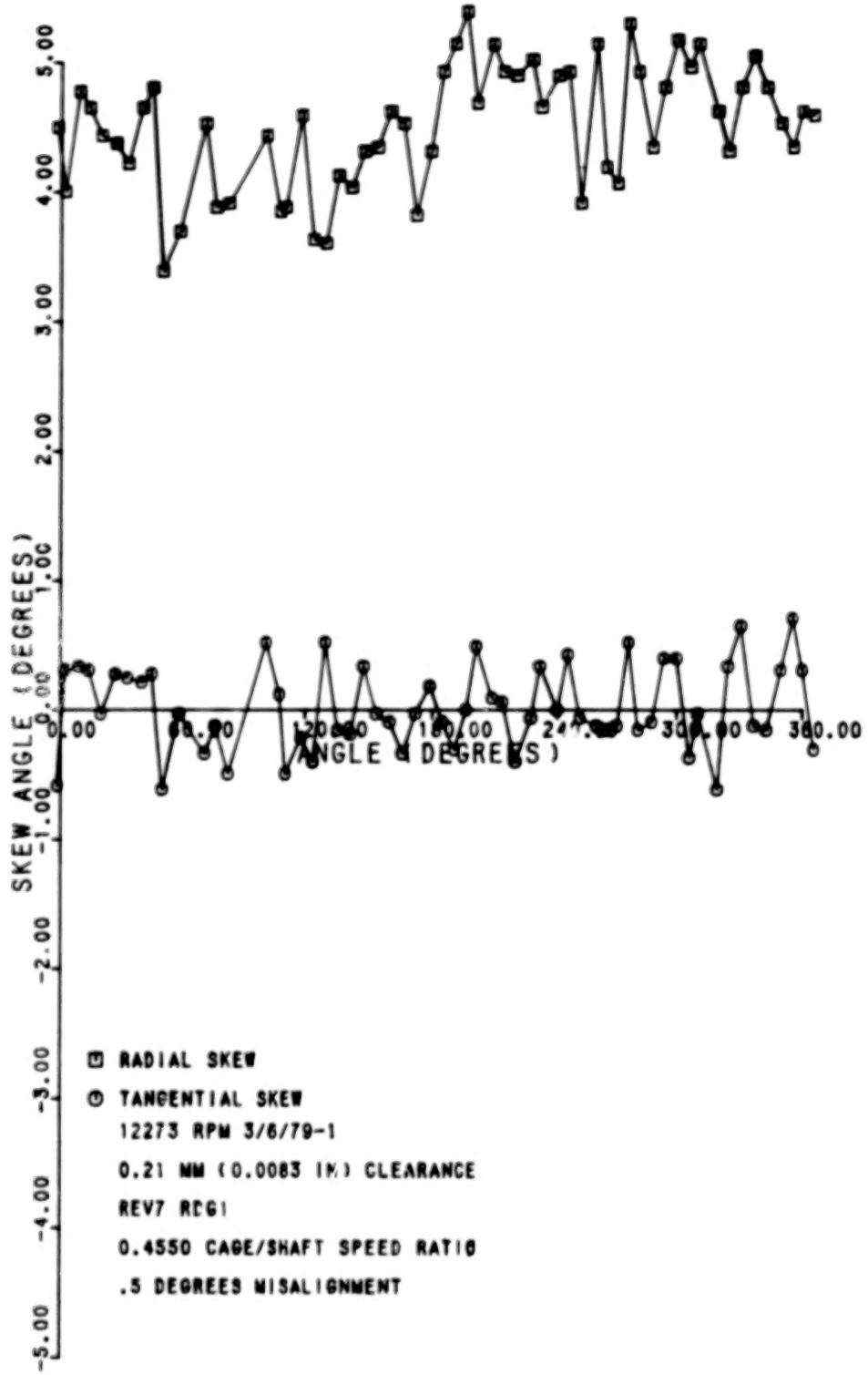

Figure 10c-6 Roller Skew, 0.21 mm Clearance Bearing, 0.50° Misalignment

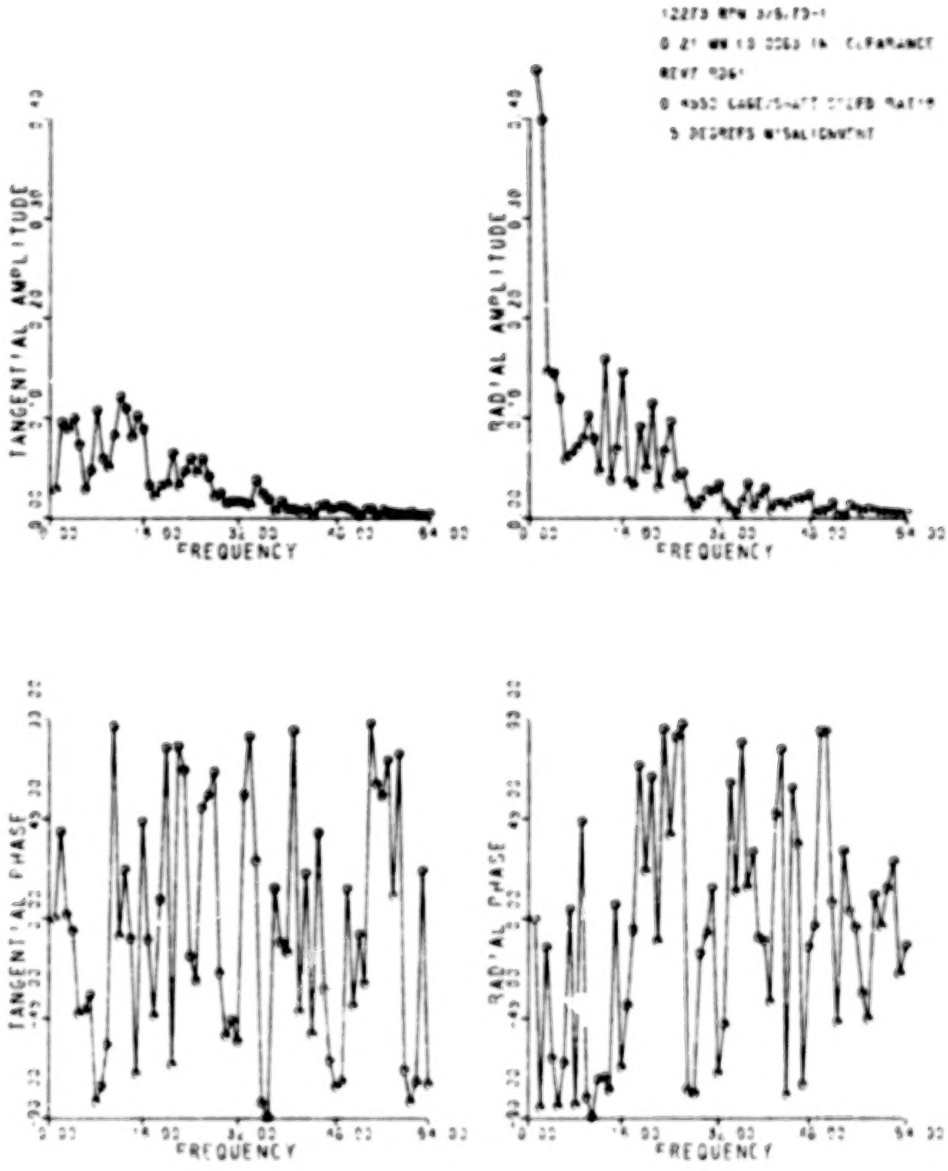

Figure 10c-6F Fast Fourier Transform of Data in Figure 10c-6

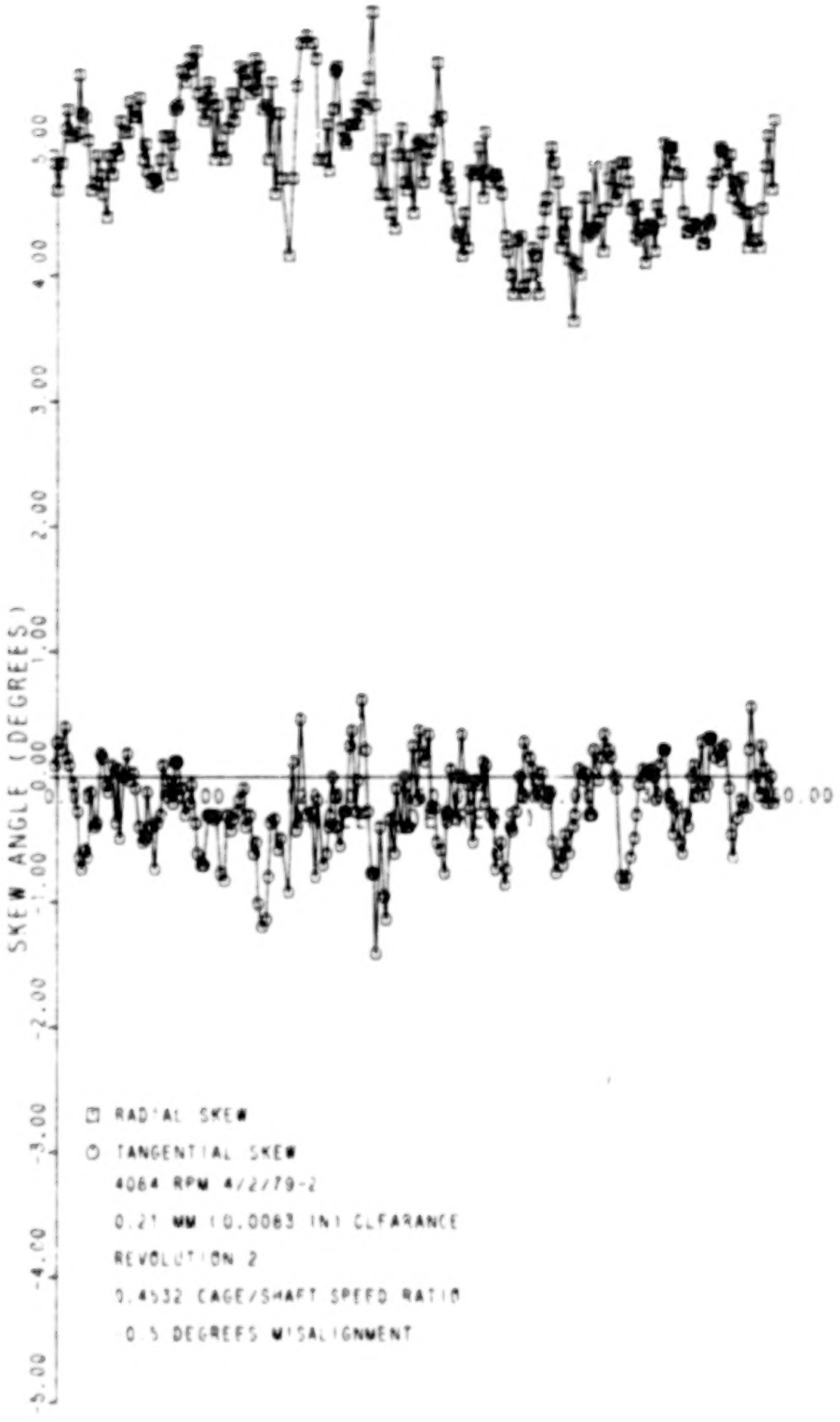

Figure 11a Roller Skew, 0.21 mm Clearance Bearing, -0.50° Misalignment

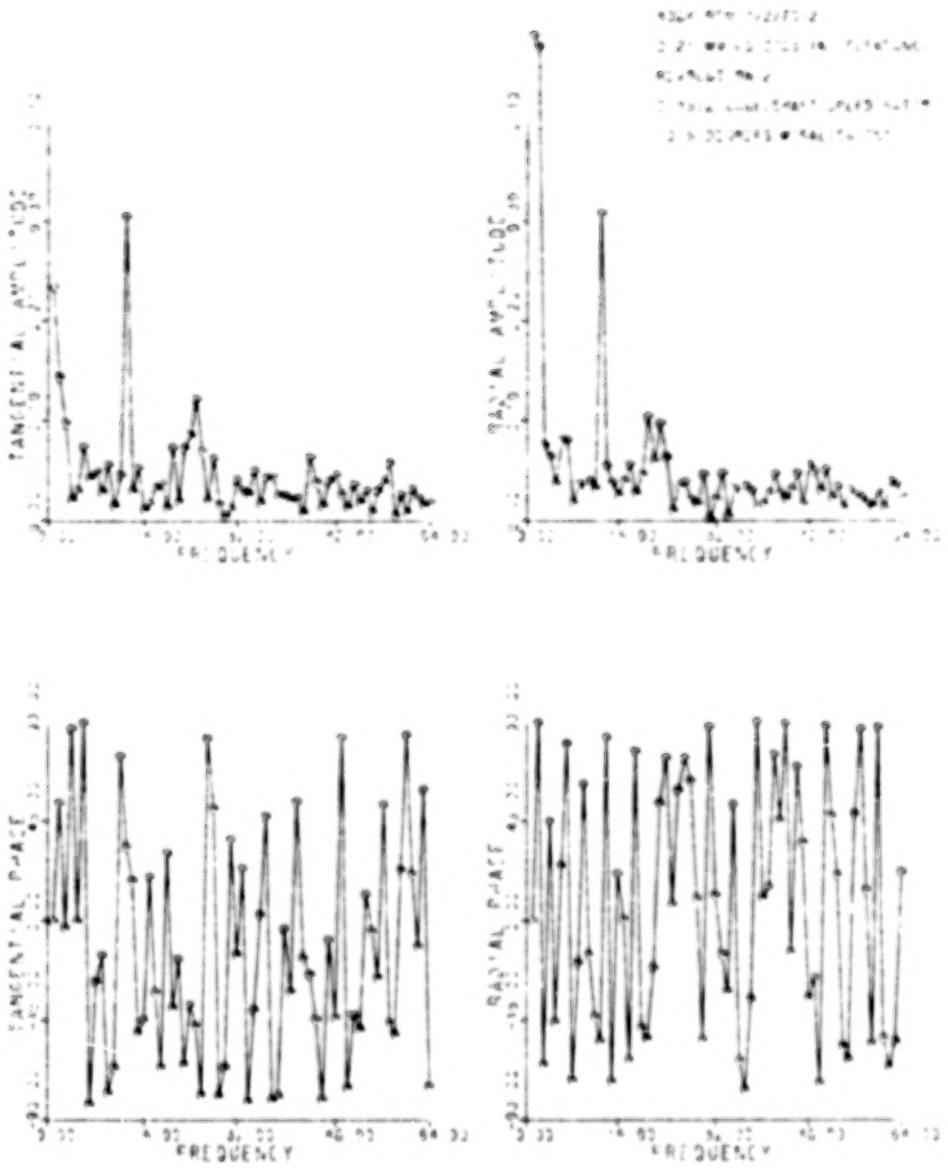

Figure 11aF Fast Fourier Transform of Data in Figure 11a

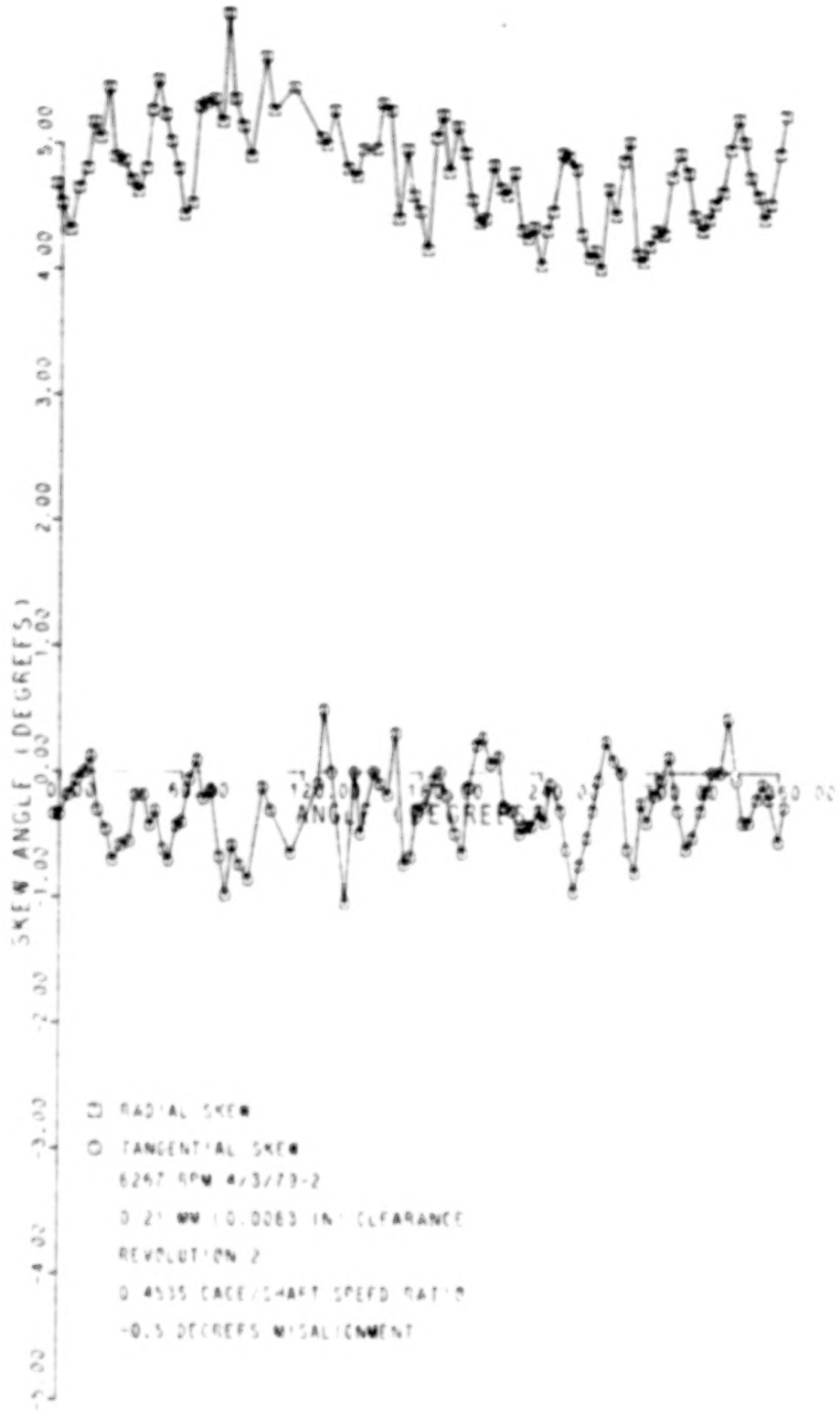

Figure 11b-1 Ro'ler Skew, 0.21 mm Clearance Bearing, -0.50° Misalignment

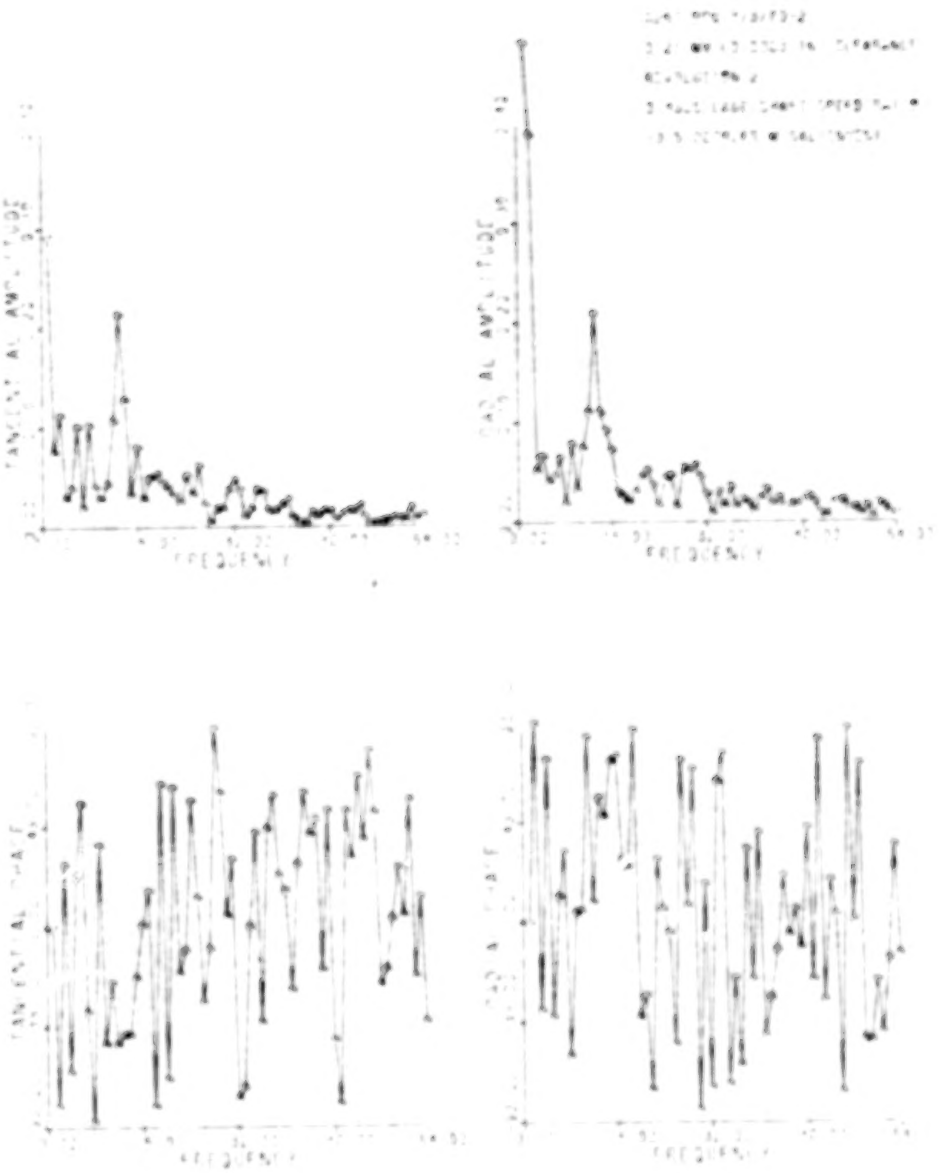

Figure 11b-1F Fast Fourier Transform of Data in Figure 11b-1

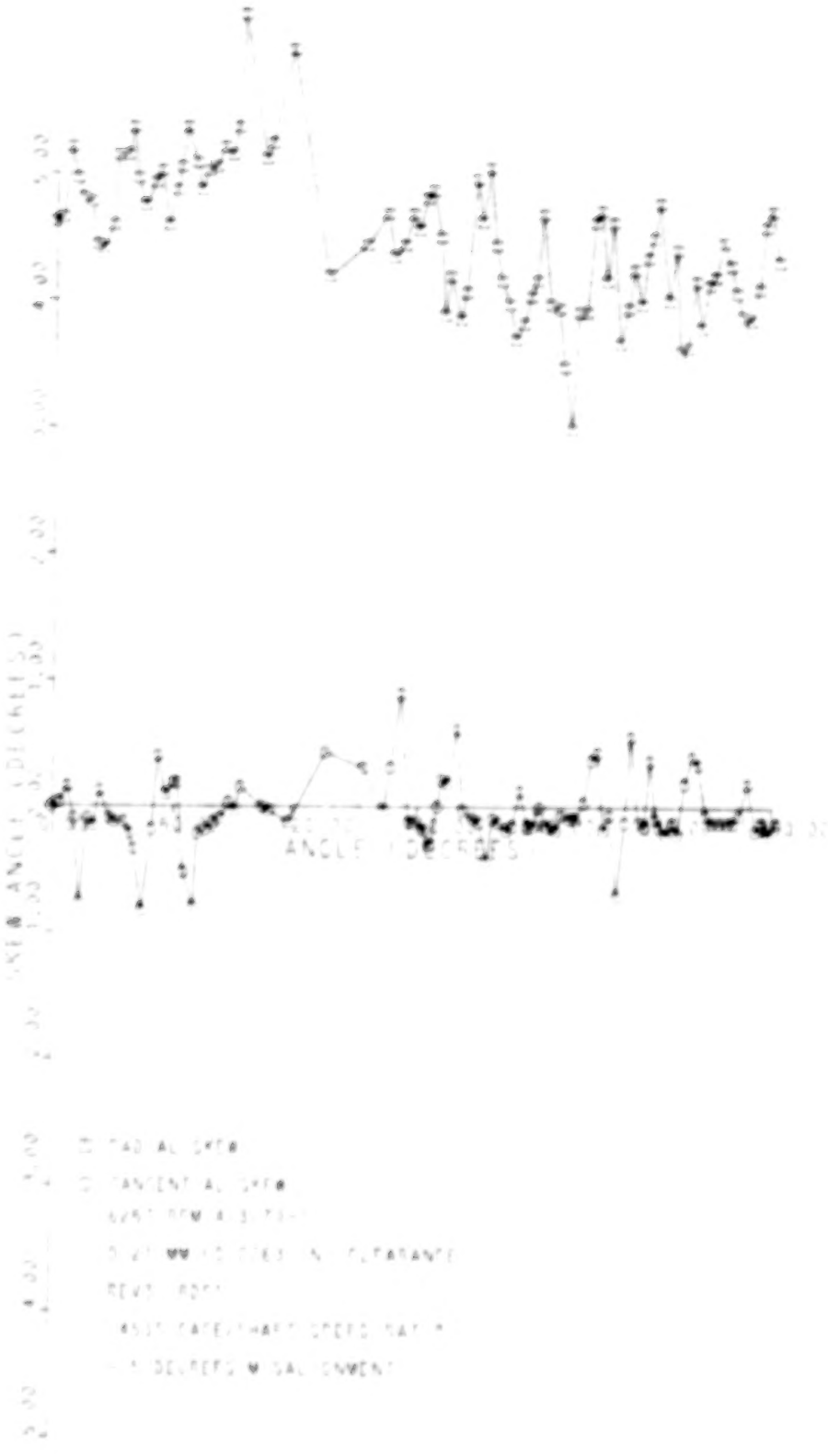

Figure 11b-2 Roller Skew, 0.21 mm Clearance Bearing, -0.50° Misalignment

Table of Contents

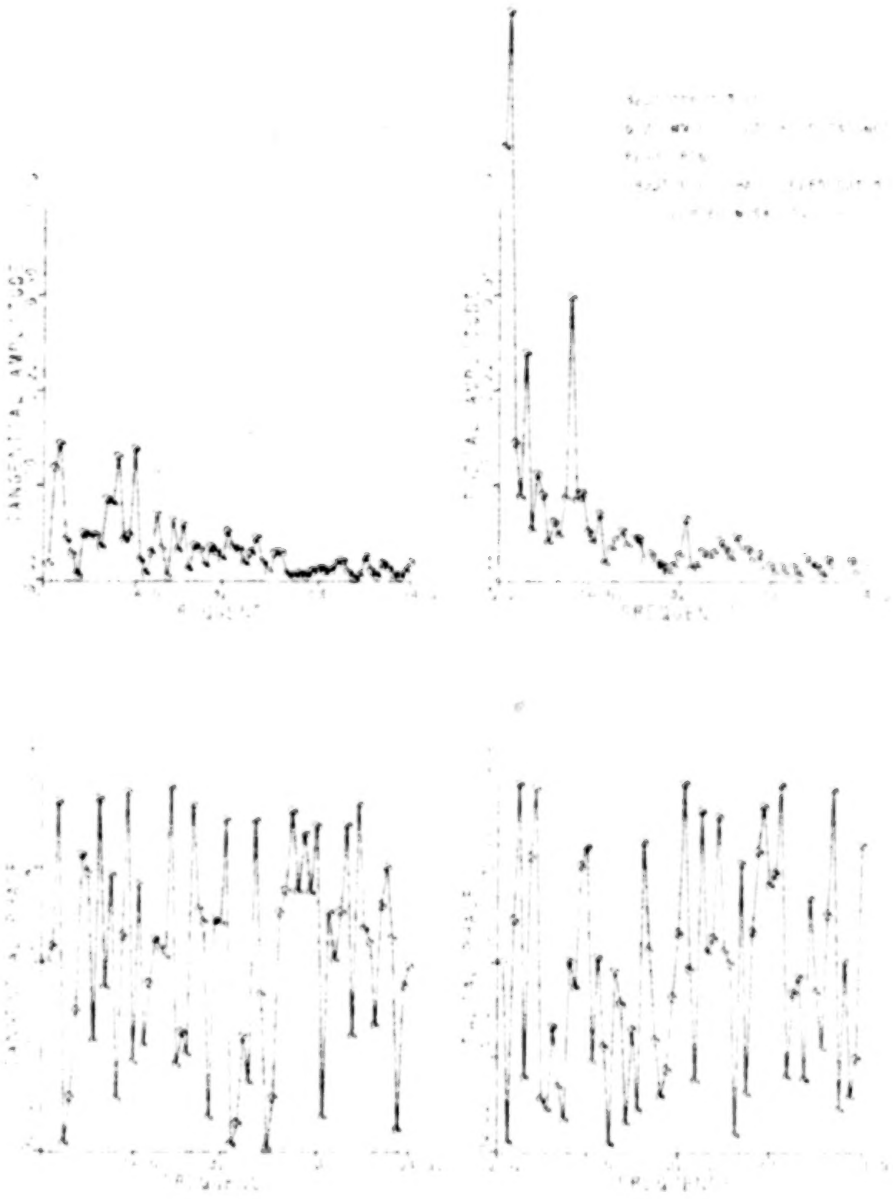

Figure 11b-2F Fast Fourier Transform of Data in Figure 11b-1

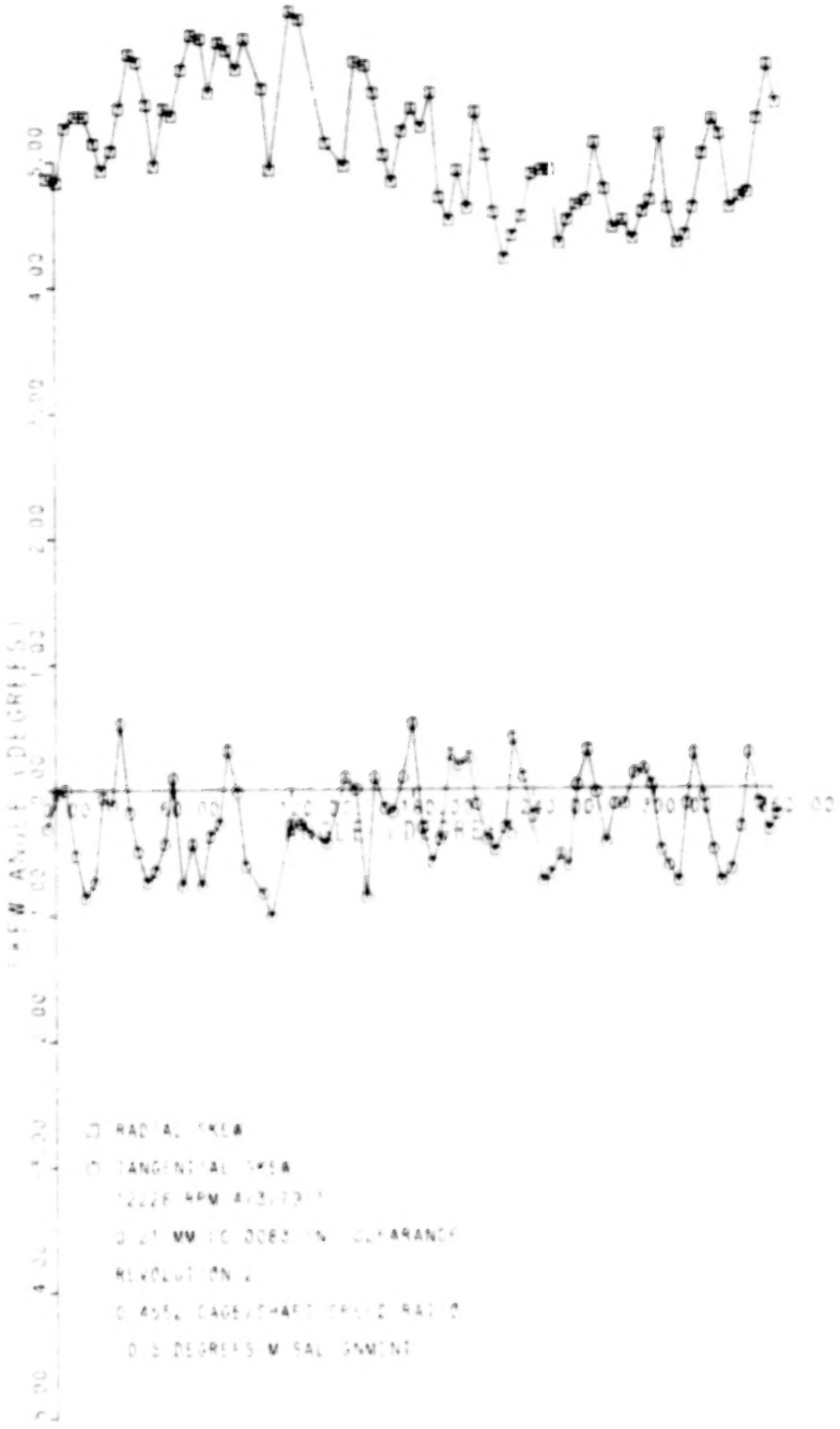

Figure 11c-1 Roller Skew, 0.21 mm Clearance Bearing, -0.50° Misalignment

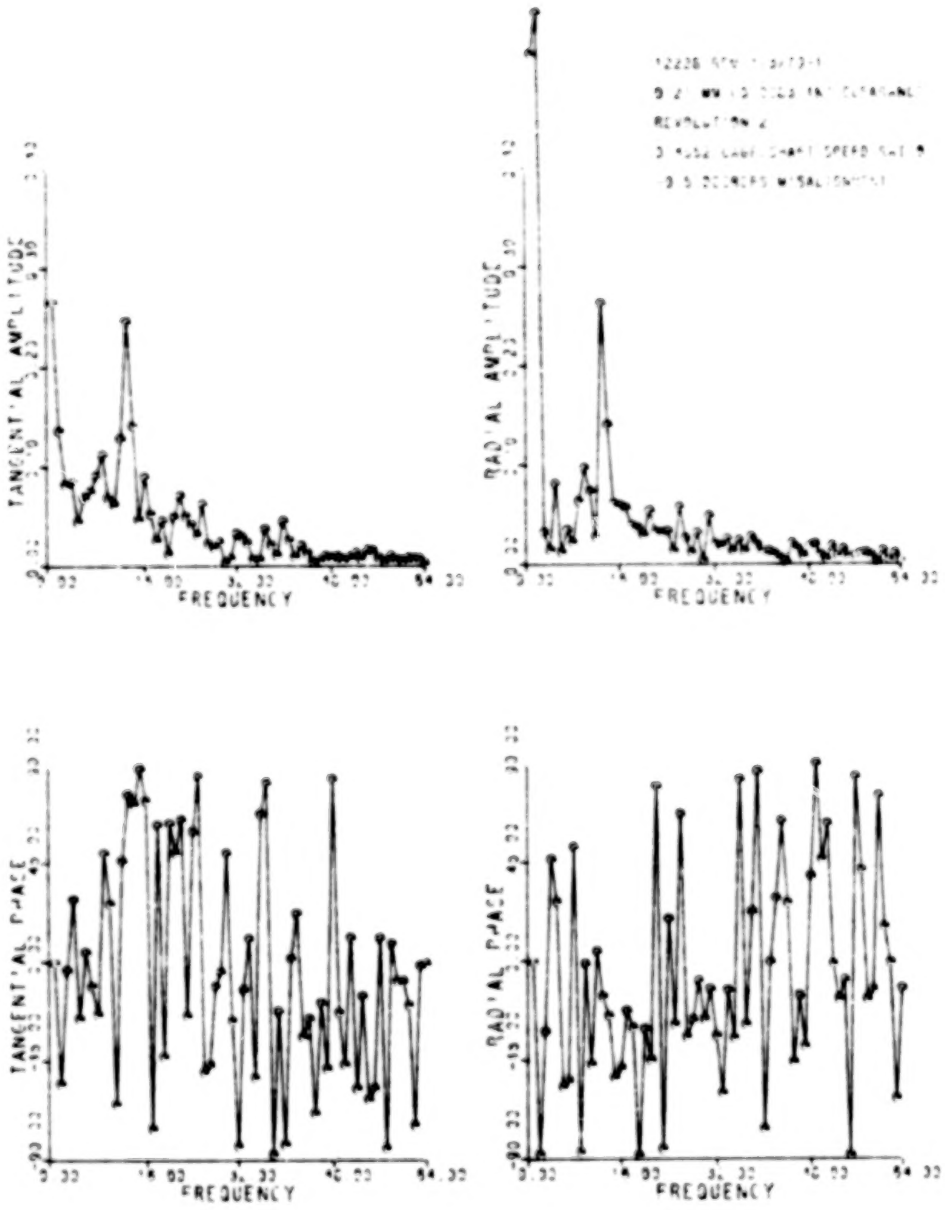

Figure 11c-1F Fast Fourier Transform of Data in Figure 11c-1

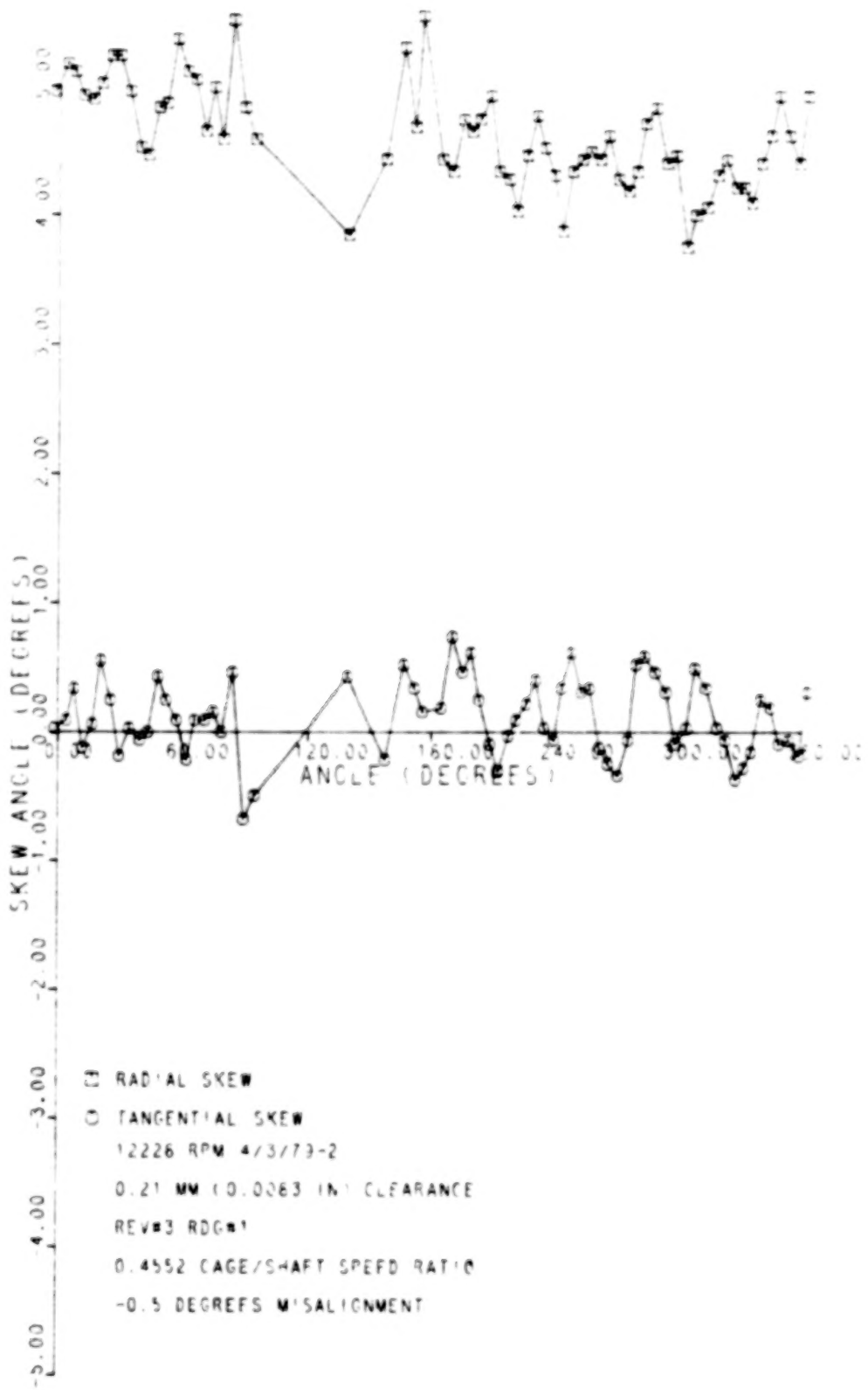

Figure 11c-2 Roller Skew, 0.21 mm Clearance Bearing, -0.50° Misalignment

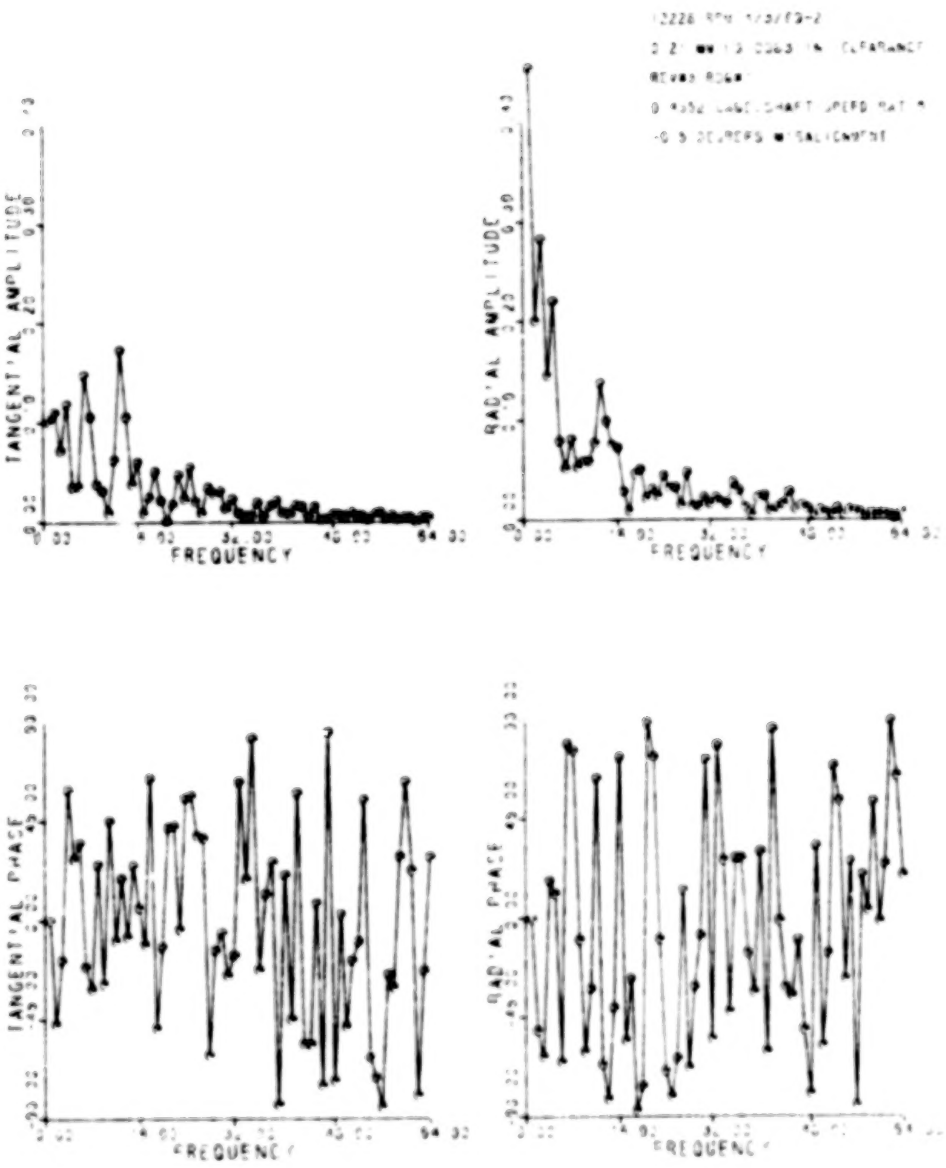

Figure 11c-2F Fast Fourier Transform of Data in Figure 11c-2

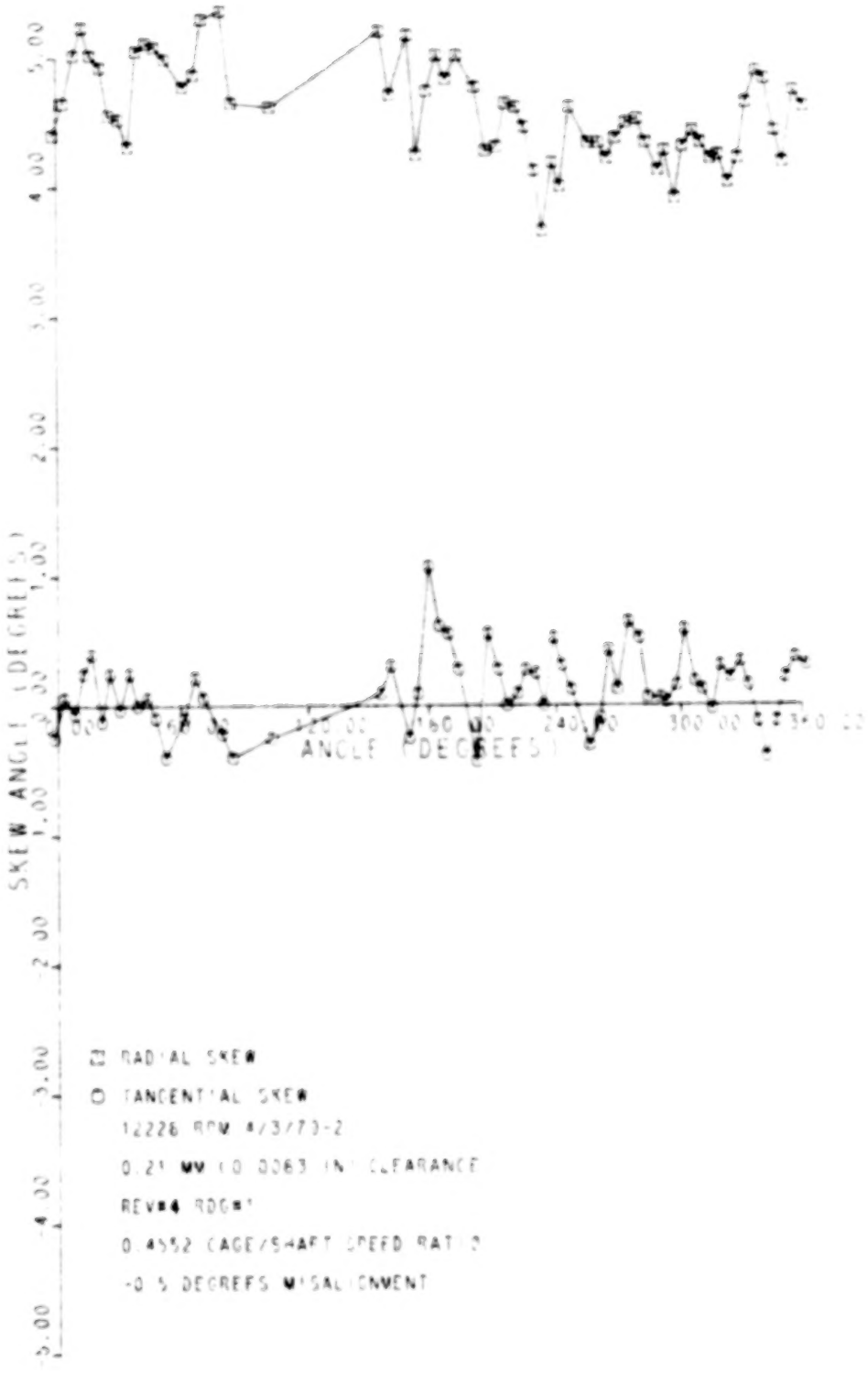

Figure 11c-3 Roller Skew, 0.21 mm Clearance Bearing, -0.50° Misalignment

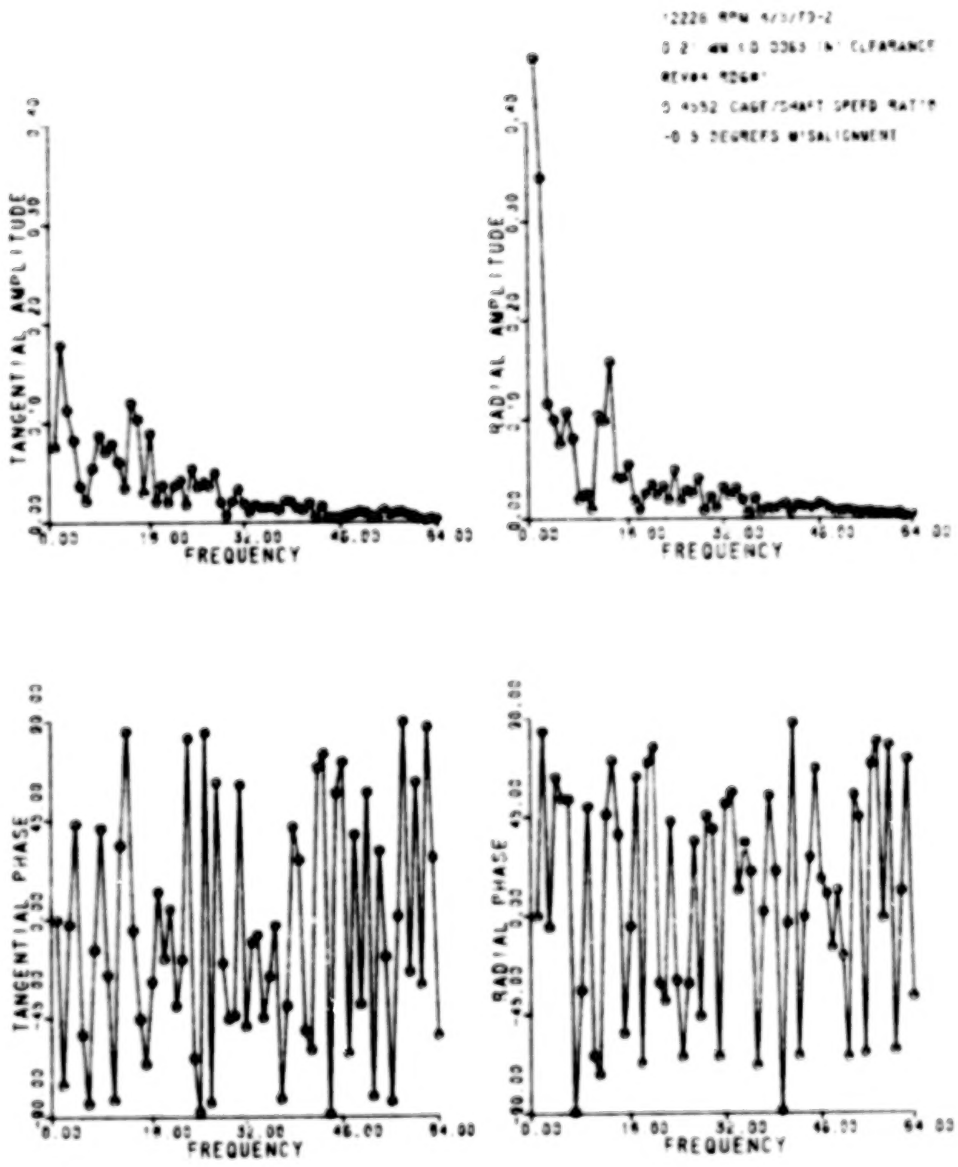

Figure 11c-3F Fast Fourier Transform of Data in Figure 11c-3

Table I

Roller Bearing Specifications

Inner Race			
Bore Dia.	mm (in)	118	(4.6457)
Raceway Dia.	mm (in)	131.66	(5.1834)
Flange Dia.	mm (in)	137.47	(5.4122)
Width	mm (in)	26.92	(1.060)
Groove Width	mm (in)	14.59	(.5746)
Flange Angle		0 degree	
Outer Race			
Outer Dia.	mm (in)	164.49	(6.4760)
Raceway Dia.	mm (in)	157.08	(6.1842)
Width	mm (in)	23.9	(.942)
Rollers			
Diameter	mm (in)	12.65	(.4979)
Length - overall	mm (in)	14.56	(.5733)
effective	mm (in)	13.04	(.5133)
flat	mm (in)	8.40	(.3307)
Crown Radius	mm (in)	622.3	(24.5)
End Radius	mm (in)	inf.	
Number		28	
Cage			
Land Dia.	mm (in)	137.95	(5.4312)
Axial Pocket Clearance	mm (in)	.020	(.0008)
Tangential Pocket Clearance	mm (in)	.221	(.0087)
Single Rail Width	mm (in)	4.6	(.18)
Clearance			
Serial No. A2284	mm (in)	0.18	(0.0073)
Serial No. A2279	mm (in)	0.21	(0.0083)

Table 2. - Summary of Test Conditions and Data
[PWA 541043]

(a) Serial No. A2284 - 0.18 mm (0.0073 in.) Clearance

Misalignment Degrees	Speed Case RPM	Figure	Exact Speed RPM	Date, Film Set	Cage to Shaft Speed Ratio	% Slip	
0	4000	4a	4 055	4/19/79-1	0.4537	0.6	Rev 2 Rdg 2
0	8000	4b	8 229	4/30/79-1	0.4545	0.4	Rev 1
0	12000	4c	12 161	4/30/79-2	0.4493	1.5	Rdg 3
0.25	4000	5a	4 135	6/1/79-2	0.4529	0.7	Rev 1 Starts 57°
0.25	8000	5b-1	8 169	5/31/79-1	0.4531	0.7	Rev 1 Starts 12°
		5b-2	8 169	5/31/79-1	0.4531	0.7	Rev 2 Rdg 2
0.25	12000	5c-1	12 346	6/1/79-2	0.4538	0.5	Rev 1 Rdg 1
		5c-2	12 346	6/1/79-1	0.4541	0.5	Rev 2
0.5	4000	6a	4 020	6/8/79-1			Rev 1 Rdg 1
0.5	8000	6b-1	8 137	6/8/79-2	0.4545	0.4	Rev Starts 193°
		6b-2	8 137	6/8/79-2	0.4545	0.4	Rev Starts 0°, inc.
0.5	12000	6c-1	12 238	6/8/79-3	0.4557	0.1	Rev 1
		6c-2	12 238	6/8/79-3	0.4557	0.1	Rev 2 Rdg 1
		6c-3	12 238	6/8/79-3	0.4541	0.5	Rev 3 Rdg 1
-0.5	4000	7a-1	4 247	6/11/79-2	0.4541	0.5	Rev 1
		7a-2	4 247	6/11/79-2	0.4541	0.5	Rev 2 Rdg 1
-0.5	8000	7b-1	8 390	8/6/79-2	0.4545	0.4	Rev 1 Rdg 1
		7b-2	8 390	8/6/79-2	0.4545	0.4	Rev 2 Rdg 1
-0.5	12000	7c-1	12 181	6/11/79-4	0.4547	0.3	Rev 1 Starts 114°
		7c-2	12 181	6/11/79-4	0.4547	0.3	Rev 2 Rdg 1

Table 2. - Summary of Test Conditions and Data
[PWA 541043]

(b) Serial No. A2279 - 0.21 mm (0.0083 in.) Clearance

Misalignment Degrees	Speed Case RPM	Figure	Exact Speed RPM	Date, Film Set	Cage to Shaft Speed Ratio	% Slip	
0	4000	8a	4 000	1/23/79-1	0.4537	0.6	Rev 2 Rdg 2
0	8000	8b	8 136	3/27/79-2	0.4521	0.9	Rev 2 After 0.5 misaligned
0	12000	8c	12 113	1/23/79-3	0.4524	0.8	Rev 1 Rdg 2
0.25	4000	9a	4 029	1/29/79-1	0.4540	0.5	Rev 2
0.25	8000	9b	8 119	1/25/79-2	0.4517	1.0	Rev 1 Rdg 1
0.25	12000	9c	12 127	1/26/79-1	0.4525	0.8	Rev 2 Rdg 2
0.5	4000	10a	4 082	2/7/79-1	0.4545	0.4	Rev 2
0.5	8000	10b-1	8 290	2/7/79-2	0.4544	0.4	Rev 1
		10b-2	8 290	2/7/79-2	0.4544	0.4	Rev 2 Rdg 1
0.5	12000	10c-1	12 273	3/6/79-1	0.4550	0.3	Rev 2
		10c-2	12 273	3/6/79-1	0.4550	0.3	Rev 3
		10c-3	12 273	3/6/79-1	0.4550	0.3	Rev 4
		10c-4	12 273	3/6/79-2	0.4549	0.3	Rev 5
		10c-5	12 273	3/6/79-2	0.4549	0.3	Rev 6
		10c-6	12 273	3/6/79-2	0.4549	0.3	Rev 7
-0.5	4000	11a	4 08[illegible]	4/2/79-2	0.4532	0.7	Rev 2
-0.5	8000	11b-1	8 267	4/3/79-2	0.4535	0.8	Rev 2
		11b-2	8 267	4/3/79-2	0.4535	0.8	Rev 3
-0.5	12000	11c-1	12 228	4/3/79-1	0.4552	0.2	Rev 2
		11c-2	12 228	4/3/79-1	0.4552	0.2	Rev 3
		11c-3	12 228	4/3/79-1	0.4552	0.2	Rev 4

1 Report No.	2 Government Accession No.	3 Recipient's Catalog No.
NASA CR-[illegible]		

4 Title and Subtitle	5 Report Date
ROLLER SKEWING MEASUREMENTS IN CYLINDRICAL ROLLER BEARINGS	January 1981
	6 Performing Organization Code

7 Author(s)	8 Performing Organization Report No.
Lester J. Nypan	None
	10 Work Unit No.

9 Performing Organization Name and Address	11 Contract or Grant No.
California State University, Northridge Northridge, California 91330	NSG-3065
	13 Type of Report and Period Covered
12 Sponsoring Agency Name and Address	Contractor Report
National Aeronautics and Space Administration Washington, D.C. 20546	14 Sponsoring Agency Code

15 Supplementary Notes

Lewis Technical Monitor: Harold H. Coe
Final Report

16 Abstract

Measurements of roller skewing in a 118 mm bore roller bearing operating at shaft speeds to 12,000 rpm are reported. High speed motion pictures of a modified roller were taken through a derotation prism to record skewing as the roller moved through loaded and unloaded regions of the bearing. Subsequent frame by frame measurement of the photographic film provided information on roller skewing. Radial and tangential skew amplitudes of 0.4 to 0.5 degrees were observed with 0.5 degree misalignment.

17 Key Words (Suggested by Author(s))	18 Distribution Statement
Roller bearings; Roller skewing; Misalignment; Skew angle; Cylindrical	Unclassified - unlimited Subject Category [illegible]

19 Security Classif. (of this report)	20 Security Classif. (of this page)	21 No. of Pages	22 Price*
Unclassified	Unclassified	104	A06

* For sale by the National Technical Information Service, Springfield, Virginia 22161

NASA-Langley, 1981

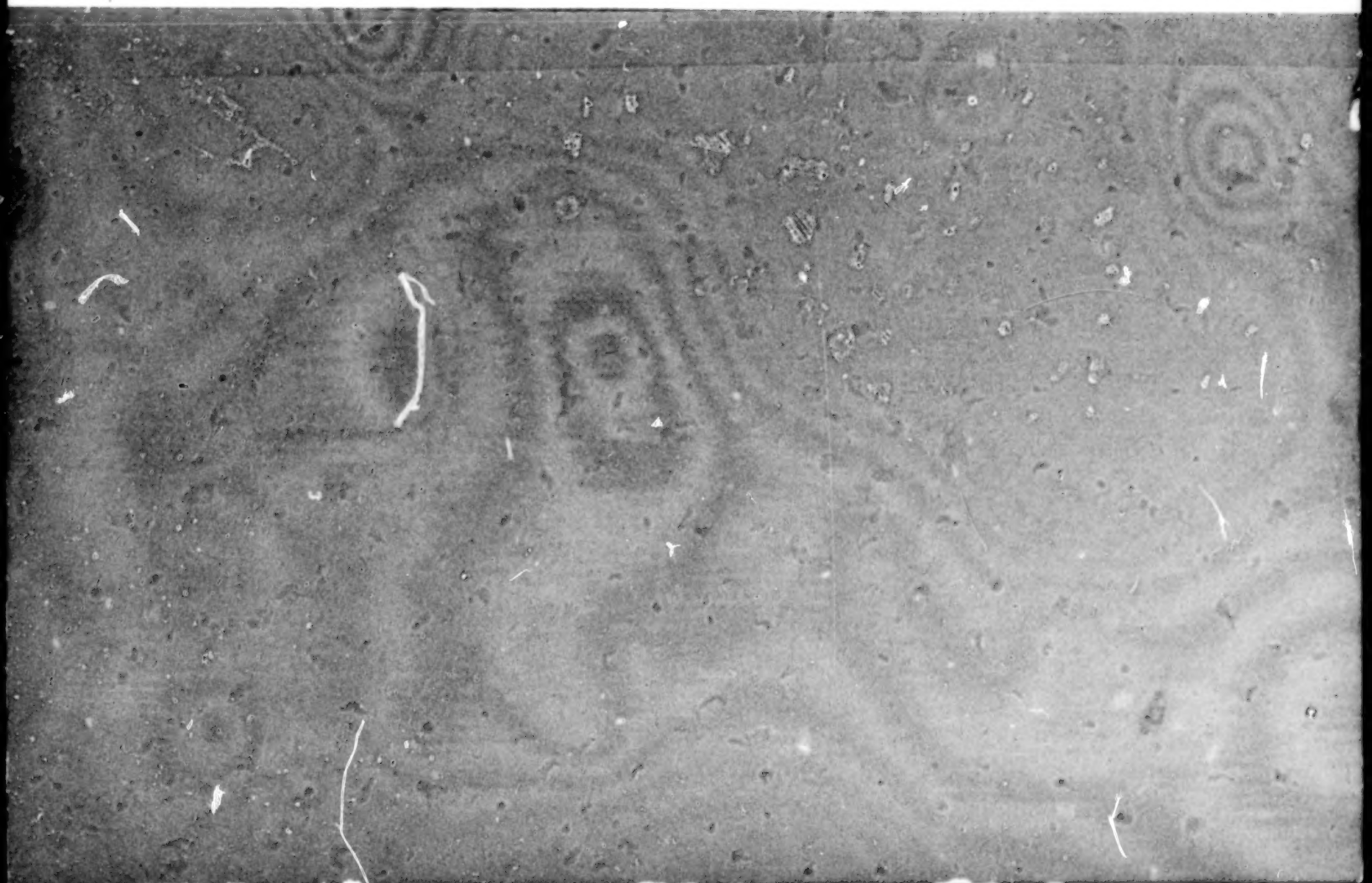

END

MARCH 4, 1981